DISSERTATION

DEVELOPMENT OF A MICROCHIP ELECTROPHORESIS ENVIRONMENTAL MONITORING SYSTEM: FROM SURFACE TO SEPARATION CHEMISTRY

Submitted by

Brian M. Dressen

Department of Chemistry

In Partial Fulfillment of the Requirements

For the Degree of Doctor of Philosophy

Colorado State University

Fort Collins, Colorado

Summer 2008

COLORADO STATE UNVERSITY

April 30, 2008

WE HEREBY RECOMMEND THAT THE DISSERTATION PREPARED UNDER OUR SUPERVSION BY BRIAN M. DRESSEN ENTITLED "DEVELOPMENT OF A MICROCHIP ELECTROPHORESIS ENVIRONMENTAL MONITORING SYSTEM: FROM SURFACE TO SEPARATION CHEMISTRY" BE ACCEPTED AS FULFILLING IN PART REQUIREMENTS FOR THE DEGREE OF DOCTOR OF PHILOSOPHY.

Committee on Graduate Work

Oren P. Anderson

C. Michael Elliott

Bruce A. Parkinson

David S. Dandy

Advisor: Charles S. Henry

Department Head: Anthony K. Rappé

ABSTRACT OF DISSERTATION

DEVELOPMENT OF A MICROCHIP ELECTROPHORESIS ENVIRONMENTAL MONITORING SYSTEM:

FROM SURFACE TO SEPARATION CHEMISTRY

Environmental contaminants are an increasing problem in today's modern world. Methods of incorporation into the human body are numerous, but perhaps the most common is ingestion with food or drinking water. Of more recent concern is perchlorate in drinking water. Human exposure to perchlorate is of concern because of the potential for impaired thyroid function, leading to a number of developmental delays and other medical problems. Its prevalence in the environment only gained interest in the late 1990's, once a method was developed for its detection at the 4 ppb level. In 2005 after being added to the Environmental Protection Agency's (EPA) Unregulated Contaminant Monitoring Rule (UCMR1) list, a sampling of 2800 large water systems and 800 smaller systems, representing less than 10% of all US water systems, revealed contamination in 153 sites over 25 states. Numerous methods of analysis exist relying on expensive bench-top analysis devices that require long analysis times. This dissertation details the development of a perchlorate sensor capable of sub ppb detection limits and 4 min analysis times, with a total cost of less than $10K. The size of the sensor device and supporting equipment lends itself to portability for near-real-time in-field monitoring. This device combines microchip capillary electrophoresis with sensitive detection technology to reliably separate and detect perchlorate in surface and waste water samples. Here I describe the

comprehensive development of the microchip system including control of surface chemistry, flow magnitude and direction, bulk material selection, and chemical selectivity to allow for the separation of perchlorate in water. Optimization of the microchip system, including the use of a selective zwitterionic surfactant to enhance on-chip separations is also presented. The final outcome of this dissertation work is a near-portable environmental sensor for perchlorate capable of meeting EPA regulations for sensitivity to perchlorate as well as several advances in controlling the chemistry within microchip electrophoresis devices through modification or bulk material selection.

Brian M. Dressen

Chemistry Department

Colorado State University

Fort Collins CO 80523

Summer 2008

AKNOWLEDGEMENTS

To my best friend and wife: Brianne Lunt Dressen. I love you forever! This would have never been possible without your love and endless support. You are the reason all of this came to be and worked out. For all that we are and will be.

I want to thank the lab members, especially from the early days, Carlos Garcia, Meghan Caulum, Jon Vickers, Brian Murphy, and David MacDonald. Thanks for making some days bearable.

Thanks to my ski buddies, you helped keep me grounded by being there with me when I needed to get out and play. Here is to powder days.

I would like to thank my family. Thanks for the encouragement and always believing in me.

Charles Henry, thanks for being my advisor, mentor, friend, and boss. Your guidance and insight will follow my career. Thank you.

TABLE OF CONTENTS

LIST OF FIGURES

LIST OF EQUATIONS

LIST OF TABLES

Chapter 1

Introduction

1.1 Perchlorate

Perchlorate is arguably the highest priority military contaminant due to its ubiquitous nature, persistence, and aqueous solubility. In military applications, it is the most common oxidizer in most solid missile and rocket fuels and is used in many pyrotechnic formulations. In solid rockets, the oxidizer is added in great excess, releasing the unconsumed ClO_4^- into the environment. ClO_4^- is known to disrupt normal hormonal development processes by inhibiting the uptake of iodine in the thyroid.[3] Furthermore, ClO_4^- is persistent in the environment since it binds weakly to soil and travels quickly with groundwater. Finally, reported releases of perchlorate have occurred in at least 25 states and contamination is known to exist at many Army facilities and is suspected at many more.[4] For these reasons, the development of sensor technology is necessary to ensure the mitigation of perchlorate contamination, to detect perchlorate presence before migration off site, and to monitor remediation processes.

Currently the EPA has several approved methods for perchlorate testing. The two most common are ion chromatography coupled to conductivity detection[5] and ion chromatography with mass spectrometry detection.[6] Other approved methods[7, 8] are variations of these two and generally have specific goals for perchlorate detection, dealing with difficult matrices or, lowering of limits of detection. While robust and capable of detecting low levels of perchlorate, these methods rely on expensive benchtop instrumentation. In my dissertation work, I developed the fundamental chemistry needed for measuring perchlorate using microchip capillary electrophoresis with conductivity detection to address the need for a fast, portable perchlorate sensor.

The starting point for this work focused on the fabrication and chemical modification of microchip capillary electrophoresis devices. Subsequent to this, novel chemistry was developed for the selective separation of perchlorate from other common inorganic anions. This chapter contains a summary of the pertinent background behind the work performed in this dissertation.

1.2 Capillary Electrophoresis.

Pioneering work by Hjertén using 3 mm tubes[9] led the way for Jorgenson and Lukacs[10, 11] to first demonstrate modern capillary electrophoresis (CE). CE is a liquid-based separation method in which analytes migrate at different rates in an applied electric field. The electric field influences the ions to move with a constant velocity as determined by the field strength, temperature, and properties of the ions. This movement is opposed by the viscous forces of the solution as governed by Stokes law.[12] Ions that migrate faster than, and in the same direction as the bulk flow are retarded by viscous drag and ions that migrate slower are accelerated by the same phenomenon. Neutral analytes are carried with the bulk flow by viscous drag. Migration rate is determined by the charge-to-hydrodynamic radius of each analyte[13] with small highly charged analytes having greater velocity than larger, lower charge species. Migration velocity v of analytes in the presence of an electric field E is given by Equation 1.1.

$$v = \mu_{app} E = (\mu_{ep} + \mu_{eo})E \qquad \textbf{Equation 1.1}$$

where μ_{app} is defined as the apparent solute mobility and is the sum of the electrophoretic mobility (μ_{ep}) and the electroosmotic mobility (μ_{eo}) and E is the field strength in V/cm. μ_{ep} is the force on the ions from the electric field, while μ_{eo} is the effect of electroosmotic flow (EOF) on the analyte. The equations presented were developed for ions in a zero ionic strength system. When ionic strength of the background electrolyte (BGE) is increased, ionic interactions reduce the mobility of the ions because a diffuse cloud of counter ions from the BGE surrounds each analyte ion, effectively increasing its Stokes radius.[14] An increase in the Stokes radius will result in a decrease in the apparent mobility of ions moving in the same direction as bulk flow but faster, while the apparent mobility of ions migrating slower than the bulk flow will increase. Increasing ionic strength also leads to a reduction in μ_{eo} because the double layer thickness is reduced.

1.3 Electroosmotic flow

First identified by Helmholtz in the late 19th century,[13] EOF is generated by the build up of charge at a solid-liquid interface, and its directions and magnitude are governed by the surface charge of the solid and the ionic strength of the BGE. In the case of the fused silica capillaries typically used for CE, the surface is negatively charged, causing a layer of cations to build up at the interface. A second, more diffuse layer is formed, radiating out into the bulk solution, decreasing in density with distance from capillary surface. The solvated cations contained in the diffuse layer migrate towards the cathode causing a "bulk flow" or EOF through viscous drag as well as hydrogen bonding of the solvating water molecules with the bulk solution

water.[15] The flow profile of EOF is flat as opposed to parabolic as in pressure driven systems (Figure 1.1), leading to reduced band broadening, and higher separation efficiency. Due to this difference, CE generally has higher separation efficiencies when compared to liquid or gas chromatography techniques.

The direction and magnitude of the EOF is controlled by the zeta potential (ζ) of the capillary. ζ will vary with capillary material, pH, and surface modification. pH affects ζ through protonation or deprotonation of silanol groups on the surface of the capillary in silica based capillaries. Zeta potential is defined by Equation 1.3.[13]

$$\xi = \sigma_0 / \varepsilon K \qquad \textbf{Equation 1.2}$$

σ_0 is the surface charge density on the capillary surface and ϵ is the dielectric constant of the material in question. 1/K is the double layer thickness. An increase in ionic strength results in a reduction in double layer thickness.

1.4 Modes of CE

There are several modes of CE commonly employed. In my dissertation, two modes were employed and are discussed in detail here. The most common mode is capillary zone electrophoresis (CZE), often referred to as free solution CE. CZE is the simplest of the CE modes relying only on the charge to Stokes radius ratios of analytes for separation.[10, 19] A second mode, micellar electrokinetic chromatography (MEKC), developed by Terabe[20, 21] adds an additional separation regime that relies on the association of analytes with surfactant micelles.

Figure 1.1 Schematic illustrating the differences between electroosmotic (plug) and pressure driven flow (parabolic)

Schematic representations of CZE and MEKC are shown in Figures. 1.2 and 1.3 as they are used in my dissertation research work.[1, 2] In MEKC analytes divide their time between the aqueous phase and the micelle. The surfactant micelles have different migration velocity and/or direction than the analytes[12] and the migration rates of ions will vary with their degree of association. Surfactant micelles act as a chromatographic pseudo-stationary phase enhancing the resolving power through selective interactions. While ionic surfactants such as sodium dodecyl sulfate are the most common stationary phases in MEKC, a number of neutral and zwitterionic surfactants have also been used. Haddad[22] and Lucy[23] described interactions of the zwitterionic surfactant N-dodecyl-N, N-dimethyl-3-ammonio-1-propanesulfonate (DDAPS) with a series of both polarizable and non-polarizable ions including ClO_4^-. DDAPS was shown to cause significant changes in migration time for ions with increasing polarity when it was added above the critical micelle concentration (CMC).

1.5 Sample preconcentration: Stacking

The mobility of a species is directly related to the ions in the BGE and generally sample stacking will occur when a boundary exists between sample regions and the surrounding BGE.[16] Ions present in low conductivity zones will have higher mobility than in high conductivity zones. The ions in the low conductivity region will migrate rapidly towards the boundary, where they will slow down and "stack" like a traffic jam. This type of sample stacking is known as field amplified sample stacking

(FASS).[15] A second method of sample stacking is known as sweeping and occurs when a BGE containing surfactant micelles is used and the sample plug does not contain micelles. The sample ions are slowed down by the micelles as they migrate into the micelle rich region and the sample is concentrated in this boundary zone. Concentration rates exceed 5000 fold.[17] Sweeping is now defined as a situation in which the BGE has a separation vector and the sample plug does not.[18]

1.6 Microchip Capillary Electrophoresis

Miniaturized fluidic technology (Microfluidics) has many advantages over current bioanalytical methods, including reduced sample and reagent consumption (nL to pL), reduced analysis times (min to s), portability, low cost, high throughput, and total sample analysis.[24] Conventional microfluidic devices have been fabricated from a variety of hard materials such as silicon and glass.[25-27] These materials take advantage of established fabrication methods from the microelectronics industry.[25, 26] Separation efficiencies of 10^4- 10^6 theoretical plates/m can be obtained when glass substrates are used for microchip CZE separations.[28, 29] However, fabrication of silicon or glass devices is expensive, time consuming, and requires clean room facilities. Additionally the devices are fragile and advanced microstructures such valves require the addition of soft materials. These issues have led to the search for less expensive, easier to fabricate polymers fro microfluidics. Polymers used in microfluidics include polyvinylchloride (PVC), poly(methylmethacrylate) (PMMA), polycarbonate (PC),

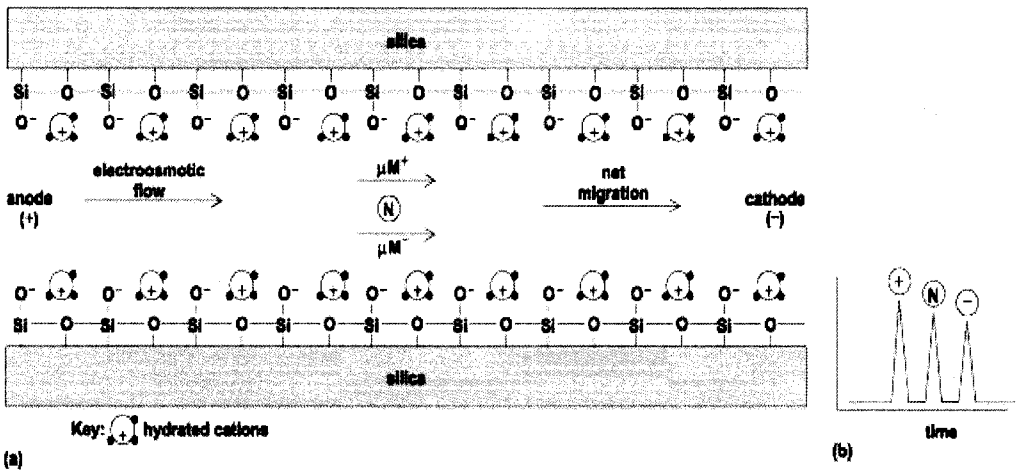

Figure 1.2. Capillary zone electrophoresis. (a) Separation mechanism showing electrophoretic mobility of the positive ion (μM^+) and negative ion (μM^-); N is a neutral molecule. (b) Migration order of the ions.[1]

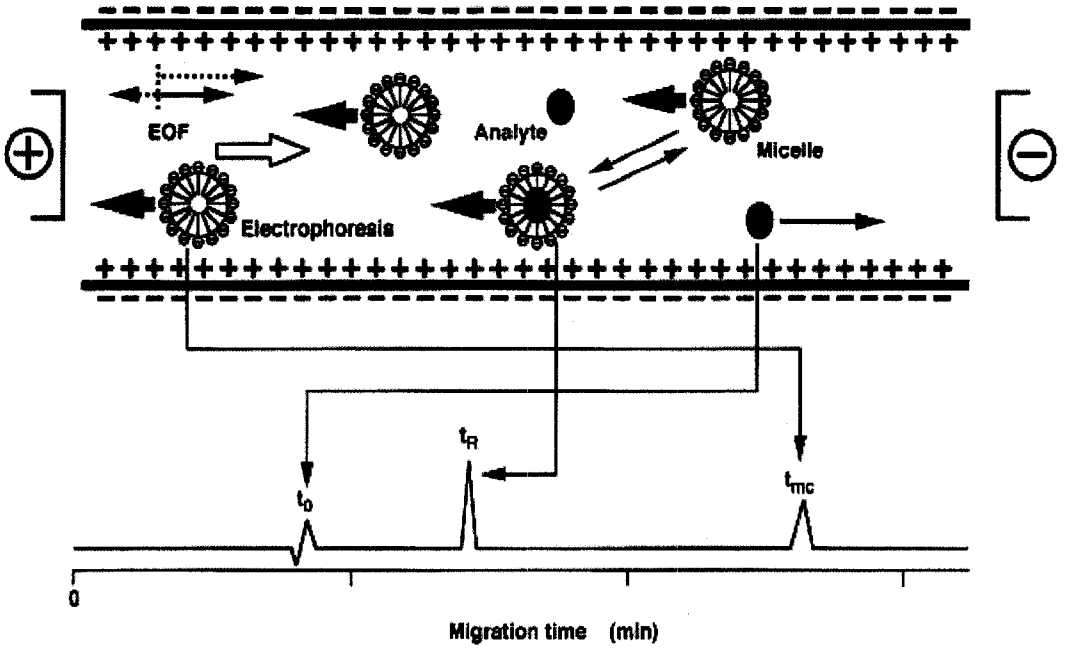

Figure 1.3. Schematic principle of MEKC with anionic micelle. t_0=migration time of a neutral 'unretained' solute, t_R='retention' time in MEKC, t_{mc}=migration time of a micellar aggregate.[2]

and poly(dimethylsiloxane) (PDMS),[30-33] with the two most common being PDMS and PMMA.[34] Compared to glass and silicon, polymer devices are inexpensive and easier to fabricate, and do not require clean room facilities, a major advantage for academic laboratories.[33] Unfortunately, polymeric devices suffer from issues not seen in glass microchips. Hydrophobicity is increased relative to glass, giving rise to poor wettability of aqueous solvents and adsorption and absorption of hydrophobic analytes. Separation efficiency is also reduced in polymeric devices and can be attributed to analyte adsorption and flow microheterogeneity inside the capillaries.[35-37] Solvent incompatibility with polymers limits applications of polymer microchips. These issues can be so severe that without significant improvements, they will continue to limit the number of applications for polymeric microfluidic devices. One focus of my dissertation has been development of novel methods of surface modification methods to reduce some of the problems noted with polymeric microfluidic devices.

1.7 Poly (dimethylsiloxane)

Poly (dimethylsiloxane) (PDMS) has been the most popular polymer used in microfluidic devices.[34] PDMS can be produced by low temperature polymerization. PDMS is an elastomer, lends itself well to mechanical pumping of fluids within the channels. PDMS characteristics include: biologically inert and non-toxic, gas permeable, transparent down to 230 nm, and seals readily with other materials.[34] While PDMS has many advantages, it is not without problems. The most prominent problem or challenge with PDMS is the hydrophobic nature of untreated PDMS as

reflected by a water contact angle of ~108°.[38] Hydrophobic PDMS surfaces interact strongly with hydrophobic domains of analytes during separation causing significant peak tailing and loss of separation efficiency.[39] The electroosmotic flow (EOF) also changes with pH and can drift run-to-run, compromising the analysis reproducibility. PDMS has a tendency to revert back to the hydrophobic state quickly following hydrophilic modification, a phenomenon known as hydrophobic recovery.[34] Hydrophobic recovery occurs when low molecular weight oligomers from the bulk polymer migrate to the surface and replace modified areas resulting in a heterogeneous surface and flow irregularities.[40] Hydrophobic recovery generally takes place in <30 min as illustrated by a measured contact angle starting at ~65° after plasma treatment and returning to 108°.[38]

Several chemical modification methods for PDMS have been investigated in an effort to address the above issues. In the literature there are three general approaches for modifying surface chemistry: dynamic coatings with surfactants, adsorbed polymer coatings, and covalent modification. Dynamic coatings have provided good EOF stability but require the continual presence of surfactant in the mobile phase.[41] Adsorbed coatings also stabilize the EOF and do not require polymer in the mobile phase.[42] Covalent modifications have shown the best performance with regards to analyte absorption.[43, 44] The difficulty in modifying PDMS is further complicated by hydrophobic recovery.[38, 40] In my dissertation, adsorbed, dynamic, and covalent coatings were studied.

1.8 Poly(methyl methacrylate)

Poly(methyl methacrylate) (PMMA) has seen use in microfluidics because it has good chemical and mechanical stability, good optical properties, and supports electroosmotic flow.[45] Ease and low cost of fabrication also make PMMA an attractive polymer.[46] Devices constructed from PMMA are not without their drawbacks, however. The hydrophobicity of PMMA (illustrated by a water contact angle of ~75° vs. ~108° for PDMS) inhibits self-wetting with aqueous solvents. Furthermore, PMMA is incompatible with many organic solvents including acetone and methanol. Chemical modification of PMMA microfluidic devices has not been as widely reported as for PDMS.[47-51]

1.9 Thermoset Polyester

Thermoset polyester (TPE) uses similar fabrication to that of PDMS, easing the transition to this material and reducing costs. TPE does not suffer from such disadvantages as hydrophobic recovery and has much lower native hydrophobicity when compared to PDMS.[52] Lower hydrophobicity leads to higher separation efficiencies from decreased analyte adsorption. The absence of hydrophobic recovery gives better stability with the use of TPE microchips for MCE-EC. TPE is not transparent and absorbs strongly in the UV range, hampering optical detection methods. While fabrication is similar to that of PDMS, the polymer is removed from the mold while partially cured and is easily damaged especially when features are small.

1.10 Dissertation Summary

The research contained in this dissertation focuses on two main areas: the control of separation conditions and EOF within polymer microfluidic devices with the use of coatings, additives, treatments, and material selection and application of the polymeric microfluidic devices for analysis of perchlorate in surface and drinking water. EOF and analytically relevant surface chemistry was controlled through the use of surfactants, polyelectrolyte multilayers, and plasma enhanced chemical vapor deposition. After studying modification chemistry, I developed the requisite separation chemistry necessary to detect perchlorate at environmentally relevant concentrations using microchip CE with contact conductivity detection. Electrophoretic stacking has enabled sub-ppb determination of perchlorate in water. After demonstration of the capability of the system to detect environmentally relevant perchlorate concentrations, two real-world studies were conducted including both relatively clean surface water and heavily contaminated waste water from an explosives packing facility. This dissertation describes the ground up process involved in the development of a sensor system for environmental perchlorate and is divided into 7 chapters. The first (this) chapter covers relevant background information such as, perchlorate information, current detection methods, and capillary electrophoresis and microchip CE. The second chapter covers surfactant modification of PDMS microfluidic chips. Chapter 3 discusses plasma vapor deposition and application to EOF and absorption control within PDMS microchips. Chapter 4 focuses is on thermoset polyester as an alternative material for device fabrication, leading to increases in separation efficiency. The fifth chapter covers use

of polyelectrolyte multilayers to alter the surface chemistry of PDMS microchips. Chapter 6 presents a novel analytical system and chemistry for perchlorate separation and detection in surface and waste water capable of high resolution separation and sub ppb detection limits. The last chapter (7) summarizes my work and outlines future directions. Chapters 2-5 are essentially reprints of published manuscripts with a section added to delineate the relative contributions of each of the authors.

1.11 References

(1) answers.com *http://content.answers.com/main/content/img/McGrawHill/Encyclopedia/images/CE226400FG0010.gif.*

(2) Watanabe, T.; Terabe, S. *Journal of Chromatography A* **2000**, *880*, 311-322.

(3) Wolff, J. *Pharmacological Reviews* **1998**, *50*, 89-105.

(4) EPA, Ed.; EPA, 2004.

(5) D.P. Hautman, D. J. M., A.D. Eaton, A.W. Haghani; Environmental Protection Agency, C., OH, 1999, Ed.; Environmental Protection Agency, 1999.

(6) Elizabeth Hedrick, T. B., Rosanne Slingsby, David Munch, ; EPA, Ed.; EPA, 2005.

(7) S.C. Wendelken, D. J. M., B.V. Pepich, D. W. Later, C. A. Pohl; EPA, Ed.; EPA, 2005.

(8) Herbert P. Wagner, B. V. P., Chris Pohl, Douglas Later, Robert Joyce, Kannan Srinivasan, Brian DeBorba, Dave Thomas, Andy Woodruff, David J. Munch; EPA, Ed.; EPA, 2005.

(9) Hjerten, S. *Chromatogr. Rev.* **1967**, *9*, 122.

(10) Jorgenson, J. W.; Lukacs, K. D. *Clin Chem* **1981**, *27*, 1551-1553.

(11) Jorgenson, J. W.; Lukacs, K. D. *Science* **1983**, *222*, 266-272.

(12) Landers, J. P. *Handbook of Capillary Electrophoresis*; CRC Press: Boston, 1997.

(13) Oda, R. P.; Landers, J. P. In *Handbook of Capillary Elecrophoresis,* 2nd ed.; Landers, J. P., Ed.; CRC Press: Boca Raton, 1997, pp 1-47.

(14) C, P. *The Essence of Chromatography; Elsivier: Amsterdam*, 2003.

(15) Landers, J. P. *Handbook of Capillary Electrophoresis*, 1 ed., 1993.

(16) Landers, J. P. *Handbook of of capillary and microhip electrophoresis and associated microtechniques* 3rd ed.; CRC Press: Boca Raton, 2008.

(17) Quirino, J. P.; Terabe, S. *Science* **1998**, *282*, 465-468.

(18) Sera, Y.; Matsubara, N.; Otsuka, K.; Terabe, S. *Electrophoresis* **2001**, *22*, 3509-3513.

(19) Jorgenson, J. W.; Lukacs, K. D. *Analytical Chemistry* **1981**, *53*, 1298-1302.

(20) Terabe, S.; Otsuka, K.; Ichikawa, K.; Tsuchiya, A.; Ando, T. *Analytical Chemistry* **1984**, *56*, 111-113.

(21) Terabe, S.; Otsuka, K.; Ando, T. *Analytical Chemistry* **1985**, *57*, 834-841.

(22) Yokoyama, T.; Macka, M.; Haddad, P. R. *Analytica Chimica Acta* **2001**, *442*, 221-230.

(23) Woodland, M. A.; Lucy, C. A. *Analyst* **2001**, *126*, 28-32.

(24) Lion, N. *Curr Opin Biotechnol* **2004**, *15*, 31-37.

(25) Harrison, D. J.; Manz, A.; Fan, Z.; Luedi, H.; Widmer, H. M. *Analytical Chemistry* **1992**, *64*, 1926-1932.

(26) Harrison, D. J.; Fluri, K.; Seiler, K.; Fan, Z.; Effenhauser, C. S.; Manz, A. *Science (Washington, DC, United States)* **1993**, *261*, 895-897.

(27) Harrison, D. J.; Glavina, P. G.; Manz, A. *Sensors and Actuators, B: Chemical* **1993**, *B10*, 107-116.
(28) Wang, J. *Talanta* **2003**, *60*, 1239-1244.
(29) Lacher, N. A.; de Rooij, N. F.; Verpoorte, E.; Lunte, S. M. *Journal of Chromatography, A* **2003**, *1004*, 225-235.
(30) Martynova, L. *Analytical Chemistry* **1997**, *64*, 4783-4789.
(31) McCormick, R. M. *Analytical Chemistry* **1997**, *69*, 2626-2630.
(32) Roberts, M. A. *Analytical Chemistry* **1997**, *69*, 2035-2042.
(33) Effenhauser, C. S.; Bruin, G. J. M.; Paulus, A.; Ehrat, M. *Analytical Chemistry* **1997**, *69*, 3451-3457.
(34) Makamba, H. *Electrophoresis* **2003**, *24*, 3607-3619.
(35) Badal, M. Y.; Wong, M.; Chiem, N.; Salimi-Moosavi, H.; Harrison, D. J. *J Chromatogr A* **2002**, *947*, 277-286.
(36) Duffy, D. C.; McDonald, J. C.; Schueller, O. J. A.; Whitesides, G. M. *Anal Chem* **1998**, *70*, 4874-4884.
(37) Ocvirk, G.; Munroe, M.; Tang, T.; Oleschuk, R.; Westra, K.; Harrison, D. J. *Electrophoresis* **2000**, *21*, 107-115.
(38) Fritz, J. L.; Owen, M. J. *Journal of Adhesion* **1995**, *54*, 33-45.
(39) Vickers, J. A.; Caulum, M. M.; Henry, C. S. *Analytical Chemistry* **2006**, *78*, 7446-7452.
(40) Kim, J.; Chaudhury, M. K.; Owen, M. J.; Orbeck, T. *Journal of Colloid and Interface Science* **2001**, *244*, 200-207.
(41) Harrison, D. J. *Electrophoresis* **2000**, *25*, 107-115.
(42) Henry, C. S.; Liu, Y.; Bledsoe, J. M.; Hopkins, C. D. *Abstracts of Papers - American Chemical Society* **2001**, *221st*, ANYL-212.
(43) Hu, S. *Electrophoresis* **2003**, *24*, 3679-3688.
(44) Xiao, D. *Analytical Chemistry* **2004**, *76*, 2055-2061.
(45) Kricka, L. J.; Fortina, P.; Panaro, N. J.; Wilding, P.; Alonso-Amigo, G.; Becker, H. *Lab on a Chip* **2002**, *2*, 1-4.
(46) Kelly, R. T.; Woolley, A. T. *Analytical Chemistry* **2003**, *75*, 1941-1945.
(47) Long, T. M.; Prakash, S.; Shannon, M. A.; Moore, J. S. *Langmuir* **2006**, *22*, 4104-4109.
(48) Llopis, S. L.; Osiri, J.; Soper, S. A. *Electrophoresis* **2007**, *28*, 984-993.
(49) Chen, G.; Xu, X. J.; Lin, Y. H.; Wang, J. *Chemistry-a European Journal* **2007**, *13*, 6461-6467.
(50) Mohamadi, M. R.; Mahmoudian, L.; Kaji, N.; Tokeshi, M.; Baba, Y. *Electrophoresis* **2007**, *28*, 830-836.
(51) Shah, J. J.; Geist, J.; Locascio, L. E.; Gaitan, M.; Rao, M. V.; Vreeland, W. N. *Electrophoresis* **2006**, *27*, 3788-3796.
(52) Kima, J. *J Colloid Interf Sci* **2000**, *226*, 231.

Chapter 2

Comparison of Surfactants for Dynamic Surface Modification of Poly(dimethylsiloxane) Microchips

This chapter covers the use of negatively charged surfactants as modifiers of the background electrolyte using poly(dimethylsiloxane) (PDMS) microchips. In particular, the use of the anionic surfactants, sodium dodecyl sulfate, phosphatidic acid, and deoxycholate, to modify the EOF and detection efficiency was studied. When surfactants were present in the run buffer, an increase in cathodic electroosmotic flow (EOF) was observed relative to unmodified PDMS. Two additional effects were also observed: (i) stabilization of the run-to-run EOF and (ii) an improvement in the electrochemical response for several biomolecules. In order to characterize the analysis conditions, the effects of different surfactant, electrolyte, and pH were studied.

EOF measurements were performed using either the current monitoring method or by detection of a neutral molecule. The first adsorption/desorption kinetics studies are also reported for different surfactants with PDMS. The separation of biologically important analytes such as glucose, penicillin, phenol, and homovanillic acid was improved in peak shape, resolution, and decreased the analysis time from 200 to 125 s. However, no significant changes in the number of theoretical plates were observed.

The chapter is largely a reprint of "Comparison of surfactants for dynamic surface modification of poly(dimethylsiloxane) microchips" Carlos D. Garcia, Brian M. Dressen, Amber Henderson, and Charles S. Henry, *Electrophoresis* **2005**, *26,* 703–709, a manuscript written by Carlos D. Garcia, a postdoctoral research associate in the Henry laboratory and myself, with the work performed equally by the individuals. Specifically, fabrication and EOF characterization was performed by me with separation experiments performed by Dr. Garcia. Some initial experimental work performed by A. Henderson.

2.1 Introduction

The chemical functionality of the capillary surface plays an important role in capillary electrophoresis (CE) separations. The exposed groups are especially important when microchip-CE is used because of the limited length of the separation channel. Separation efficiencies of 10^4–10^6 theoretical plates/m can be obtained when glass is used as the substrate.[1-4] However, the procedures required to fabricate glass microchips are not accessible to every laboratory and the devices are cost and time-intensive to manufacture. Polymeric substrates, such as poly(dimethylsiloxane) (PDMS), can be used to overcome some of these problems.[5] PDMS microchips can be fabricated in hours by casting a polymer against a mold. In addition, PDMS can be sealed to a wide variety of substrate materials and is optically transparent above 230 nm, flexible, nontoxic, inert, and gas-permeable.[6] PDMS also has some limitations. Probably the most prominent is the hydrophobicity that is reflected in a PDMS/water contact angle of 108° for untreated PDMS.[7] The hydrophobic PDMS surfaces have a strong interaction with the hydrophobic domains of the analytes during the separation step causing significant peak tailing and loss of separation efficiency. Another problem of PDMS is drifting electroosmotic flow (EOF) which can compromise the reproducibility of the analysis.[7-9] In order to control the magnitude and stability of the EOF on polymeric microchips, several approaches have been reported[10] including the study of sealing methods,[11] coatings with inorganic anions,[12] polyelectrolytes,[4, 13-16] and the addition of surfactants to the background electrolyte.[17-19] These compounds typically interact with the surface, changing the zeta potential[20, 21] and therefore affecting the EOF and the separation.

Surfactants, such as Brij-35, Tween 20, cetyltrimethylammonium bromide (CTAB)[22], sodium dodecyl sulfate (SDS)[23], didodecyldimethylammonium bromide (DDAB), 1,2-di-lauroyl-*sn*-phosphatidylcholine (DLPC), Triton X-100, and palmityl sulfobetaine, have shown to have a strong influence on the EOF and separation efficiency in fused-silica capillaries and microdevices.[4] In particular, the addition of SDS may increase the EOF and improve the electrochemical signal of various biomolecules, such as carbohydrates,[24-26] metabolites,[26, 27] and catechols.[27] Detection after microchip-CE separations has been traditionally performed by LIF, due to the low detection limits that can be achieved and the ease of the instrumental configuration. Electrochemical detection (EC) is an alternative detection method that is well-suited for small molecules.[28] Direct EC of many biological compounds is possible using pulsed amperometric detection (PAD). Briefly, PAD consists of a simple three-potential waveform where the electrode is first cleaned at a high positive potential (to oxidize the electrode material), then reactivated at a negative potential (to redissolve the surface oxide), and finally used to measure the analyte at a moderately positive potential. PAD has been applied for the detection of carbohydrates after separations by CE[24, 29] and HPLC.[30] In general, the advantages of using PAD (with respect to constant potential amperometry) include longer electrode lifetimes and the possibility of detection of nonelectroactive biomolecules, such as amines. One concern when using PAD (or any other EC detection mode) is the ability of surfactants to foul the electrode. Previous results from our laboratory have shown that PAD is not only compatible with SDS, but also a signal enhancement occurs.[24-26] In this report, we extend our studies to additional surfactants, to further

investigate modification in device performance as function of surfactant chemistry. The use of negatively charged surfactants as background electrolyte modifiers was studied with PDMS microchips. The structure of the three surfactants (sodium dodecyl sulfate, sodium deoxycholate, and phosphatidic acid) is shown in Fig. 2.1. The addition produces a self adsorbing nonpermanent coating that increases the EOF and reduces the interaction of the analytes with the channel surface.[9] The effects of different surfactant chemistry, electrolyte composition, and pH were studied. In general, the EOF increased with the addition of surfactants. Using optimized conditions, the analysis of biologically important analytes (glucose, penicillin, phenol, and homovanillic acid) was improved, decreasing the analysis time and increasing the electrochemical response.

2.2 Materials and methods

2.2.1 Reagents and solutions. SU-8 2035 photoresist and XP SU-8 developer were purchased from MicroChem (Newton, MS, USA), Sylgard 184 silicone elastomer and curing agent were obtained from Dow Corning (Midland, MI, USA). Aqueous solutions were prepared using analytical grade reagents and 18 $M\Omega\,cm^{-1}$ resistance water (Milli-Q; Millipore, Bedford, MA, USA). The running electrolytes were prepared by weighing the desired amount of sodium tetraborate ($Na_2B_4O_7{\cdot}10H_2O$) (Fisher, Springfield, NJ, USA) or sodium phosphate (either Na_2HPO_4 or NaH_2PO_4) and adjusting the pH with either 2 M NaOH (Fisher) or 2 M HCl (Fisher). Following the pH adjustment, the desired amount of surfactant was added to the running buffer. Sodium dodecyl sulfate (SDS; Aldrich, Milwaukee, WI, USA), sodium deoxycholate

(DOCh; Aldrich) and phosphatidic acid (PA; Aldrich) were selected for the present study (see Fig. 2.1 for structure). Glucose (Fisher), penicillin (Fluka, Buchs, Switzerland), phenol (liquefied; Fisher), and homovanillic acid (Aldrich) stock solutions (approx. 10 mM) were prepared daily by dissolving the desired amount in 1 mL running electrolyte. Samples were prepared by the dilution of the stock. A 25 μm diameter, 99.99% gold wire (Goodfellow, England) was used as the working electrode for EC. For pH measurements, a glass electrode and a digital pH meter (Denver Instruments) were used. Methanol was of ACS-certified quality and purchased from Fisher. All chemicals were used as received without any further purification. All experiments were performed at room temperature (22 ± 2°C) and unless noted, the points and error bars on the plots represent the average and standard deviation obtained for at least three measurements.

2.2.2 Instrumentation. A 3-channel (two positives and one negative) laboratory built high-voltage power supply, with an adjustable voltage range between 0 and ±4000 V, was used for all the experiments involving an injection/separation step [29]. Cross injection was used for all experiments. During the injection, +410 V, -150 V, and +410 V were applied to the reservoirs S (sample), SW (sample waste), and B (buffer) respectively. During the separation procedure the potential applied to reservoir B was raised to

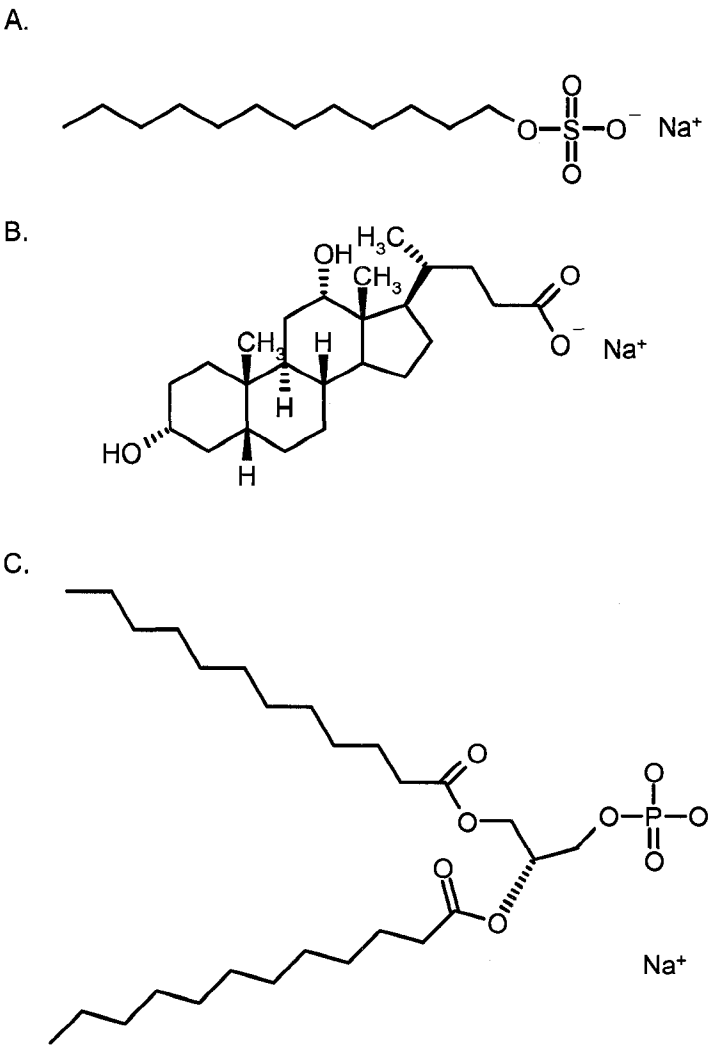

Figure 2.1 Structure of selected surfactants. (A) SDS, (B) DOCh, and (C) PA

+1000 V (or the corresponding separation potential) while the potential applied to reservoir SW was changed to +410 V. The waste reservoir (W) was always grounded. In order to avoid Joule heating in the S-B channel during the injection, a 1 MΩ resistor was included in series with the chip.

2.2.3 Fabrication of the PDMS microchip. Depending on the purpose, two different PDMS microchips were fabricated using a previously described method.[29] For the current monitoring method, single straight channels (Fig. 2.2A) 4.5 cm long were chosen to simplify the experimental design (no injection needed). For the experiments involving injections and separations a previously described design was used (Fig. 2.2B).[29] Briefly, a clean 76 mm silicon wafer (Silicon Inc.) was coated with SU-8 2035 negative photoresist. A digitally produced mask (2400 dpi) containing the channel pattern was placed on the coated wafer exposed to light *via* a near-UV flood source and then baked. The positive relief was developed by placing the wafer in propylene glycol methyl ether acetate for 15 min, rinsing with methanol, and drying under an N_2 stream. The height of the positive pattern on the molding master, which is equal to the channel depth created on the PDMS layer, was 50 μm when measured with a profilometer. PDMS layers were fabricated by pouring a degassed mixture of Sylgard 184 silicone elastomer and curing agent (10:1) onto either a molding master or a blank wafer, followed by curing for at least 2 h at 65°C. The cured PDMS was separated from the mold and reservoirs were excised at the end of each channel using a 6 mm circular punch. When necessary, a 25 μm diameter gold wire was aligned at the end of the separation

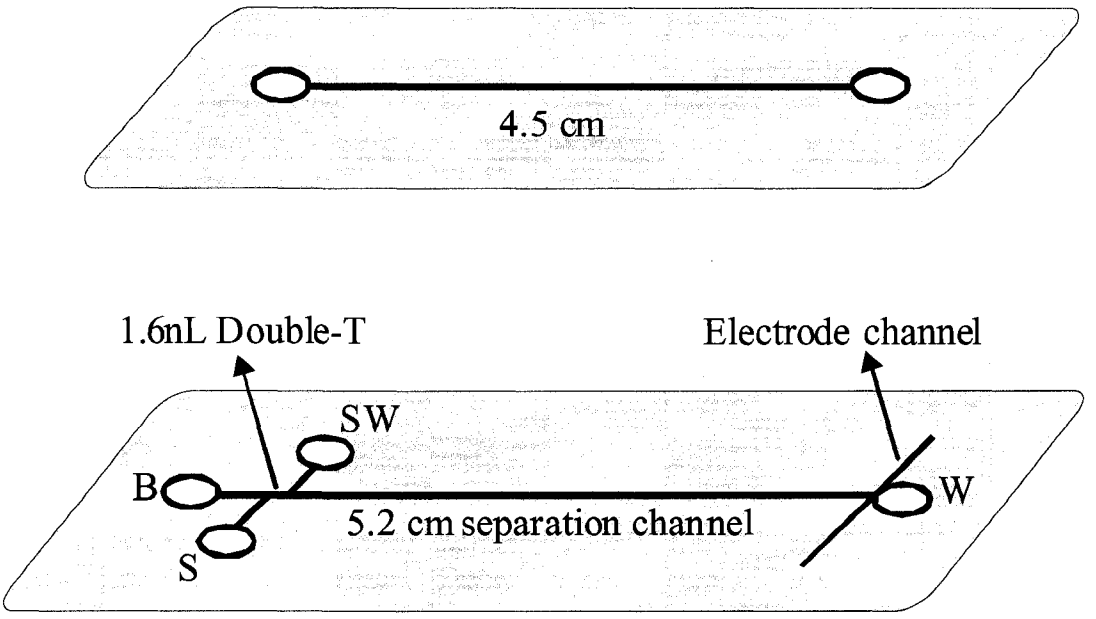

Figure 2.2 (A) Schemaic drawing of the microchip used for the current monitoring experiments. Channel, 50 μm wide, 50 μm deep. (B) Schematic drawing of the microchip-CE with PAD. Channels, 50 μm wide, 50 μm deep. Double-T volume, 1.6 nL: separation channel, 52 mm. Double-T arms, 10 mm long. Solution reservoirs, 6 mm diameter.

channel in a perpendicular electrode channel. After that, the two PDMS layers were placed in an air plasma cleaner (Harrick PDC-32G Plasma Cleaner/Sterilizer), oxidized for 20 s and immediately brought into conformal contact to form an irreversible seal. Finally, if an electrode was included, the extremities of the electrode channel were sealed with super-glue and electrical connection to the working electrode was made using silver paint (Structure Probe, PA, USA) and a copper wire.

2.2.4 EOF measurements. The EOF measurements were performed using the current monitoring method. Experiments were performed by measuring the voltage drop across a 1 kΩ resistor using a standard voltmeter (RadioShack). Only one of the channels of the power supply was used to drive the flow. The microchip consisted of a single straight channel (4.5 cm long, see Fig. 2.2A). Briefly, the first reservoir and the channel were filled with 10 mM buffer and the second reservoir was filled with 9 mM buffer. Upon application of the voltage (900 V), electroosmotic flow took place and the lower concentration electrolyte solution from the second reservoir gradually displaced the higher concentration background electrolyte in the channel, resulting in an increase in the electrical resistance of the channel. The change in separation current under a constant applied voltage difference was monitored using a voltmeter. Once a constant current was obtained, the potential was then applied to the reservoir with concentrated buffer and the above procedure repeated. The time required to reach a current plateau was used to calculate EOF based on Eq. (1) where L is the

length of the separation channel (4.5 cm), V is the total applied voltage (900 V), and t is the time in seconds required to reach the new current plateau.

$$\mu_{EOF} = L^2/Vt \qquad \textbf{Equation 2.1}$$

In all cases, electrical connections to the microfluidic devices were made with platinum electrodes placed into reservoirs.

2.2.5 Electrochemical detection. EC was performed using PAD with a two-electrode setup (CHI660B; CH Instruments, Austin, TX, USA). As mentioned previously, a gold wire (25 μm diameter) was used as the working electrode and the corresponding detection potential was optimized for each compound. A platinum wire placed in the waste reservoir was used as both auxiliary and reference electrode.

2.3 Results and discussion

2.3.1 Effect of the presence of surfactants on the EOF. Anionic surfactants are known to adsorb to the surface of PDMS. Adsorbed molecules affect the surface charge density and thus the zeta potential which is necessary for the generation of EOF. It has been reported that the hydrophobic part of the surfactants interact with the PDMS surface, exposing the charged head and therefore increasing the EOF.[8] However, the exact mechanism for the interaction is not yet clear. The effect of the addition of three different surfactants (SDS, DOCh, and PA, see Fig. 2.1) was studied at three different pH values (4, 7, and 10). In order to avoid the formation of

micelles, a concentration corresponding to 0.1X critical micelle concentration (CMC_{SDS}= 8mM [31], MW = 288.4) was selected for the present studies. The channels were in contact for at least 30 min with each solution prior to EOF measurements to minimize kinetic contributions in the adsorption stage. As can be observed in Fig. 2.3, at higher pH, higher EOF values were obtained. It can also be observed as a general trend that the addition of any negatively charged surfactant increased the EOF at all pH. In order to explain the differences between the surfactants it is necessary to consider their structure and molecular weight. We believe that the hydrophobic tail of SDS can be adsorbed to the PDMS producing the highest EOF (5.46 ± 0.02 ($x10^{-4}$) $cm^2/(sV)$, pH 10, $n = 5$). It is also reasonable to think that a double tailed, larger molecule such as PA (CMC_{PA} = 0.05 mM[32], MW = 502.6) will occupy a larger surface area and therefore provide a lower EOF value (4.52 ± 0.04 (x 10^{-4}) $cm^2/(sV)$, pH 10, $n = 5$) than SDS coated channels. Following the same model, if an aromatic surfactant like DOCh (CMC_{DOCh} = 5mM [33], MW = 414.6) is added, a lower EOF should be obtained (4.31 ± 0.03 (x 10^{-4}) $cm^2/(sV)$, pH 10, $n = 5$). It is worth noting that the hydrophobic part of DOCh is composed of four fused rings, significantly increasing the rigidity of the molecule. The additional rigidity and cross-sectional area of the tail may prevent it from absorbing into the PDMS. The result is the lowest EOF of any of the three surfactants.

2.3.2 Effect of the concentration of surfactants. The effect of the surfactant concentration was studied using the concentrations corresponding to 0 (no surfactant added), 0.16*CMC, 1.06*CMC, and 9.06*CMC of each surfactant. As can be observed in Fig. 2.4, in all cases an increase in the EOF was observed even at low surfactant concentration (0.16*CMC) with respect to the initial EOF (3.99 ± 0.25 ($x10^{-4}$) $cm^2/(sV)$, pH 10, n = 5, 3 chips). For the case of PA (CMC = 0.05 mM) a gradual increase was observed until a maximum was observed at the highest concentration (0.54 mM ,9.06CMC). For the case of SDS and DOCh the maximum was reached at a lower surfactant concentration, probably due to the higher affinity of SDS and DOCh for the surface, when compared to PA. These results are in good agreement with previously published results for SDS[24, 25] and with the adsorption kinetics discussed in the following section. It is worth noting that in all cases, the maximum EOF was achieved when the surfactant concentration was 1 mM, independent of the CMC for each surfactant. As mentioned before, moderate EOF values can be achieved if less than 1 mM PA or more than 1 mM SDS or DOCh are used. In the case of PA, the moderate EOF is the result of a series of factors including low affinity for the PDMS surface, slow kinetics, large molecular weight, and size. The decrease in EOF observed at concentrations higher than 1 mM SDS or DOCh can be attributed to an increase in the ionic strength of the background electrolyte. Similar results were also reported by Badal *et al.*[9] when they studied the effect of surfactant mixtures on the separation efficiency of proteins. Another advantage of the use of anionic surfactants is the possibility to induce EOF below the CMC (0.16*CMC), allowing the separation of proteins without denaturation.

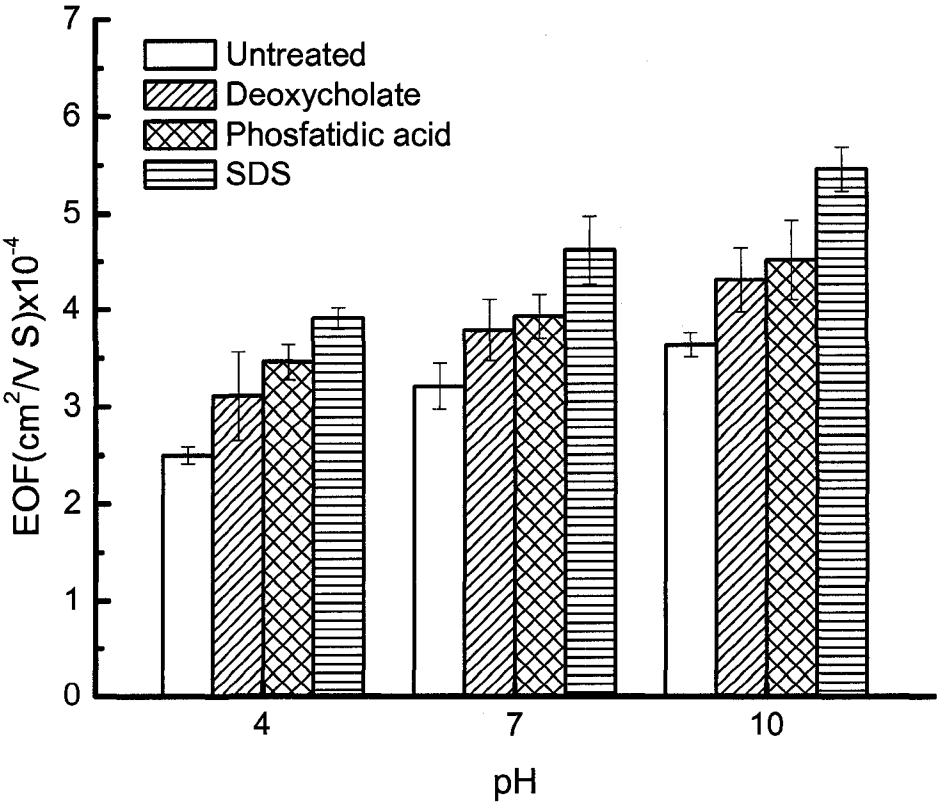

Figure 2.3 Effect of the addition of surfactants on the electroosmotic flow at different pH values measured using the current monitoring method. Conditions: current monitoring method, 10 mM–9 mM phosphate buffer (pH 10.0), E = 900 V, 0.8 mM SDS, 0.5 mM DOCh, 0.006 mM PA.

2.3.3 Adsorption/desorption kinetics of surfactants. Different experiments were performed in order to evaluate the adsorption and desorption kinetics of different surfactants using a concentration corresponding to 0.16 CMC. Pulsed amperometric detection (PAD) was performed using the previously described conditions [24, 29, 34] using glucose (p*K*a 12.1) as a neutral marker. The initial EOF was measured using 10 mM borate (pH 9.4) as the supporting electrolyte. After five consecutive runs, the solutions in reservoirs B, SW, and D were replaced with 10 mM borate (pH 9.4) containing the corresponding surfactant and the analysis was repeated until a constant migration time (*t*M) was achieved. Finally, the initial solution was placed in the reservoirs and the analysis repeated until a stable *t*M was obtained. As can be observed in Fig. 2.5A, an initial EOF = 4.07 ± 0.01 (x 10^{-4}) $cm^2/(sV)$ (n = 5) was observed for native PDMS without SDS. Once the solution was replaced and the SDS flowed through the chip, a significant decrease in the *t*M was observed, as a result of an increase in the EOF. The equilibrium was reached after approximately 20 min, where an EOF of 4.96 ± 0.02 (x 10^{-4}) $cm^2/(sV)$ (n = 3) was obtained for SDS. As can be observed also in Fig. 2.5A, when the solution containing SDS was replaced with the solution without SDS, the EOF gradually decreased towards the initial value. However, the desorption reaction proceeded at a much lower rate in comparison to the adsorption and the initial EOF value was never reached (final EOF=4.12 ± 0.02(x 10^{-4}) $cm^2/(sV)$ (n = 5)), even after 50 min. With this final EOF value, the remaining amount of SDS (attached to the PDMS) was calculated to be, 8%. Similar

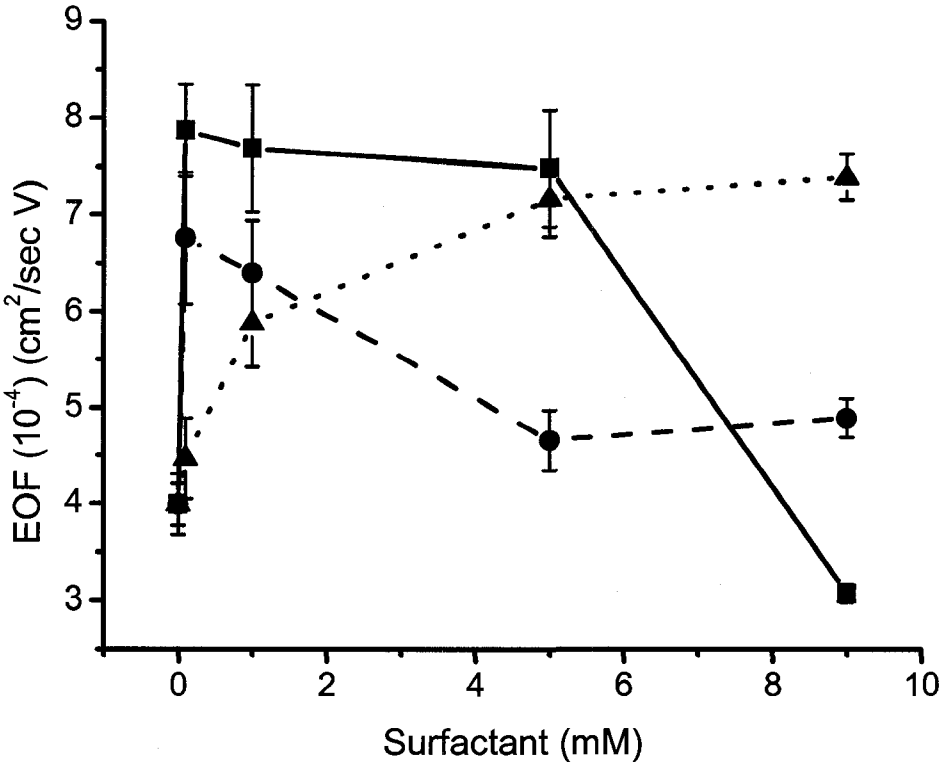

Figure 2.4 Effect of the addition of surfactants at different concentrations on the electroosmotic flow. (-■-) SDS, (--●--) DOCh, (··▲··) PA. Conditions: current monitoring method, 10 mM–9 mM phosphate buffer (pH 10.0), E = 900 V.

behavior was observed when DOCh was added to the background electrolyte. As can be observed in Fig. 2.5B, the initial EOF increased from 3.67 ± 0.01 (x 10^{-4}) cm^2/ (sV) (n = 5) up to EOF = 4.76 ± 0.01 (x 10^{-4}) cm^2/(sV) (n = 3).

Again, the observed desorption rate was much slower reaching an EOF of 3.75 ± 0.01 (x 10^{-4}) cm^2/ (sV) (n = 5) 70 min after the surfactant was removed from the solution reservoirs. After 70 min, 12% of the total DOCh remained attached to the PDMS. When PA was added to the background electrolyte, the slowest adsorption reaction was observed (Fig. 2.5C). In addition, the EOF increased from 3.21 ± 0.01 (x 10^{-4}) cm^2/(sV) (n = 4) to only 4.48 ± 0.01 (x 10^{-4}) cm^2/(sV) (n = 2). The difference observed in the initial EOF value for different untreated PDMS microchips is the result of differences in the plasma oxidation and normal chip-to-chip variations. Differences in EOF values between the current monitoring experiments and the detection of a neutral marker are also attributed to the use of borate instead of phosphate as background electrolyte.

A second set of experiments was performed in order to evaluate the possibility of performing successive coatings. Due to its intermediate adsorption-desorption kinetics and EOF, DOCh was selected for the studies. As can be observed in Fig. 2.6, similar EOF values were obtained between different adsorption/desorption cycles. In addition, the coating can be deposited and partially removed, without affecting the next adsorption/desorption cycle. However, the calculated initial adsorption and desorption rates are very inconsistent. This is because only one point can be obtained every 80–100 s, allowing only a rough estimation of the kinetics, based on EOF values between with and without coatings.

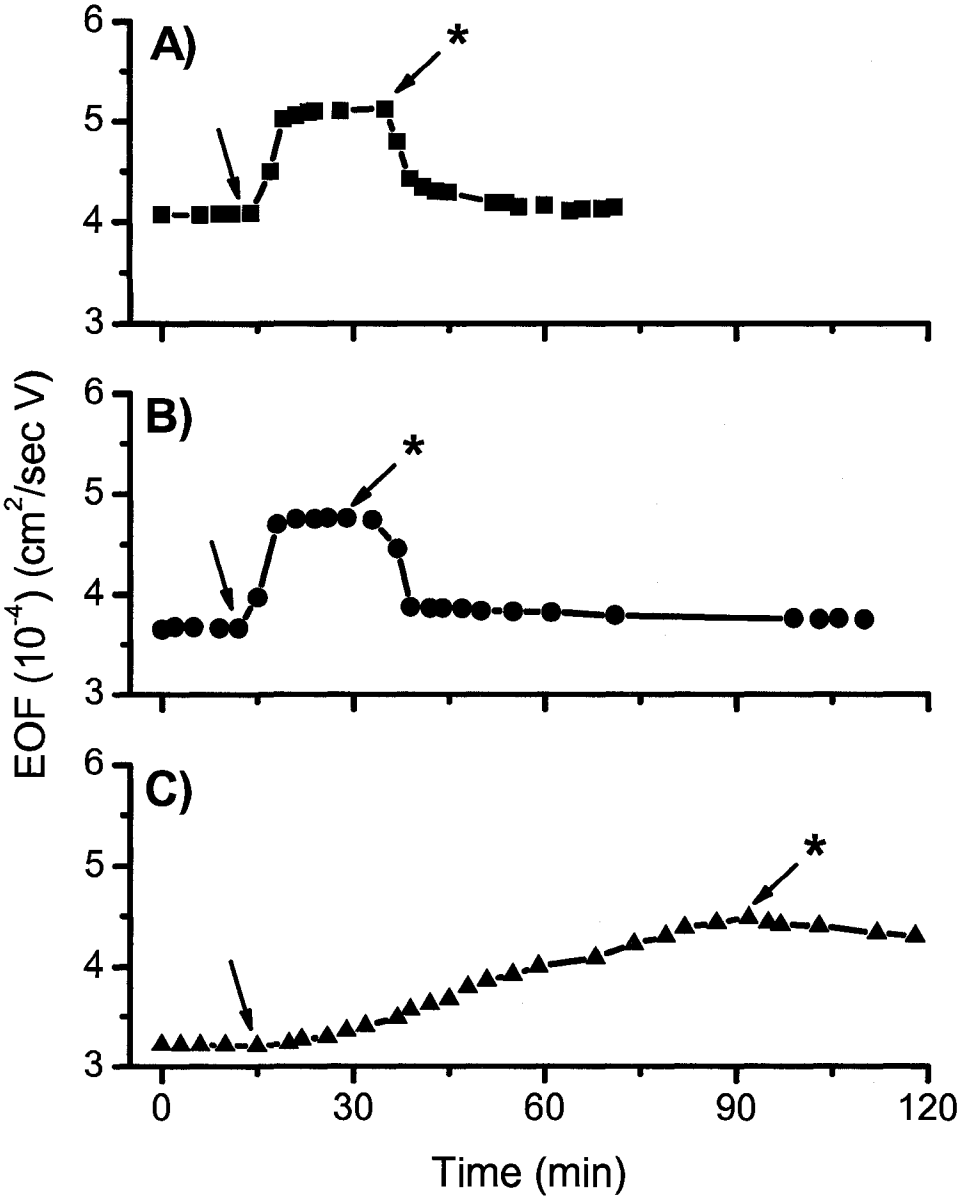

Figure 2.5 Adsorption/desorption experiments with different surfactants. (A) 0.8 mM SDS, (B) 0.5 mM DOCh, (C) 0.006 mM PA. The arrow denotes the point when the surfactant was added and the arrow* denotes the point when the surfactant was removed from the solution reservoirs.
Other conditions: EC of a neutral marker (7 mM glucose), 10 mM borate buffer, pH 9.4, E_{SEP} = 1000 V, T_{INJ} = 5 s, E_{DET} = 0.7 V.

2.3.4 Effect on the separation efficiency and analytical signal. In order to demonstrate the advantages of the use of surfactants on PDMS microchips, the separation of four compounds with biological activity was performed under different conditions. A carbohydrate (glucose), an antibiotic (penicillin), phenol, and a phenolic acid (homovanillic acid) were analyzed in the presence of surfactants and compared to native PDMS. Due to the slower kinetics of PA (requiring a 1 h chip preparation time), SDS and DOCh were selected for the comparison. As can be observed in Fig. 2.7A, longer migration times and wider peaks were obtained when only 10 mM borate (pH 12.0) was used as the background electrolyte as compared to buffers containing surfactants. A significant improvement in the separation can be observed in Fig. 2.7B and C where the modification of the capillary wall was performed with SDS and DOCh, respectively. The analysis time was reduced from 200 s (without surfactants) to 150 s and 125 s when DOCH or SDS was added, respectively. No significant change was observed in the average number of theoretical plates. For example, the separation efficiency for homovanillic acid was 49 800 ± 1000 plates/m (n = 2) when no surfactant was present, 42 400 ± 1350 plates/m (n = 2) when SDS was added, and 55 800 ± 1400 plates/m (n = 2) when DOCh was added. As it was observed in our previous works, [24, 26] the peak current (ip) obtained was significantly larger when SDS was added to the background electrolyte. For example, glucose increased 6%, penicillin increased 27%, phenol increased 64%, and homovanillic acid increased 96% with respect to the analysis performed without surfactants. However, DOCh provided a different behavior,

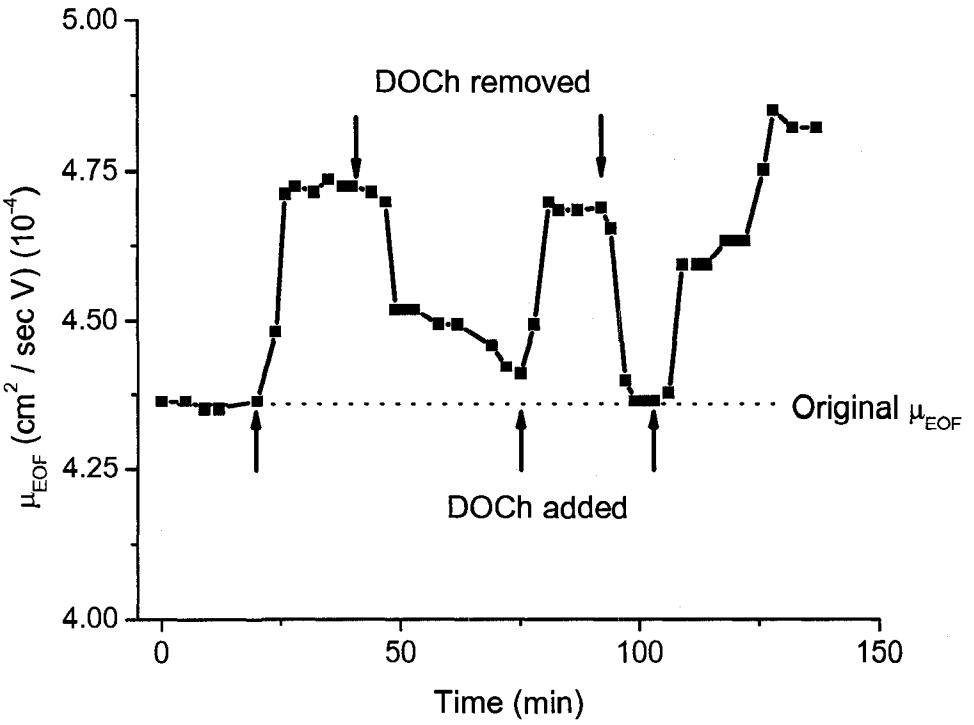

Figure 2.6 Repetitive adsorption/desorption experiments. 1.2 mM DOCh. Conditions: EC of a neutral marker (5 mM glucose), 10 mM borate buffer, pH 9.4; E = 1000 V, T_{INJ} = 5 s.

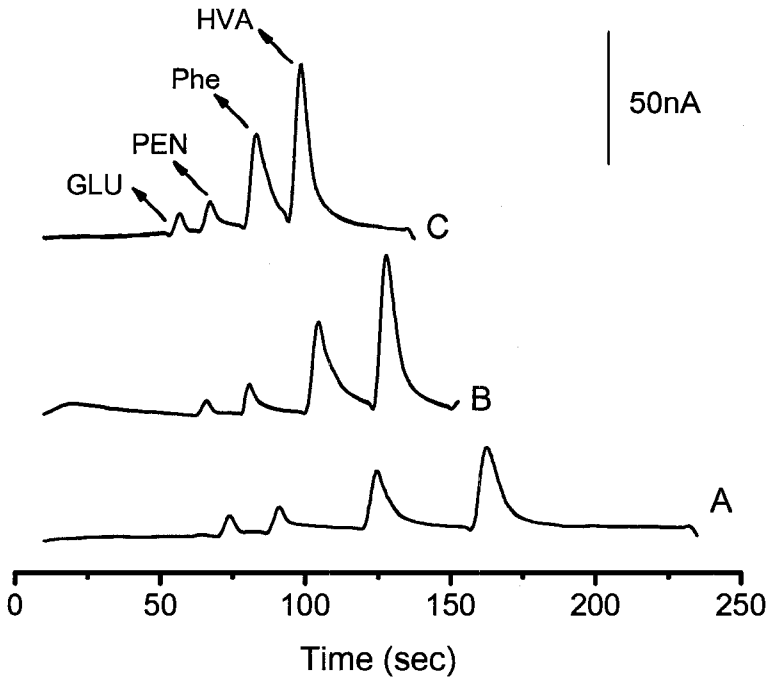

Figure 2.7. Electropherograms showing the effect of the presence of surfactants on the separation of 2 mM glucose, 0.6 mM penicillin, 0.9 mM phenol, and 1 mM homovanillic acid. (A) No surfactant added; (B) 1.3 mM DOCh (C) 1.2 mM SDS. Other conditions: E_{DET} = 0.7 V; 5 mM borate buffer, pH 12.0; E = 1500 V, T_{INJ} = 5 s.

decreasing the i_p for glucose by 50% and increasing the i_p for homovanillic acid by 76% when compared to experiments without surfactants.

2.4 Conclusion

The possibility of using anionic surfactants to increase the EOF and enhance the detection signal was demonstrated for microchip-CE-PAD. Different anionic surfactants were studied showing in all cases spontaneous accumulation at the PDMS surface and a significant increase in the EOF. The fastest adsorption and desorption kinetics were observed with SDS, followed by DOCh and then PA. In all cases, the initial EOF was not achieved after removal of the surfactant, showing a residual amount of surfactant semi-permanently attached to the PDMS. For the cases of SDS and DOCh, the remaining amount was about 9 and 12%, respectively, which is lower than compared to those obtained with Brij 35-SDS mixtures[9] but still significant. The use of surfactants also improved the separation of biologically important compounds like carbohydrates, antibiotics, and phenolic compounds causing a decrease in the separation time by up to 38% for SDS. However, the addition of negatively charged surfactants produced an uneven effect on the electrochemical response. Additional experiments are currently in progress to further exploit this phenomenon towards a wider application of surfactants to the analysis of biomolecules by microchip-CE-PAD.

2.5 References

(1) Wang, J.; Chen, G. *Talanta* **2003**, *60*, 1239-1244.

(2) Hebert, N. E.; Kuhr, W. G.; Brazill, S. A. *ELECTROPHORESIS* **2002**, *23*, 3750-3759.

(3) Lacher, N. A.; de Rooij, N. F.; Verpoorte, E.; Lunte, S. M. *Journal of Chromatography, A* **2003**, *1004*, 225-235.

(4) Doherty, E. A.; Meagher, R. J.; Albarghouthi, M. N.; Barron, A. E. *Electrophoresis* **2003**, *24*, 34-54.

(5) Becker, H.; Locascio, L. *Talanta* **2002**, *56*, 267-287.

(6) Ng, J. M.; Gitlin, I.; Stroock, A. D.; Whitesides, G. M. *Electrophoresis* **2002**, *23*, 3461-3473.

(7) Duffy, D. C.; McDonald, J. C.; Schueller, O. J. A.; Whitesides, G. M. *Analytical Chemistry* **1998**, *70*, 4974-4984.

(8) Ocvirk, G.; Munroe, M.; Tang, T.; Oleschuk, R.; Westra, K.; Harrison, D. J. *Electrophoresis* **2000**, *21*, 107-115.

(9) Badal, M. Y.; Wong, M.; Chiem, N.; Salimi-Moosavi, H.; Harrison, D. J. *J Chromatogr A* **2002**, *947*, 277-286.

(10) Norton, D.; Shamsi, S. A. *Electrophoresis* **2004**, *25*, 586-593.

(11) Duffy, D. C.; McDonald, J. C.; Schueller, O. J. A.; Whitesides, G. M. *Anal. Chem.* **1998**, *70*, 4974-4984.

(12) Tabuchi, M.; Katsuyama, Y.; Nogami, K.; Nagata, H.; Wakuda, K.; Fujimoto, M.; Nagasaki, Y.; Yoshikawa, K.; Kataoka, K.; Baba, Y. *Lab Chip* **2005**, *5*, 199-204.

(13) Liu, Y.; Fanguy, J. C.; Bledsoe, J. M.; Henry, C. S. *Anal. Chem.* **2000**, *72*, 5939-5944.

(14) Bauer, F.; Blum, W.; Dietl, H.; Kotov, S.; Kroha, H.; Manz, A.; Ostapchuk, A.; Richter, R.; Schael, S.; Chouridou, S.; Schaile, D.; Staude, A.; Strohmer, R.; Trefzger, T.; Bouzakis, K.; Krepouri, A.; Paschalias, P.; Petridou, C.; Sampsonidis, D.; Tsiafis, I.; Valderanis, C.; Wotschack, J.; Avramidou, R. M.; Dris, M.; Gazis, E. N.; Katsoufis, E. C.; Maltezos, S.; Stavropoulos, G.; Fassouliotis, D.; Ioannou, P.; Kourkoumelis, C.; Birioukov, V.; Chelkov, G. A.; Dedovitch, D. V.; Evtoukhovitch, P. G.; Gongadze, A. L.; Gostkin, M. I.; Khartchenko, D. V.; Potrap, I. N.; Rogalev, E. V.; Tskhadadze, E. G.; Zhuravlov, V. V.; Diehl, E.; Levin, D.; McKee, S.; Neal, H.; Tarle, G.; Thun, R.; Zhou, B. *Nuclear Instruments & Methods in Physics Research, Section A: Accelerators, Spectrometers, Detectors, and Associated Equipment* **2002**, *478*, 153-157.

(15) Belder, D.; Deege, A.; Maass, M.; Ludwig, M. *Electrophoresis* **2002**, *23*, 2355-2361.

(16) Pittman, J. L.; Henry, C. S.; Gilman, S. D. *Analytical Chemistry* **2003**, *75*, 361-370.

(17) Ocvirk, G.; Munroe, M.; Tang, T.; Oleschuk, R.; Westra, K.; Harrison, D. J. *Electrophoresis* **2000**, *21*, 107-115.

(18) Badal, M. Y.; Wong, M.; Chiem, N.; Salimi-Moosavi, H.; Harrison, D. J. *J. Chromatogr. A* **2002**, *947*, 277-286.

(19) Sakai-Kato, K.; Kato, M.; Toyo'oka, T. *Anal Chem* **2003**, *75*, 388-393.
(20) Kirby, B. J.; Hasselbrink, E. F., Jr. *Electrophoresis* **2004**, *25*, 203-213.
(21) Kirby, B. J.; Hasselbrink, E. F., Jr. *Electrophoresis* **2004**, *25*, 187-202.
(22) Youssouf Badal, M.; Wong, M.; Chiem, N.; Salimi-Moosavi, H.; Harrison, D. J. *Journal of Chromatography, A* **2002**, *947*, 277-286.
(23) Deyl, Z. *J chromatogr A* **2003**, *990*, 153-158.
(24) Garcia, C. D.; Henry, C. S. *Analytica Chimica Acta* **2004**, *508*, 1-9.
(25) Garcia, C. D.; Henry, C. S. *Electroanalysis* **2005**, *17*, 1125-1131.
(26) Garcia, C. D.; Henry, C. S. *Analyst* **2004**, *129*, 579-584.
(27) Wallingford, R. A.; Ewing, A. G. *Analytical Chemistry* **1988**, *60*, 1972-1975.
(28) Wang, J. *Talanta* **2002**, *56*, 223-231.
(29) Garcia, C. D.; Henry, C. S. *Analytical Chemistry* **2003**, *75*, 4778-4783.
(30) Stroop, C. J. M.; Bush, C. A.; Marple, R. L.; LaCourse, W. R. *Analytical Biochemistry* **2002**, *303*, 176-185.
(31) Lin, C.-E.; Chen, M.-J.; Huang, H.-C.; Chen, H.-W. *Journal of Chromatography A* **2001**, *924*, 83-91.
(32) Lee, E. N. *J. Neurochem* **2003**, *84*, 1128-1142.
(33) Matsuoka, K. *Biochim Biophys Acta* **2002**, *1580*, 189-199.
(34) Garcia, C. D.; Liu, Y.; Anderson, P.; Henry, C. S. *Lab Chip* **2004**, *3*, 324-328.

Chapter 3

Plasma Modification of PDMS Microfluidic Devices for Control of Electroosmotic Flow

Polydimethylsiloxane (PDMS) capillary electrophoresis microchips were modified using plasma-enhanced chemical vapor deposition (PECVD), resulting in modified electroosmotic flow (EOF) values. Octafluoropropane (C_3F_8) and acrylic acid (AA) plasmas were chosen as initial test systems for device modification. Argon plasma pretreatments were used to improve adhesion of the fluorocarbon (FC) and AA films. Contact angle measurements and X-ray photoelectron spectroscopy data demonstrated that the Ar/C_3F_8 plasma treatment of PDMS results in the deposition of a hydrophobic, crosslinked FC film, whereas the Ar/AA plasma treatment results in the deposition of a hydrophilic film with ionizable acid groups. The extent of plasma modification within the device channels was explored using scanning Auger microscopy and dye absorption measurements. EOF values were measured for plasma-treated chips as a function of pH, and aging studies were performed to determine the durability of the plasma treatments. Results show that EOF is decreased in Ar/C_3F_8 plasma-treated chips, and varies less with pH than untreated devices. Additionally, EOF measurements are constant for a minimum of 5 days. In contrast, EOF for Ar/AA plasma-treated devices is dependent on pH. EOF measurements of C_3F_8 and AA treated chips without the Ar pretreatment are less stable, particularly in the AA case. In addition to improving adhesion, the Ar plasma treatment results in a decreased hydrophobic dye absorption into the PDMS, which is attributed to the crosslinking of the polymer by the Ar plasma.

This chapter is a reprint of" Plasma Modification of PDMS Microfluidic Devices for Control of Electroosmotic Flow" Ina T. Martin, Brian Dressen, Mark Boggs, Yan Liu, Charles S. Henry, Ellen R. Fisher, Plasma Process. Polym. 2007, 4, 414–424, a manuscript written by Ina T. Martin and Brian M. Dressen. Some preliminary experiments performed by Mr. Mark Boggs and Yan Liu. Plasma deposition performed by Ina Martin and Brian Dressen. All fabrication, EOF, and absorption characterization of microchips shown in this chapter was performed by Brian Dressen. Surface analysis was performed by Ina Martin and Brian Dressen with help from Dr. Patrick R. McCurdy.

3.1 Introduction

Capillary electrophoresis (CE) microchips combine the powerful separation capabilities of CE with the advantages of microdevices such as nL scale reagent and sample consumption and portability.[1, 2] CE microchips have been constructed from both hard materials, including silicon and glass, and soft materials, such as polydimethylsiloxane (PDMS).[3, 4] In comparison to soft materials, silicon and glass device construction is costly, labor intensive, and requires a clean room environment.[3, 4] Consequently, construction of microfluidic devices from soft materials such as PDMS has become increasingly popular.[3-5] In addition to the straightforward fabrication, PDMS is inexpensive, many devices can be constructed from a single molding master, and a variety of detection schemes can be coupled to the separation devices, including laser induced fluorescence, mass spectrometry, and electrochemistry.[1, 3, 4, 6, 7] In spite of these desirable properties, there are unresolved issues with the implementation of PDMS in microfluidic devices. The primary disadvantage of PDMS is that it is an unstable hydrophobic material. The instability of the polymer is due to the presence of low molecular weight oligomers that diffuse to the surface,[8] and the hydrophobicity leads to the adsorption and absorption of hydrophobic analytes and makes the channels difficult to fill with aqueous solutions. Thus, chemical modifications that address these issues are of considerable interest.

In the literature, there are three general approaches for modifying PDMS surface chemistry: dynamic coatings with surfactants, adsorbed polymer coatings, and covalent modification. One of the overarching goals of these studies is to generate reproducible and controllable electroosmotic flow (EOF) in the microfluidic devices,

as this would improve both the range and reproducibility of analyses. This bulk flow is dependent on the surface charge of the polymer; thus, treatments that modify or stabilize the surface charge lead to stable EOF values. In the literature, dynamic coatings have been shown to provide a good EOF stability but require the continuous presence of a surfactant in the mobile phase.[9] Adsorbed polymer coatings also stabilize the EOF and do not require the presence of the polymer in the mobile phase.[10] Both of these techniques have minimal impact on analyte adsorption and absorption. Covalent coatings, including plasma-deposited films have given the best performance with regards to analyte absorption.[5, 7, 11, 12] There are several examples of PDMS modification via polymer grafting and plasma deposition in the literature. Hu et al. have modified PDMS microfluidic devices by UV grafting monomer mixtures [poly(ethylene glycol), poly(ethylene glycol) diacrylate, and acrylic acid (AA)] onto the surfaces. Their crosslinked, mixed monomer grafted PDMS resulted in more hydrophilic surfaces, considerably larger EOF values, and highly efficient separations of biologically relevant peptides.[7] Xiao and coworkers demonstrated the separation of proteins using PDMS microchips modified with grafted polyacrylamide. The multistep deposition process involved surface oxidation of the PDMS channels, the formation of a self-assembled monolayer of benzyl chloride initiators, and atom-transfer radical polymerization.[11] The modified devices were hydrophilic and had considerably greater resistance to protein adsorption when compared to adsorbed or dynamic coatings. In addition, a recent study suggests that plasma-polymerized acrylic acid (p-AA) coatings improve fluid velocity in microchannels.[12] We propose plasma modification of preassembled PDMS microfluidic devices as a

straightforward method to tailor the surface chemistry of chips for a variety of applications in microfluidics and lab-on-a-chip systems. Experimentally, these plasma treatments involve simple, one or two step dry processes, which result in minimal waste. Low pressure plasmas are widely used both to create polymers and to chemically alter the surface properties of polymeric materials.[13-20] Non-depositing plasma treatments can result in both functional group implantation and crosslinking of the polymer. Previous work in our laboratories involved the use of H_2O and CO_2 plasmas to permanently modify various polymeric membranes.[16-18] Alternatively, plasma-enhanced chemical vapor deposition (PECVD) can be used to modify polymers by creating new organic or inorganic materials covalently bound to the original polymer. Plasma-deposited thin films are typically conformal, pinhole free, can provide stable and sterile surfaces, and are able to adhere to a wide variety of substrates.[13] Previous work in our laboratories has demonstrated the efficacy of PECVD in coating diverse sample geometries.[21]

Another advantage of PECVD is the virtually unlimited range of plasma monomers available. As a result, an expansive collection of potential materials can be created via plasma polymerization. The aim of this work is to coat CE microchips with plasma-deposited thin films that result in a different surface charge than the native PDMS, thus allowing us to tailor the EOF which in turn has tremendous utility for separation applications. We chose two plasma-deposited materials to modify CE microchips: plasma-polymerized fluorocarbon (FC) and p-AA. We are interested in the former system as the FC surface should not be ionizable in the buffers typically used for microchip separations, giving rise to low EOF. In contrast, we chose p-AA

because these materials are typically hydrophilic in comparison to FC materials and they also contain carboxylic acid groups. These properties are attractive for microchip modification as the hydrophilic surface could result in decreased protein adsorption compared to bare PDMS, and the carboxylic acid functionalities could lead to improved channel wetting capacity.

Here, we present results for microfluidic devices modified by PECVD. PDMS microdevices were assembled, and then coated with either FC or p-AA films. Effectiveness of the surface modification was determined by X-ray photoelectron spectroscopy (XPS), contact angle measurements and scanning Auger microscopy (SAM). Subsequently, the current monitoring method was used to measure the EOF as a function of the pH of the buffer and the age of the device.[22-24] In general, FC films proved to be more stable, and reduced both the EOF magnitude and pH dependence. AA films were less stable, and gave a greater variation in EOF with pH than native PDMS. Including an Ar plasma treatment before the deposition step reduced the absorption of a hydrophobic fluorescent dye into the PDMS and improved the adhesion of the plasma-deposited thin films.

3.2 Experimental

3.2.1 Fabrication of PDMS Device. PDMS devices were fabricated using a replica molding method reported previously.[25] Briefly, for molding device construction, SU-8 2035 negative photoresist was spin-coated onto a 4 in. silicon wafer that was cleaned and oxidized with piranha solution (2:1 H_2SO_4/H_2O_2), and then baked at 65 °C for 2 min and 95 °C for 5 min to evaporate the solvent. A mask containing the

4.5 cm long and 150 μm wide channel pattern was placed over the coated wafer, and exposed to near-UV light for 5 min. This was followed by a 5 min postbake at 95 °C to crosslink the exposed portions of the film to the wafer. Developing and hard baking of the exposed SU-8 patterns were followed by pouring a degassed mixture of Sylgard 184 (Dow Corning) silicone elastomer and its curing agent (10:1 ratio) onto the mold. After curing (2 h at 65 °C), the PDMS replica was removed from the mold to yield a pattern of negative relief channels and reservoirs in the PDMS. Buffer reservoirs were opened with a 6mm circular punch. The bottom layers (blanks) of the PDMS chips were formed by casting the PDMS mixture on a clean, dry silicon wafer. Irreversible sealing was accomplished by thoroughly rinsing two PDMS replicas with methanol and drying them separately in an oven at 65 °C. The two pieces were then treated with an air plasma (ambient humidity) for 30 s in a Harrick plasma cleaner/sterilizer (PDC-32 G, 13.56 MHz, 1.5-2 Torr, 100 W), and immediately brought into conformal contact. Alternatively, reversible sealing was achieved by rinsing the pieces with MeOH and bringing them into conformal contact, followed by drying at 65 °C for 10 min. Unless otherwise specified, chips were irreversibly sealed. In all the cases, a simple straight channel design was used. The channel was 4.5 cm long, 150 μm wide, and 50 μm deep.

3.2.2 Plasma Treatment of PDMS Samples and Microchips. PDMS, silicon wafers [p-type, (100)], and sealed PDMS CE microchips were treated in our home-built, inductively coupled RF plasma reactor.[26] Microchips were placed in the reactor such that the channels were oriented parallel to the gas flow and the upstream edge of

the microchip was located 8 cm downstream from the RF coil (Figure 3.1). PDMS and Si samples were also oriented parallel to the gas flow and centered 8 cm downstream from the coil. In the Ar plasmas, the plasma glow extended past the substrates. All the samples were removed from the chamber for analysis.

A nickel-plated copper coil was used to couple RF power to the reactor, and was tuned with a Jennings 100 pF variable capacitor. The pressure in the chamber was monitored with an MKS Baratron capacitance manometer which is insensitive to differing gas compositions. All the gases were used without further purification. A liquid nitrogen cold trap was used to prevent fouling of the pump with condensable plasma products. A standard set of conditions was used for the C_3F_8 and AA plasma treatments. These parameters were chosen based on results from previous work in our laboratories.[19, 27] Prior to film deposition, some of the PDMS samples were subjected to a 10 min Ar (General Air, 99.985%) plasma pretreatment wherein gas flow and applied RF power (P) were kept constant at 10 sccm (standard cubic centimeters per minute, pressure ≈300 mTorr) and 30 W, respectively. After this pretreatment, the reactor was evacuated, and the film deposition step was performed immediately. For C_3F_8 (Air Products, 99%), gas flow was kept constant at 10 sccm (pressure ≈220 mTorr), and P = 50 W. The substrate was placed 8 cm downstream from the glow and the deposition time was 4 min, resulting in a film thickness of ≈35 nm when deposited directly on Si.[19] AA (Aldrich, 99%), a liquid monomer, was subjected to multiple freeze-pump-thaw cycles to remove dissolved gases prior to use. Control of AA vapor entry into the

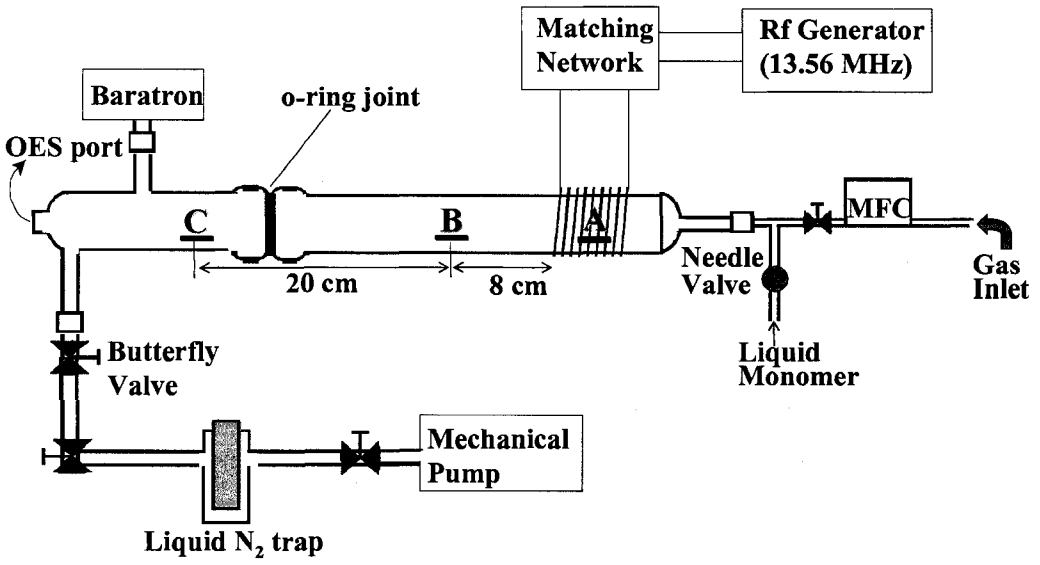

Figure 3.1 Schematic diagram of the inductively coupled plasma reactor used for thin film deposition.

reactor was achieved via a Nupro bellows-sealed valve, resulting in a pressure of approximately 150 mTorr. These depositions employed a pulsed plasma, with a 16% duty cycle (d.c.), a 10 ms on-time, and an applied peak power of 150 W. Duty cycle is defined as the ratio of pulse on time to the total cycle time. The substrate was placed 8 cm downstream of the RF coil, and a 5 min deposition time was used for all the AA treatments.

3.2.3 Surface Analysis of Plasma-Treated PDMS. Static water contact angles were measured with a contact angle goniometer (Krüss DSA 10). Water drop profiles were fit using the tangent method. Reported contact angles for each experimental condition are the mean and standard deviation of three to five measurements on two to three samples.

XPS analyses were performed on a Physical Electronics PE5800 ESCA/AES system. Spectra were collected using a monochromatic AlK_α X-ray source (1 486.6 eV), hemispherical analyzer, and multichannel detector. A photoelectron take-off angle of 45° was used for all the spectra. A low energy (≈1 eV) electron neutralizer was used for charge neutralization. Survey spectra were collected with a pass energy of 93.90 eV, and high resolution spectra were acquired at an analyzer pass energy of 23.50 eV. Percent compositions were calculated from high resolution spectra, and values reported are the mean and standard deviation of three to four measurements from one to two samples. Curve fitting of the high resolution spectra of plasma-deposited materials on PDMS was performed using Gaussian functions with the FWHM (full width at half maximum) ≤2 eV, unless otherwise specified. Binding

energy scales were referenced to the C_{1s} peak at 284.8 eV.[28, 29] These fitting parameters are typical for plasma polymers.[30]

SAM was carried out using the PE 5800 with the analyzer in the fixed retarding ratio mode. The Auger images were obtained using an accelerating potential of 10 kV. The electron beam had a current of 10 nA, operating in a vacuum better than 10^{-9} Torr. Images shown here are 32 × 32 pixels.

3.2.4 Dye Absorption. Dye absorption experiments were performed using an inverted fluorescence microscope (Nikon Eclipse TE2000-4) with a Photometrics Cool Snap cf camera to image and measure the intensity of fluorescence from a buffer (10×10^{-3} M borate, pH 10) containing rhodamine 6G fluorescent dye (Lambda Physik, Ft. Lauderdale, FL). The channel was filled with the rhodamine solution and images were collected at regular time intervals. The extent of the dye absorption into the PDMS channel walls was monitored by the change in the width of fluorescence signal across the channel with time. All the experiments were carried out in a darkened room and UV illumination was blocked during incubation to prevent photobleaching.

3.2.5 EOF Measurments. EOF was measured using the current monitoring method, as reported previously.[22-24] The running buffer for electrophoresis experiments was pH 4-9 phosphate buffer. All the buffers were prepared in deionized water, passed through a 0.20 μm pore size syringe filter (Whatman) and degassed for 5 min in a sonicator (Fisher Scientific, FS 20) before use. Electrical connections to the

microfluidic devices were made with Pt electrodes placed into reservoirs at the ends of each channel. The current monitoring experiments were performed by measuring the voltage drop across a 1 kΩ resistor (0.5 W, RadioShack) using a voltmeter (RadioShack) and the high voltage power supply (Spellman CZE1000R). For a typical current monitoring measurement, the first reservoir and the channel were filled with 20×10^{-3} M buffer and the second reservoir was filled with 18×10^{-3} M buffer. When the voltage (900 V) was applied and electroosmosis occurred, the lower concentration buffer from the second reservoir gradually displaced the higher concentration buffer in the channel, resulting in an increase in the electrical resistance of the channel. The change in current under a constant applied voltage difference was monitored using a 1 kΩ resistor in series between the cathode and ground. After a constant voltage was obtained, the potential was applied to the reservoir with concentrated buffer and the above procedure repeated. The time required to reach a current plateau was used to calculate EOF based on Equation 3.1, where L is the length of the separation channel (4.5 cm), V is the total applied voltage (900 V), and t is the time in seconds required to reach the new current plateau.

$$\mu_{EOF} = L^2 / V \cdot t \qquad \textbf{Equation 3.1}$$

3.3 Results and Discussion

3.3.1 Plasma-Deposited Materials' Analyses. Table 1 lists the static water contact angles measured on untreated and treated PDMS. Air plasma treatments were performed in the commercial cleaner; all the other plasma treatments were performed in our inductively coupled RF plasma reactor. The air plasma treatment used to seal the PDMS chips initially results in a 30° contact angle, with some hydrophobic recovery within 60 min. After 3 h, contact angles increase to 108°. This broad range of values is the result of the marginal parameter control available in the plasma cleaner; the increase in contact angle arises from the well-known hydrophobic recovery that PDMS exhibits after plasma oxidation.[3] The extent of modification via the sealing process does not affect the surface properties of the deposited films.

To better adhere our plasma-deposited material to the PDMS, we included an Ar plasma pretreatment step before the deposition.[18] The following material analysis results pertain to samples subjected to both an air plasma treatment and an Ar plasma pretreatment before the film deposition step. The contact angle of the FC film deposited from the C_3F_8 plasma on PDMS is 115 ± 5°. This measurement is within the combined experimental error of that of the material deposited on Si wafers using the same deposition parameters (110 ± 2°).[19] The average contact angle measured for the p-AA sample is 65 ± 9°, lower than that of p-AA deposited on Si using the same

Table 1. Contact angles and elemental analysis of plasma-treated PDMS. (Values in parentheses for selected measurements represent the standard deviation of the mean of several measurements).

Plasma source[a)]	Buffer[b)]	Contact angle	C	O	Si	F	N	F/C
			%					
None	None	113 (3)	47.6 (0.3)	27.3 (0.1)	25.2 (0.4)	0	0	-
Air	None	30-60	20.1 (1.2)	51.8 (0.9)	28.2 (0.3)	0	0	-
Ar	None	30-60	13.1 (0.5)	53.9 (0.8)	31.1 (0.9)	0	1.9 (1.0)	-
Ar/C_3F_8	None	115 (5)	41.7 (0.5)	2.5 (0.8)	1.3 (0.6)	53.0 (1.4)	1.6 (0.2)	1.27 (0.04)
Ar/C_3F_8	1×	-	45.7 (0.2)	7.4 (0.4)	4.0 (0.1)	41.1 (0.1)	1.9 (0.1)	0.90 (0.00)
Ar/C_3F_8	4×	-	46.8 (0.7)	23.0 (2.8)	14.9 (1.4)	12.4 (4.1)	2.9 (0.4)	0.26 (0.08)
Ar/AA	None	65 (9)	65.3 (0.7)	25.9 (2.5)	8.8 (1.9)	0	0	-
Ar/AA	1×	-	48.3 (8.3)	31.7 (4.8)	18.0 (3.3)	0	2.0 (0.5)	-

[a)] Plasma parameters are detailed in Experimental Part;
[b)] The value in this column indicates if and how often the sample was exposed to buffer before the measurement was taken. 1× denotes the sample was soaked once in buffer for 30 min; 4× denotes the sample was soaked in buffer four times, in 30 min increments.

deposition parameters (85 ± 2°).[19] The p-AA sample is much more hydrophilic than both the untreated and FC plasma-treated PDMS. The FC film appeared smooth and featureless to the naked eye, whereas the AA film appeared to have small cracks on the surface.

The elemental surface composition of plasma-treated PDMS was quantified via XPS, Table 1. The experimentally measured composition of PDMS (47.6% C, 27.3% O, 25.2% Si) is in good agreement with the stoichiometric composition of the polymer (50% C, 25% O, 25% Si). The air plasma treatment leads to a significant increase in oxygen content (51.8%) and a concomitant decrease in C (20.1%); these values do not change significantly 5 days after treatment. Compositionally, Ar plasma-treated PDMS that is exposed to atmosphere resembles air plasma-treated PDMS: a standard Ar treatment results in an increase in O content to 53.9%, a decrease in C content to 13.1%, and a slight increase in Si content to 31.1%. Additionally, a small amount of N (1.9%) is incorporated into the PDMS. The incorporation of both the N and additional O are attributed to postdeposition atmospheric reactions. Thus, the Ar plasma successfully creates active sites on the PDMS surface, as expected, which improve the adhesion of the plasma-deposited films. Note that the elemental compositions of air and Ar plasma-treated PDMS correspond well to the literature results that demonstrate that the non-depositing plasma treatment of PDMS leads to the formation of a thin silica-like layer on the polymer surface.[17, 31]

The elemental composition of the FC film deposited from the C_3F_8 plasma is primarily F and C, Table 1, consistent with our prior film deposition work.[19] The

trace N (1.6%) is likely from a small amount of air in the reactor for this particular deposition, as neither the PDMS substrate nor the FC monomer contains N. Si, however, is present exclusively in the PDMS, which makes Si content a good gauge of substrate coverage. The trace Si (1.3%) present in the FC film indicates a good initial coverage of the underlying PDMS (Table 1).

High resolution XPS spectra yield information on the bonding environments of the deposited films. Figure 3.2(a) shows the high resolution C_{1s} spectrum of untreated PDMS. It was fit with one peak (FWHM = 1.5 eV), representing the single molecular environment of C in the polymer (C—H, 284.8 eV).[17] Figure 3.2(b) is the high resolution C_{1s} spectrum of an FC film deposited on Si using a C_3F_8 plasma with the same deposition parameters discussed earlier; this C envelope is considerably more complex, and has been decomposed into four chemical environments: CF_3 (294.0 eV), CF_2 (292.1 eV), CF (290.0 eV), and $\underline{C}$-CF_x (287.3 eV). The spectrum for the C_3F_8 plasma-treated PDMS, Figure 3.2(c), is decomposed into five chemical environments, the first four correspond to those seen in Figure 3.2(b), and the fifth is the C-C/C-H (284.8 eV) peak, which could also include a contribution from C-Si bonds. The underlying PDMS is most likely the main contributor to the C-C/C-H peak, as it is not present in the spectrum of the FC film on Si [Figure 3.2(b)]. Note that the assignment for CF includes contributions from both CF-C and CF-CF_x, making the FWHM (2.16 eV) slightly greater than those of the other peaks.

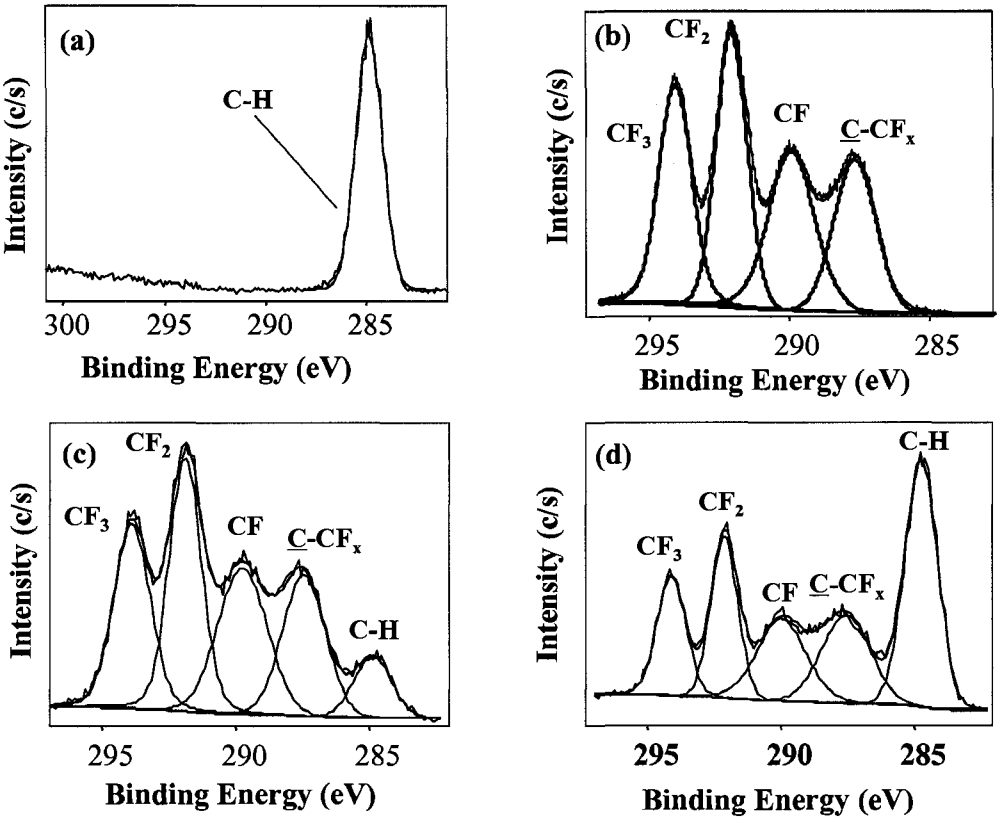

Figure 3.2. High resolution XPS C1s spectra of (a) untreated PDMS, (b) p-C_3F_8 on Si, (c) p-C_3F_8 on PDMS, and (d) p-C_3F_8 on PDMS after an exposure to buffer for 30 min.

During a typical set of EOF measurements, the plasma-treated microfluidic device is exposed to the buffer for approximately 30 min. To determine the effect buffer exposure has on film composition, a sample of C_3F_8 plasma-treated PDMS was soaked in the buffer, and XPS analysis was then performed. The Table 1 values indicate an increase in both O and Si content, to 7.4 and 4.0%, respectively, and a decrease in F content to 41.1% after an exposure to the buffer. After repeated exposures to the buffer, the O and Si components are even greater, 23.0 and 14.9%, respectively, and the F is decreased to 12.4%. The high resolution C_{1s} spectrum of FC plasma-treated PDMS after a 30 min exposure to the buffer [Figure 3.2(d)], shows both a significant reduction in the intensity of the CF_x peaks attributed to the FC film, and an increase in the intensity of the PDMS substrate peak located at 284.8 eV. This, combined with the increase in Si and O content, is attributed to an increase in these signals from the underlying PDMS substrate, which suggests either removal of the FC film in the buffer or rearrangement of the PDMS over the FC film due to the diffusion of uncrosslinked oligomers to the solid-air interface.[8] Previous experiments involving cell-culturing on the FC materials demonstrated that the materials were stable during the exposure to aqueous solutions (10% FBS/media); thus, the former explanation is the more likely one.[27] This is supported by a series of extraction experiments that demonstrated that oligomers did contribute to the rearrangement of the PDMS surface after air plasma treatments using the Harrick PDC-32 G.[32] Future plasma modifications will include this extraction step prior to the plasma treatment to minimize the contribution of unreacted oligomers to PDMS surface rearrangement. Initially, the elemental composition of our p-AA film is primarily O and C, Table 1,

Figure 3.3(a). The Si content is 8.8%, slightly higher than that measured for the FC film. After exposure to the buffer, the Si increases to 18.0%, this suggests that the p-AA film is less robust than the FC material. The fitting used for the high resolution C_{1s} spectra of our p-AA films, Figure 3.3(b), uses five peaks and closely matches that found in the literature.[33] The most significant deviation from p-AA spectra in the literature is that the FWHM of the C—C/C—H peak (2.58 eV) is wider than that typically found in this type of plasma polymer. We attribute this to contributions from C—C/C—H in the film, and C—H in the underlying PDMS substrate: variations in the molecular environments of identical groups contribute to broader FWHMs.[30] The most interesting feature in the high resolution spectrum of p-AA is the COOH/R peak at 289.88 eV, as this is the ionizable functionality of interest in electrophoresis applications. The contribution of this moiety to the total area is 6% which indicates extensive crosslinking of the p-AA film.[33] Films deposited under less energetic conditions that result in a higher retention of the AA monomer are typically water soluble, and are therefore not useful for our applications.

3.3.2 Chip Coatings. The surface analysis data presented above pertain to pieces of PDMS treated with different plasmas. The microfluidic devices were irreversibly sealed before plasma treatment, so a series of experiments was carried out to determine the extent of plasma modification within the reservoirs and channels. For the plasma to treat the interior of the device, the gas phase species must enter the channel via the reservoirs,

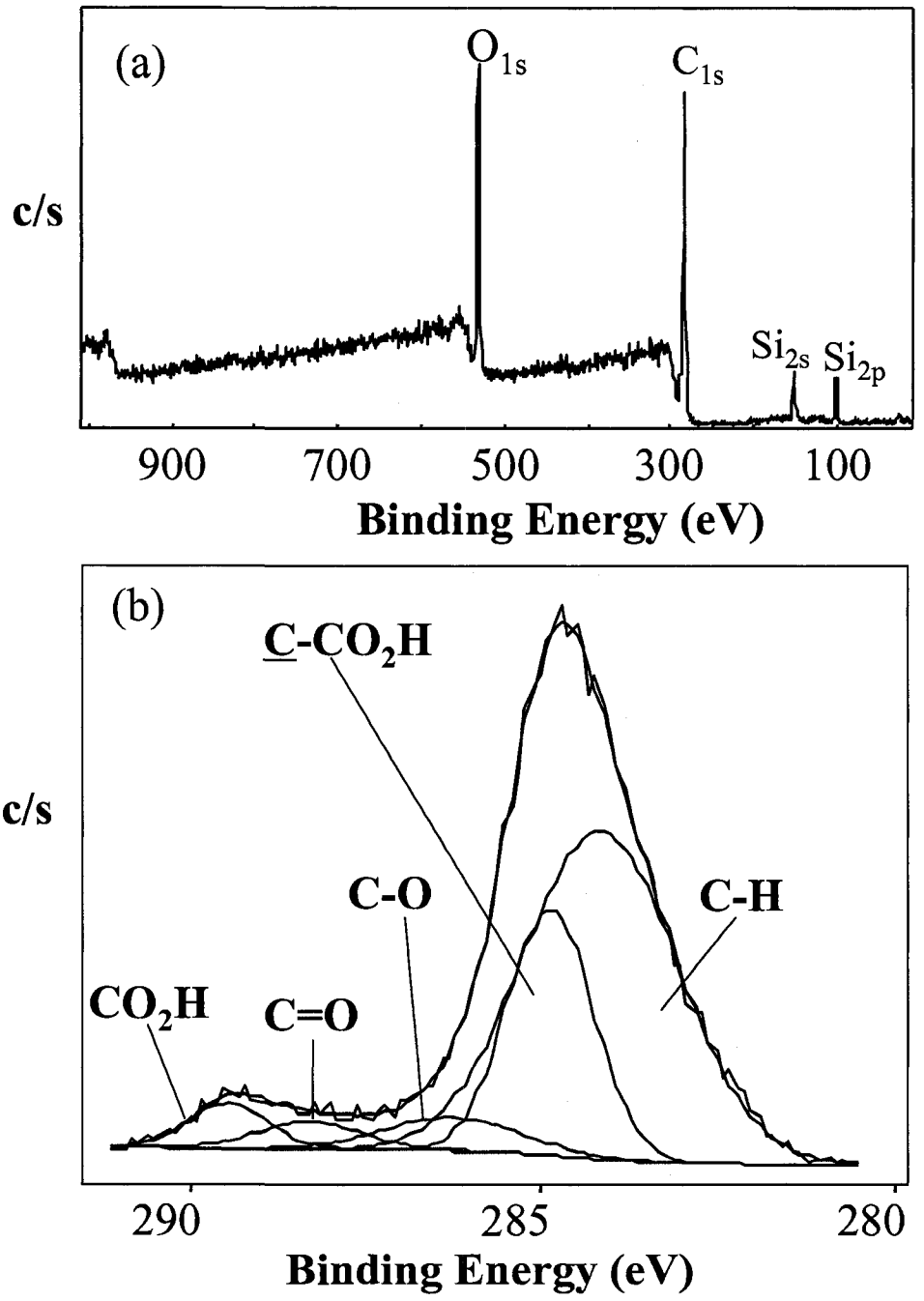

Figure 3.3 (a) Survey and (b) high resolution XPS C_{1s} spectra of PDMS coated with p-AA.

or through the porous PDMS. To ascertain the extent of coverage in the channel, we performed SAM imaging of the blank of a microfluidic device. For this particular experiment, we used a Si wafer as the blank instead of PDMS to improve our imaging capabilities. The Si blank was reversibly sealed to the PDMS replica and treated with a C_3F_8 plasma. The blank was then removed and imaged using SAM; Figure 3.4 shows the F_{KLL} maps taken of the Si. F is apparent in both the reservoirs and the channel, but not outside the channel area. As the Si blank does not contain F prior to the treatment, the F_{1s} signal should exclusively appear on the area treated by the FC plasma. The presence of F in restricted areas confirms that the plasma enters the channels through the reservoirs and not through the porous PDMS. Figure 3.4(a) is the F_{KLL} map of the reservoir located closest to the RF coil in the reactor during the deposition. Clearly there is a good coverage of the underlying Si, and the F is limited to the channel and reservoir areas that were exposed to the plasma. Figure 3.4(b) is the map of the channel further downstream; full coverage of the Si is still apparent. Farther downstream, Figure 3.4(c), the F_{1s} signal becomes less intense, and there are small areas without any signal. This is also true at the reservoir located downstream from the plasma source [Figure 3.4(d)]. The areas where F is not detected suggest incomplete coverage of the channel.

Another method of determining the extent that the plasmas treat the channels in sealed devices is via dye absorption measurements, as described in the Dye Absorption section. A solution of rhodamine dye was introduced into untreated and treated chips, and the width of the fluorescence across the channel with the dye removed, was measured as a function of time (Figure 3.5). An increase in apparent

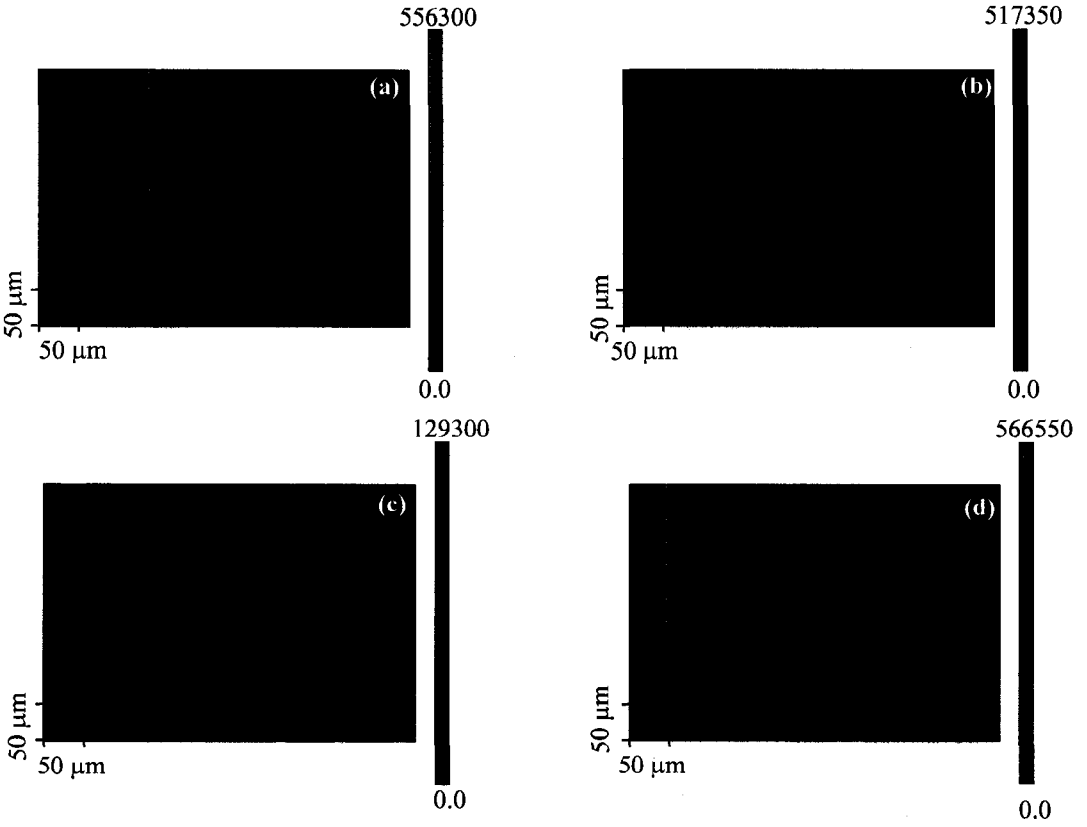

Figure 3.4 SAM maps of FKLL signal of the Si base of a PDMS icrochip; (a) shows the upstream reservoir and beginning of the channel; (b) and (c) are images of the channel farther downstream (≈500 mm and ≈3.0 cm, respectively); and (d) is the downstream reservoir and channel.

channel width indicates the absorption of the rhodamine dye into the PDMS, a generally undesirable result. The kinetics of dye absorption for the untreated chip were sufficiently rapid, hence, we could not obtain fluorescent images of the channel without some degree of rhodamine absorption into the channel walls. Initially, there was a rapid increase in the width (from 100 to 127 pixels) of the fluorescence, which was followed by a plateau wherein the width no longer increased. Given that the channels are 150 μm wide, each pixel corresponds to 1-1.5 μm. After 60 minutes, the extent of absorption remained constant, Figure 3.5. The error calculated for the untreated chip was 3%; we estimate it to be similar for the plasma-treated devices. Note that the increase in channel width observed in these fluorescence measurements could be the result of inadequate sealing between the top and bottom layers of PDMS. We do not, however, believe this to be the mechanism for dye spreading as the different devices exhibit different behaviors with respect to the spreading of the dye. Moreover, the results presented in Figure 3.5 represent measurements made on multiple ($\geq$3) different chips. Also note that similar data were acquired along the entire length of the channel, and exhibited no significant differences at different positions along the channel, which may be expected if imperfect sealing had occurred.

Fluorescence width measurements for a sealed chip treated only with an Ar plasma show a drastic decrease in the absorption of dye into the channel, Figure 3.5. The fluorescence width increases only slightly over time; this ability to inhibit dye absorption lasts for a minimum of 5 days after Ar plasma treatment. Fluorescence measurements for devices coated with FC and p-AA films that included an Ar plasma

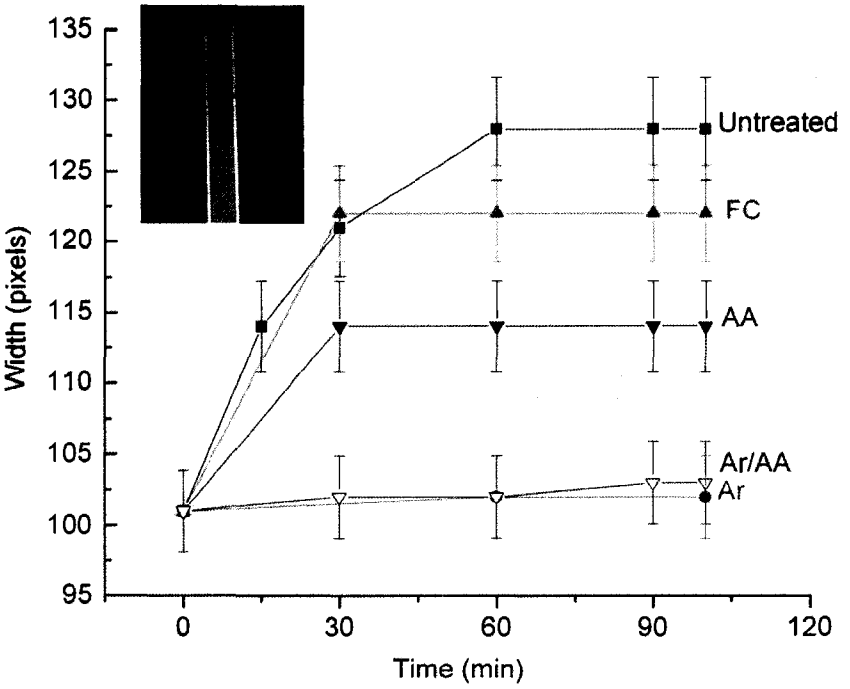

Figure 3.5 The width of the fluorescent signal of rhodamine containing buffer across the channel as a function of time for unmodified and Ar, Ar/AA, AA, and C_3F_8 plasma-treated devices. The inset shows a photograph of the dye-filled channel taken with a microscope.

pretreatment were within the error limit of the results for devices treated only with an Ar plasma. Samples coated with p-AA contain small cracks on the surface. These cracks are the only parts of the channel that fluoresce after the rhodamine solution is rinsed out, indicating that the dye absorbed into the PDMS through the cracks but did not absorb into the surface of the AA film. Fluorescence measurements were also obtained for chips treated with either AA or FC plasmas, without the Ar plasma pretreatment. The AA treatment alone has some capacity to lower the dye absorption, whereas results for the FC film resemble the untreated device, Figure 3.5. These data demonstrate that the Ar plasma pretreatment step is the critical factor for inhibiting dye absorption.

XPS data show that an Ar plasma treatment followed by exposure to atmosphere changes the surface elemental composition of PDMS by decreasing C and increasing O content, Table 1. This is consistent with the literature results for Ar plasma-treated PDMS membranes.[20] Plasma treatments based on inert gases such as Ar typically result in the formation of free radicals on the surface that recombine to crosslink the surface, and react with O_2 and N_2 after exposure to the atmosphere.[20] SEM (scanning electron microscopy) images of Ar plasma-treated PDMS (not shown) reveal surface damage (pitting, cracking) that is typical of a crosslinked polymer. Crosslinking of the PDMS surface makes it less porous, thereby limiting dye absorption. As this is a physical effect, Ar plasma treatment followed by a film deposition step also inhibits dye absorption, even when the deposited material is hydrophobic, such as the FC film. The ability of the Ar plasma-treated samples to minimize the absorption of a hydrophobic dye is promising in that it may also inhibit the absorption of other

hydrophobic analytes, such as proteins, which would allow for their separation and detection in PDMS microchips. Further work is underway to characterize the effect of coatings on separations of proteins and peptides.

In summary, the SAM images suggest that the FC coating within the channel may be incomplete; however, all of the dye absorption data show conformal treatment throughout the length of the channel. If the plasma treatment did not extend throughout the channel, there would be a broadening of the fluorescent signal where the dye solution was in direct contact with unmodified PDMS. The inhibition of dye absorption throughout the chip suggests that we are able to treat the entire length of a sealed channel; however, we may not be able to image the channel with high enough resolution to verify this hypothesis completely. Note that previous work in our laboratory has shown a complete treatment of microporous and ultrafiltration membranes (≈300 μm thick) using a variety of plasma treatments.[14, 15, 21, 34, 35] Thus, it is reasonable to suggest that the plasma treatment extends throughout these device channels.

3.3.3 EOF Measurements. The generation of EOF in a capillary depends on the net charge density on the surface of the capillary that is in contact with the aqueous solution. This gives rise to an electrical double layer, which results in the generation of EOF in the presence of an electrical field.[36] The potential at the liquid-surface interface is known as the zeta potential, ζ, and changes affecting the zeta potential will have an effect on the EOF. For example, in PDMS chips, higher pH creates an increase in the zeta potential and therefore the EOF.[9, 10] The ability to generate reproducible and controllable EOF would improve the reproducibility of analyses.

EOF of plasma-treated samples was measured as a function of pH, over a 5 day period. EOF measurements of Ar plasma-treated chips were within the error limit of untreated devices up to 48 h after the treatment. Figure 3.6 contains the EOF values measured in the Ar/C_3F_8 plasma-treated PDMS. EOF is the lowest for a newly coated chip; on Day 1, there is 30% reduction in EOF at all the pH values. On Day 2 and beyond, EOF values are 10% lower than untreated channels for pH 5 and 7, and 21% lower at pH 9. The variation in the EOF for untreated devices is 32.3% between pH 5 and 9. The change in EOF in treated devices, however, is less than that observed in the uncoated channel: the variation between pH 5 and 9 is 23% on Day 1, but decreases to less than 17% after this. The aged chip had a 7.4% variance in EOF for this pH range. Note that the EOF measured on an aged Ar/C_3F_8 treated chip is within the error limit of devices used multiple times, which suggests that some stabilization of the surface occurs within the first 24 h of treatment. Additionally, twelve consecutive runs of the chip yielded a constant EOF, indicating that the coating is quite robust. EOF values for a microchip treated only with a C_3F_8 plasma have greater daily fluctuations, and are $\approx$13% higher than those measured in the Ar/C_3F_8 plasma-treated device, Figure 3.6. This shows that the Ar plasma pretreatment increases the stability of the FC coating.

Overall, these data show that the Ar/FC treatment leads to a decrease in EOF, and an increase in the stability of the EOF with respect to pH. In comparison to previous work involving dynamic coatings, the Ar/FC plasma treatment is on par with anionic

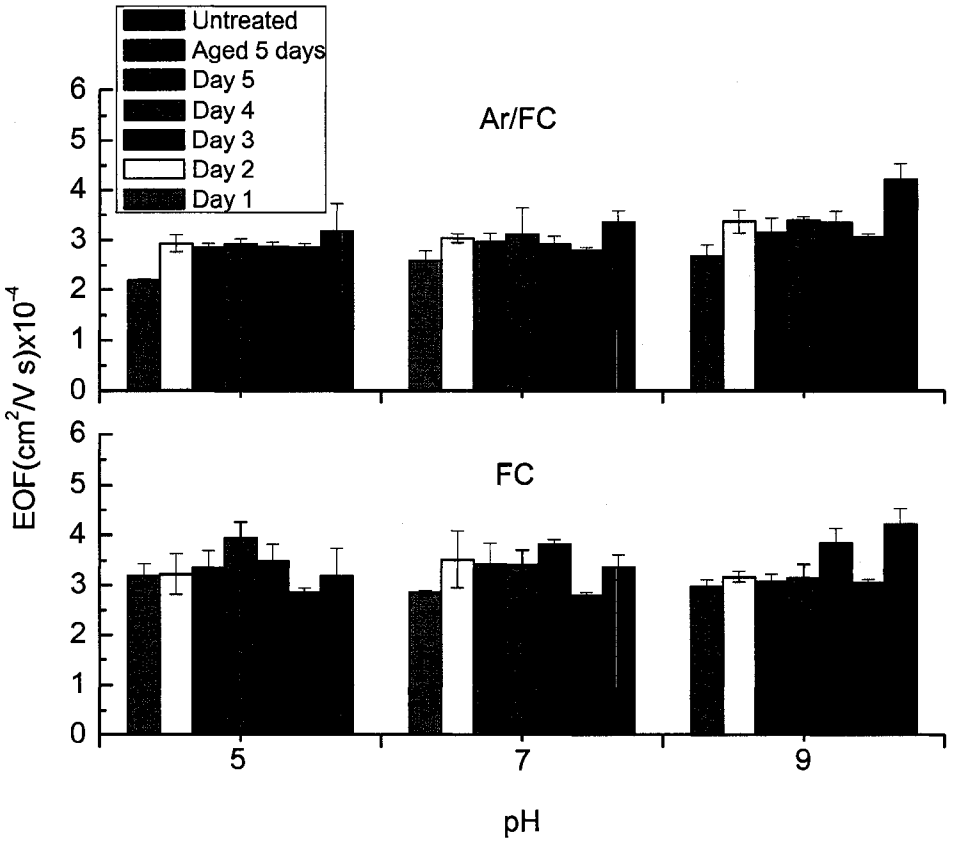

Figure 3.6 EOF values for C_3F_8 plasma-treated microchips as a function of pH and age of the sample. The EOF of an unmodified device is shown for comparison.

polybrene (PB-) coated devices (variation of 17.7% between pH 5 and 10), but less effective than the cationic polybrene/dextran sulfate (PB/DS) coated devices (1.6% between pH 6 and 10).[23] The reduction in EOF seen in FC plasma-treated microchips indicates that the treatment reduces the zeta potential across the pH range tested. The source of EOF in both native and oxidized PDMS is a subject of interest in the literature.[37] For plasma oxidized PDMS, silanol groups are suggested as the source of the charge for EOF.[38] The change in EOF with pH is well characterized with higher pH buffer resulting in higher EOF. The FC coating should not have any SiO_x ionizable groups. Although the EOF is reduced with FC coatings, it is still supported, which could be caused by an incomplete coverage of the surface. Alternatively, the underlying negative charges from the PDMS may be exerting their influence on the solution through the thin film. This behavior has been seen before for polyelectrolyte coatings on fused-silica capillaries.[39] The stability of the EOF with changing pH suggests that the coating is complete enough to control the surface charge along the channel. Greater EOF stability with changing pH is a benefit to analysis, as changes in migration time with pH would not occur. The exact mechanism involved in the generation of the zeta potential is not known presently but is under investigation in our laboratories.

Figure 3.7 shows the EOF for Ar/AA treated chips at different pHs. This treatment produces a 17% increase in EOF compared to untreated PDMS at pH 9. At pH 7, the EOF remains unchanged (0.003%) and there is a reduction in EOF at both pH 4 (37%) and pH 5 (31%). The largest decrease in EOF occurs at pH 4, the value where the buffer pH is lower than the pK_a of AA ($pK_a = 4.25$[40]). Both this result and

the pH dependence of the EOF suggest some retention of the acid functionality in the p-AA film, consistent with XPS results [Figure 3.3(b)]. When a weak acid is at a pH below its pK_a, most of the sites are protonated, which reduces the negative surface charge, resulting in a low EOF. At pH 5 only partial deprotonation occurs and the surface charge will be dominated by the neutral acrylic acid, resulting in a lower EOF than untreated. The EOF at pH 7 is almost identical to that of an untreated chip, which may be due to equivalent charged sites being created both from deprotonation of the acid and charging of silanol groups within the PDMS. An increased EOF at pH 9 may be due to the large number of deprotonated sites of the AA and the charging of silanol groups in the PDMS, resulting in a higher EOF than the native PDMS. The variability of the EOF across the pH range may provide the possibility for tuned EOF.

The durability of the AA coating appears to be inferior to the FC coating and required the use of an Ar pretreatment to obtain a usable stability (Figure 3.7). After 3 d, for Ar/AA treated devices, EOF values return to that of an untreated chip, indicating the loss of coating or continued migration of unreacted PDMS oligomers, as discussed above. This agrees with the XPS data (Table 1) that reveal a substantial loss of film after exposure to the buffer. However, loss of EOF control occurs regardless of the use of the chip: EOF measured for the first time on a device 5 d after plasma treatment had a similar EOF to an untreated device, which demonstrates a lack of film stability in the air. EOF values were also measured for chips treated with an AA plasma, without the Ar plasma pretreatment, Figure 3.7. These values have the greatest variance over the pH range studied in this work. The same general trend for

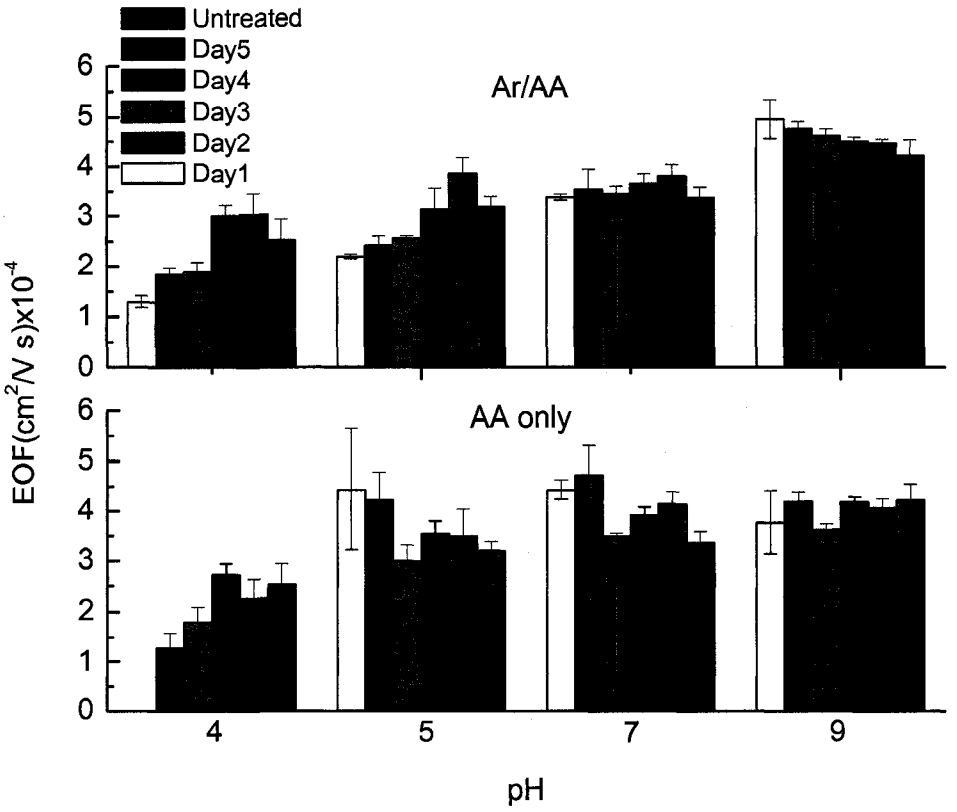

Figure 3.7 EOF values for AA plasma-treated microchips as a function of pH and age of the sample. The EOF of an unmodified device is shown for comparison.

EOF versus pH was seen as for the Ar/AA coating, but with more significant daily changes. Note that the addition of the Ar pretreatment resulted in only 3 d of stability; further efforts are being directed toward developing a more stable AA coating.

3.4 Conclusion

We have demonstrated that PECVD can be used to treat preassembled polymer microfluidic devices, resulting in modified EOF. An Ar plasma pretreatment was used to increase the stability of both the FC and p-AA coatings. The Ar plasma treatment was also found to be important for reducing dye absorption. Experiments currently underway in our laboratories are exploring separations within these systems, alternate coatings, and non-depositing plasmas as a way to control the surface properties of the PDMS.

3.5 Acknowledgements

Financial support for this work was provided by the *National Science Foundation (ERF; NSF-0137664)* and *Colorado State University (CSH).*

3.6 References

(1) Wang, M.; Cui, D. F.; Wang, L.; Chen, X.; Zhao, Q. *International Journal of Nonlinear Sciences and Numerical Simulation* **2002**, *3*, 207-210.
(2) Ding, Y. S.; Garcia, C. D. *Electroanalysis* **2006**, *18*, 2202-2209.
(3) Duffy, D. C.; McDonald, J. C.; Schueller, O. J. A.; Whitesides, G. M. *Analytical Chemistry* **1998**, *70*, 4974-4984.
(4) Quake, S. R.; Scherer, A. *Science* **2000**, *290*, 1536-1540.
(5) Berdichevsky, Y.; Khandurina, J.; Guttman, A.; Lo, Y. H. *Sensors and Actuators B-Chemical* **2004**, *97*, 402-408.
(6) Martin, R. S.; Gawron, A. J.; Lunte, S. M. *Anal Chem* **2000**, *72*, 3196-3202.
(7) Hu, S. W.; Ren, X. Q.; Bachman, M.; Sims, C. E.; Li, G. P.; Allbritton, N. *Electrophoresis* **2003**, *24*, 3679-3688.
(8) Fritz, J. L.; Owen, M. J. *Journal of Adhesion* **1995**, *54*, 33-45.
(9) Harrison, D. J. *Electrophoresis* **2000**, 107-115.
(10) Henry, C. S.; Liu, Y.; Bledsoe, J. M.; Hopkins, C. D. *Abstracts of Papers - American Chemical Society* **2001**, *221st*, ANYL-212.
(11) Xiao, D. Q.; Van Le, T.; Wirth, M. J. *Analytical Chemistry* **2004**, *76*, 2055-2061.
(12) Dhayal, M.; Jeong, H. G.; Choi, J. S. *Applied Surface Science* **2005**, *252*, 1710-1715.
(13) d'Agostino, R. *Academic Press, Inc., San Diego* **1990**, 95-143.
(14) Steen, M. L.; Jordan, A. C.; Fisher, E. R. *Journal of Membrane Science* **2002**, *204*, 341-357.
(15) M. S. Steen, L. H., E. D. Havey, N. E. Capps, D. G. Castner, E. R. Fisher *Journal of Membrane Science* **2001**, *188*, 97-114.
(16) Wavhal, D. S.; Fisher, E. R. *Journal of Polymer Science Part B-Polymer Physics* **2002**, *40*, 2473-2488.
(17) Williams, R. L.; Wilson, D. J.; Rhodes, N. P. *Biomaterials* **2004**, *25*, 4659-4673.
(18) Egitto, F. D.; Matienzo, L. J. *Ibm Journal of Research and Development* **1994**, *38*, 423-439.
(19) Martin, I. T.; Malkov, G. S.; Butoi, C. I.; Fisher, E. R. *Journal of Vacuum Science & Technology A* **2004**, *22*, 227-235.
(20) Matsuyama, H.; Teramoto, M.; Hirai, K. *Journal of Membrane Science* **1995**, *99*, 139-147.
(21) Steen, M. L.; Flory, W. C.; Capps, N. E.; Fisher, E. R. *Chemistry of Materials* **2001**, *13*, 2749-+.
(22) Pittman, J. L.; Henry, C. S.; Gilman, S. D. *Analytical Chemistry* **2003**, *75*, 361-370.
(23) Liu, Y.; Fanguy, J. C.; Bledsoe, J. M.; Henry, C. S. *Anal Chem* **2000**, *72*, 5939-5944.
(24) Huang, X. H.; Gordon, M. J.; Zare, R. N. *Analytical Chemistry* **1988**, *60*, 1837-1838.
(25) Garcia, C. D.; Henry, C. S. *Analytical Chemistry* **2003**, *75*, 4778-4783.

(26) Butoi, C. I.; Mackie, N. M.; Gamble, L. J.; Castner, D. G.; Barnd, J.; Miller, A. M.; Fisher, E. R. *Chemistry of Materials* **2000**, *12*, 2014-2024.
(27) Godek, M. L.; Malkov, G. S.; Fisher, E. R.; Grainger, D. W. *Plasma Processes and Polymers* **2006**, *3*, 485-497.
(28) G. Beamson, D. B. *High Resolution XPS of Organic Polymers, The Scienta ESCA Data Base*; J. Wiley & Sons, New York 1992.
(29) McCurdy, P. R.; Sturgess, L. J.; Kohli, S.; Fisher, E. R. *Applied Surface Science* **2004**, *233*, 69-79.
(30) Sandrin, L.; Silverstein, M. S.; Sacher, E. *Polymer* **2001**, *42*, 3761-3769.
(31) A. Delacorte, S. B., C. Poleunis, M. Troosters, P. Bertrand *Adhesion Aspects Thin Films* **2004**, 1.
(32) Vickers, J. A.; Caulum, M. M.; Henry, C. S. *Analytical Chemistry* **2006**, *78*, 7446-7452.
(33) Candan, S.; Beck, A. J.; O'Toole, L.; Short, R. D. *Journal of Vacuum Science & Technology A* **1998**, *16*, 1702-1709.
(34) Kull, K. R.; Steen, M. L.; Fisher, E. R. *Journal of Membrane Science* **2005**, *246*, 203-215.
(35) Steen, M. L.; Butoi, C. I.; Fisher, E. R. *Langmuir* **2001**, *17*, 8156-8166.
(36) Kirby, B. J.; Hasselbrink, E. F. *Electrophoresis* **2004**, *25*, 187-202.
(37) Wheeler, A. R.; Trapp, G.; Trapp, O.; Zare, R. N. *Electrophoresis* **2004**, *25*, 1120-1124.
(38) Ren, X. Q.; Bachman, M.; Sims, C.; Li, G. P.; Allbritton, N. *Journal of Chromatography B-Analytical Technologies in the Biomedical and Life Sciences* **2001**, *762*, 117-125.
(39) Sui, Z. J.; Schlenoff, J. B. *Langmuir* **2003**, *19*, 7829-7831.
(40) Harris, D. C. *Quantitative Chemical Analysis, 6th edition*; Freeman and Company, New York 2003, 2003.

Chapter 4

Thermoset Polyester as an Alternative Material for Microchip Electrophoresis and Electrochemistry

Microchip capillary electrophoresis coupled with electrochemical detection (MCE-EC) is an up and coming method for the direct detection of many small molecule analytes because the technique is sensitive and readily miniaturized. Polymer materials have become increasingly used with MCE due to their affordability and ease of fabrication. While poly(dimethylsiloxane) (PDMS) has become arguably the most widely used material in MCE-EC due to the simplicity of microelectrode incorporation, it suffers from a lack of separation efficiency, lower surface stability, and a tendency for analyte sorption. Other polymers such as poly(methylmethacrylate) (PMMA) and poly(carbonate) (PC) have higher separation efficiencies but require more difficult fabrication techniques for electrode incorporation. In this report, thermoset polyester (TPE) was characterized as an alternative material for MCE-EC. TPE microchips were characterized in their native and plasma oxidized forms and after coating with polyelectrolyte multilayers (PEM). TPE provides higher separation efficiencies when compared to PDMS microchips, while still using simple fabrication protocols. In this work, separation efficiencies as high as 295,000 N/m were seen when using TPE MCE-EC devices. Furthermore, the electroosmotic flow was 38% higher and more consistent as a function of pH for both native and plasma treated TPE than PDMS. Finally, TPE is amenable to modification using simple polyelectrolyte multilayer coatings as another way to control surface chemistry and surface charge.

The chapter is a reprint of "Thermoset polyester as an alternative material for microchip electrophoresis/electrochemistry" Jonathan A. Vickers, Brian M. Dressen, Melissa C. Weston, Kanokporn Boonsong, Orawan Chailapakul, Donald M. Cropek, and Charles S. Henry, Electrophoresis 2007, 28, 1123–1129 a manuscript written by Jonathan A. Vickers and Brian M. Dressen, with work performed equally by both individuals. Brian Dressen performed fabrication and characterization of the devices while Jonathan Vickers performed the separations. Melissa Weston and Kanokporn Boonsong provided initial studies on TPE modification and separations respectively.

4.1 Introduction

The development of miniaturized, multifunctional devices for chemical analysis is becoming increasingly important, particularly for point-of-measurement applications. Such 'lab-on-a-chip' devices have the potential to serve as portable analytical tools, increase efficiencies in sample preparation, delivery, and analysis, and reduce overall analysis costs.[1] Lab-on-a-chip devices using capillary electrophoresis (CE) offer a fast and efficient means for chemical separation relative to traditional instrumentation. The benefits of these systems include reduced analyte and sample consumption, fast analysis times, and high-resolution separations using exceptionally small volumes relative to HPLC and even conventional CE. Fabrication of microchip capillary electrophoresis (MCE) devices also offers benefits including excellent precision and reproducibility of structural elements and inexpensive mass fabrication of complicated microstructures.[2]

As MCE devices grow in popularity, there is a need for multiple detection methods to increase the number of detectable analytes, particularly for point-of-measurement applications. Absorbance,[3, 4] mass spectrometry,[5, 6] laser-induced fluorescence (LIF),[7, 8] electrochemical (EC) techniques[9, 10] and other detection methods[11-13] have been successfully coupled with microchip CE. EC instrumentation is particularly attractive for small molecule analysis because it is less complex and expensive than many other detection systems such as laser-induced fluorescence[7, 8] and mass spectrometry[5, 6] and can range in selectivity from general through the use of conductivity[14, 15] to very specific through careful potential selection.[16, 17] EC has

shown potential for many applications and offers mass sensitivity levels similar to fluorescence detection while not requiring derivitization with a fluorophore.[18-20]

One concern with the use of EC is the appropriate choice of substrate material and the impact it has on separation performance. Glass is known to give the best separation performance among microchip materials; however, the high temperatures used in bonding can damage or destroy electrodes. Polymeric substrates, on the other hand, are more amenable to the incorporation of electrodes but give a lower separation performance.[16, 19] Polymers such as poly(dimethylsiloxane) (PDMS), poly(methyl-methacrylate) (PMMA), and polycarbonate (PC) have been studied for use in the fabrication of MCE devices.[21-23] The interest in polymer microchips has come about due to their relative ease of fabrication compared to glass and low materials cost. A range of fabrication methods can be applied to polymers, including soft lithography,[24] casting,[25] laser ablation,[26] injection molding[27] and hot embossing.[28] These processes have shown to be easier, faster, and simpler than etching channels into glass.[2] Polymer microchips also do not require the same high temperatures as glass for bonding, preventing electrode damage. Polymer CE microchips have, however for the most part been disappointing with regards to separation efficiency with a few notable exceptions.[29-31] PDMS microchips in particular, are easy to fabricate with soft lithography and inexpensive but the separation efficiencies are low and surface charge is unstable.[24, 32, 33] PMMA and PC have shown higher separation efficiencies, better EOF stability and a less likelihood of analyte absorption into the bulk material, but the fabrication and sealing processes are more challenging than the soft lithography of PDMS.[21, 29] Several methods for the chemical modification of the

PDMS surface have been demonstrated in an effort to address some of these issues with varying degrees of success.[34-36]

The introduction of thermoset polyester (TPE) as an alternative microchip material has shown promise as a merger between the ease of fabrication and cost effectiveness of PDMS with the higher separation efficiencies and increased stability of PMMA and PC.[37] The process of fabricating TPE as a microfluidic device has been described previously by Fiorini et al.[37, 38] With fabrication techniques similar to PDMS, little to no modification to existing soft lithography techniques is needed.[39, 40] Here, TPE microchips were fabricated and used for MCE-EC for the first time. Native and polymer modified TPE were studied to investigate effects on surface stability and EOF. Amperometric and pulsed amperometric detection (PAD) were used to demonstrate the compatibility of TPE with different modes of electrochemical detection. An 8-fold increase in separation efficiency is seen when going from PDMS microchips (42,000 ± 2100 N/m) to TPE microchips (295,000 ± 12,000 N/m) using the same SU-8 mold and analyte solution. Finally, TPE was modified with polyelectrolyte multilayers to demonstrate the potential for further control of the surface chemistry of TPE.

4.2 Experimental

4.2.1 Chemicals. Sylgard 184 silicone elastomer and curing agent were obtained from Dow Corning (Midland, MI). Sodium phosphate monobasic (F.W. 137.99) was purchased from Acros Organics and *o*-phosphoric acid (85%) and methanol were purchased from Fisher Scientific (Fair Lawn, NJ). Gold (99.9% diameter 25 μm) and

palladium (99.9% diameter 25 μm) wire were obtained from Goodfellow (Huntingdon, England). SU-8 2035 negative photoresist and XP SU-8 developer were obtained from Microchem Corp (Newton, MA). All polyelectrolytes were obtained from Aldrich. The polymers tested included hexadimethrine bromide (polybrene, PB) and dextran sulfate (sodium salt) (DS) (Av. M.w. 5,000). All chemicals were used as received.

4.2.2 Microchip Fabrication. Silicon masters were fabricated following techniques published elsewhere.[41] Briefly, SU-8 2035 negative photoresist was spun onto a 100 mm silicon wafer (<100>Silicon Inc, Boise, ID) to a thickness of 50 μm. A digitally printed mask was used to define channel structures. After exposure and developing, patterned silicon masters were treated with hexamethyldisilazane (HMDS) by vapor deposition to aid in the removal of the both TPE and PDMS. Vapor deposition was performed by placing the wafer and a small vial containing 500 μL of HMDS in a crystallization dish, the dish was then covered with foil and placed in a 65° C oven for 4-6 hrs. PDMS walls and posts were used to define the molding area and create reservoirs in the TPE devices.

TPE was prepared by mixing resin (TAP Clear-Lite Casting Resin) with additional styrene, UV photoinitiator (2,2-dimethoxyphenylacetophenone) and methyl ethyl ketone peroxide (MEKP) catalyst following published protocols.[37] Approximately 0.2 g of photoinitiator was dissolved in 0.5 g of styrene and then

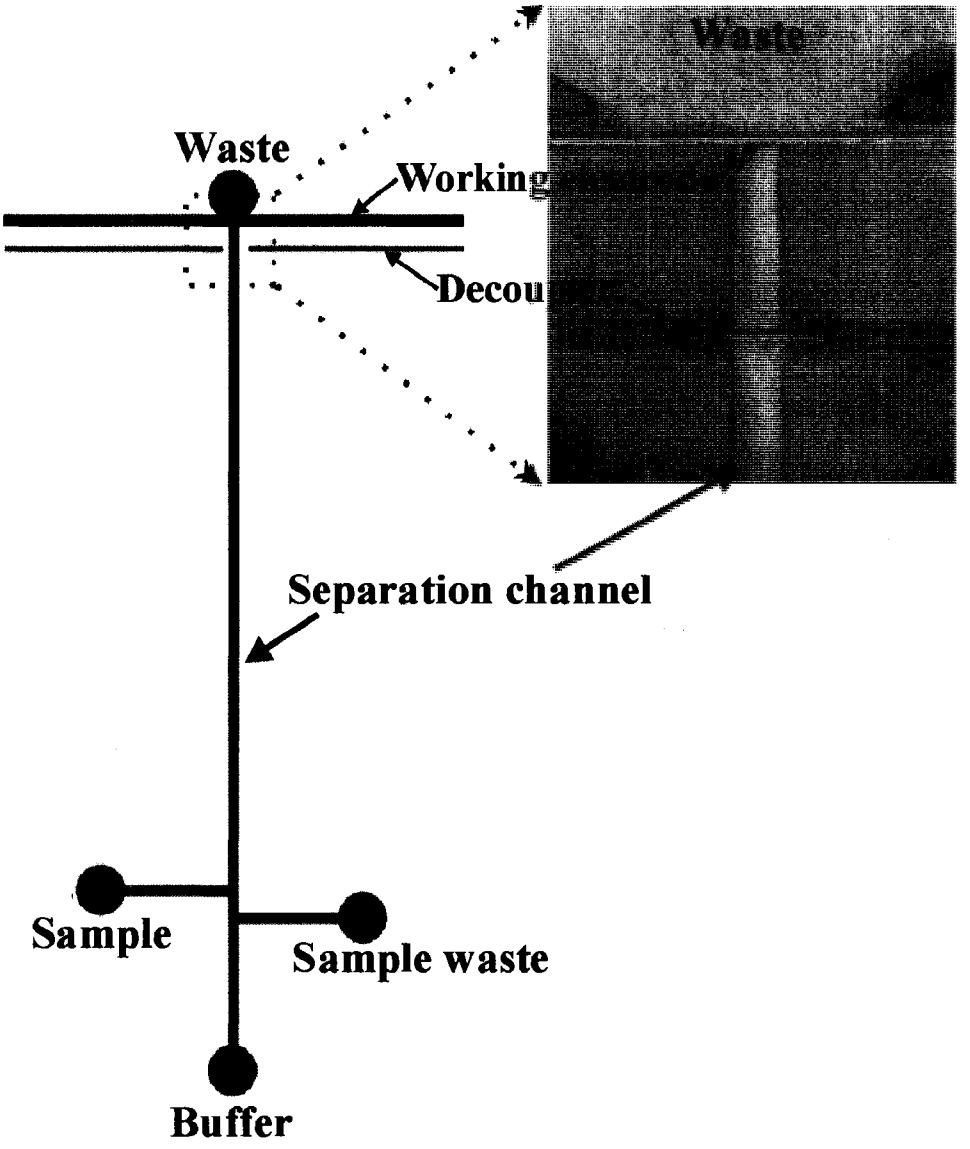

Figure 4.1: Schematic of the TPE microchips (50 μm x 50 μm x 6 cm) showing the double-T injector (100 μm) on the right and electrode alignment channels (decoupler 25 μm x 50 μm and working 50 μm x 50 μm) on the left. A 50 μm gap separates the decoupler channel from the separation channel. To the right is a photograph showing the electrode alignment in a completed microchip.

added to 20 g of resin. Six drops of MEKP catalyst were added and the mixture was stirred and degassed. After degassing, the TPE resin was poured onto the prepared master and either transparency film or a glass microscope slide was used to cover the TPE. The cover material was allowed to make contact with TPE mixture to ensure a flat top surface during UV curing. HMDS was used to treat the glass cover slides to ease removal from cured TPE. TPE was partially cured by UV radiation in a flood lamp (364 nm) (Inteli-ray 400) at 50% power for 100 s and then, carefully pulled away from the mold while still slightly soft. While still soft, the PDMS posts were removed to expose the reservoirs. Microwire electrodes were then placed in the designated electrode channels located at the end of the separation channel according to previously published work in PDMS microchips from the Henry group.[39, 40] Care had to be taken while inserting the microwires because TPE is easily scratched, torn, or otherwise damaged when not fully cured. Once the electrodes were in place a blank piece of TPE was prepared in the same manner with a UV exposure of 100 s. The two pieces were then placed together to form the microchannels. A final UV exposure was necessary to set the bond between the 2 pieces and fully cure the TPE (four, 30 s exposures separated by 90 s cooling periods). The chip was then placed on a 65° C hot plate for 30 min followed by transfer to a 120° C hotplate for 90 min for final curing. Figure 4.1 shows a schematic of the microchip design as well as a zoomed in picture of the detection electrodes in a fully assembled TPE microchip.

4.2.3 Electroosmotic Flow Measurements. Electroosmotic flow was measured using the current monitoring method developed by Huang et al[42] and further established by many groups. A straight 50 x 50 μm channel with a length of 4.5 cm was used for all EOF measurements. One reservoir and the channel were filled with 20 mM buffer while the second reservoir was filled with 18 mM buffer. During electroosmosis, the lower concentration electrolyte solution from the second reservoir gradually displaced the higher concentration buffer in the channel, resulting in an increase in the electrical resistance of the channel and therefore a different separation current. The change in separation current under a constant applied voltage was monitored and the time required to reach a constant separation current was used to calculate EOF. The separation current was monitored using a digital multimeter (Fluke 189) to follow the voltage drop across a 1 kΩ resistor in series between the cathode and ground. A 900 V separation potential (200 V/cm) was used for EOF measurements.

4.2.4 Coating Procedure. TPE microchips were coated with polyelectrolyte multilayers using previously reported methods.[32] The channel was preconditioned with 0.1 M NaOH for 10-15 min, followed with a 5 min water rinse. A cationic polymer (Polybrene (PB)) layer was deposited onto the channel wall by filling the channel with a 5% polyelectrolyte solution. The channel was then immediately rinsed with water for 5 min. Double layer coatings were formed by repeating this procedure with an anionic polyelectrolyte solution of dextran sulfate (DS). After the final water rinse, the channel was filled with buffer and electrophoresis is performed.

4.2.5 Electrochemical Detection. Amperometric and pulsed amperometric detection (PAD) were used for the detection of electrochemically active analytes using a previously published chip design.[39, 43] Amperometry was used for the detection of dopamine, catechol, and ascorbic acid. PAD was used in the detection of carbohydrates and thiols. Both amperometry and PAD were performed using a commercially available potentiostat (CHI812 or CHI660b, CH Instruments). Amperometry had a constant potential of 0.8 V applied to the working electrode. The PAD waveform had a cleaning/oxidation potential of 1.6 V for 0.05 s, the reduction/regeneration potential was -0.5 V for 0.025 s and the detection potential was 0.6 V for 0.15 s. Amperometry and PAD experiments were run in a two-electrode configuration with a Pt wire (1.6 mm diameter) as the counter electrode in all cases. An Au microwire (25 μm) was placed in the microfluidic devices and used as the working electrode. Cleaning and conditioning of the Pd decoupler was done initially by running cyclic voltammetry (CV) from -1.0V to 1.0V at 0.1 V/s for 50 cycles. Cleaning of the working electrode was done initially by running a CV from -1.0V to 1.0V at 0.1 V/s until 6 sweep segments overlapped each other. While using amperometry the working electrode was cleaned every 15 runs via CV with 20 sweep segments from -1.0V to 1.0V at the rate of 0.1 V/s while buffer was flowed over the electrode.[43]

4.3 Results and Discussion

TPE has been reported previously in three separate publications.[37, 38, 44] In the previous work, EOF was measured for only five days. Furthermore, no surface modification studies were presented. Finally, all previous detection was performed using laser-induced fluorescence (LIF). LIF in previous reports was complicated by background fluorescence inherent in the fundamental polymer materials. In our quest to achieve high efficiency separations for MCE-EC using polymer microchips, we sought to both further establish the material characteristics of TPE as well as demonstrate its use with EC detection.

4.3.1 Electroosmotic Flow Studies. Figure 4.2 shows EOF values measured over 18-days for native TPE. No statistical decrease in EOF was seen over the first 4 days with the chips stored in water between measurements. A 55% decrease from 4.85 ± 0.57 to 2.16 ± 0.53 $cm^2/V{\cdot}s \times 10^{-4}$ in EOF is seen between 4 and 18 days (n = 5). Similar EOF values and trends are seen for microchips stored in air. EOF values were also measured for plasma oxidized microchips over a period of 11 days. As can be seen in Figure 4.2, the EOF for plasma treated TPE is higher and more stable with time than unmodified TPE. EOF as a function of pH was further established for TPE microchips in comparison to PDMS. Figure 4.3 shows a comparison of EOF values as they are affected by a change in pH for PDMS, native TPE and plasma oxidized TPE. EOF values are 22% larger and more stable for native TPE across the pH values than EOF seen on PDMS microchips. EOF values of plasma oxidized TPE devices were 5.13 ± 0.34, 5.56 ± 0.22 and 5.61 ± 0.35 $cm^2/V{\cdot}s \times 10^{-4}$ (n = 5) for pHs 4,

7 and 10 respectively, a 38% increase in EOF over PDMS and a 21 % increase over native TPE. Chip-to-chip reproducibility of the TPE microchips was also established. The RSD from chip-to-chip for five chips was 2.7, 5.1 and 7.1% for pH 4, 7 and 10 respectively. The reproducibility of EOF for TPE microchips shows that small changes in the volume or mass of TPE components have little to no effect on the EOF. The stability of the EOF as a function of time for both native and plasma oxidized TPE is much better than PDMS microchips and similar to that measured in PMMA or PC.[45] The comparison to PDMS is however, more relevant because of the similar fabrication methods and times for the two materials. PDMS lacks stability because of the diffusion of hydrophobic low molecular weight oligomer to the surface.[46-48] TPE lacks this property because it is denser and the starting materials are less hydrophobic. The lack of long-term stability of native TPE could result from the conversion of carboxylic acids back to esters over time. Plasma treatment presumably perturbs the surface enough to separate reactive acids and alcohols. The exact chemical mechanism that leads to enhanced stabilization is currently under investigation.

4.3.2 Polyelectrolyte Modification. PEM coatings provide a method for controlling the surface chemistry in microchip devices.[32, 49] PEM coatings have shown to be beneficial when working with PDMS microchips because they increase the EOF, surface stability, and hydrophilicity of the devices. Figure 4.4 shows EOF values measured for native

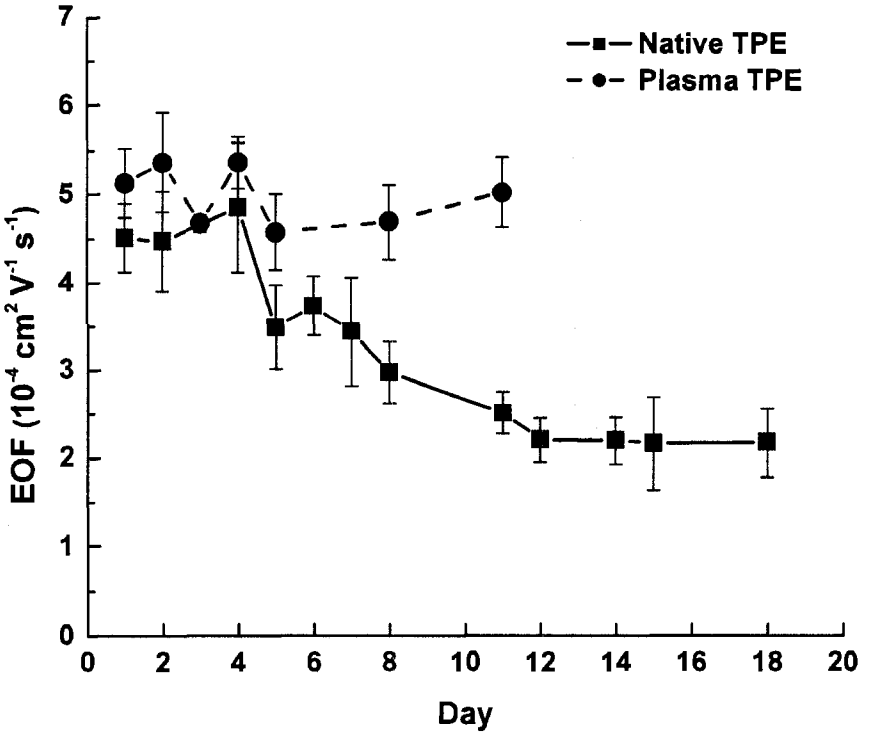

Figure 4.2: Day-to-day EOF reproducibility of TPE microchips. EOF stability is shown for native TPE over an 18 day period (■) and for plasma treated TPE over an 11 day period (●). EOF was determined by the current monitoring method. Experimental conditions: Field strength: 200 V/cm; Background electrolytes: 20 mM phosphate and 18 mM phosphate.

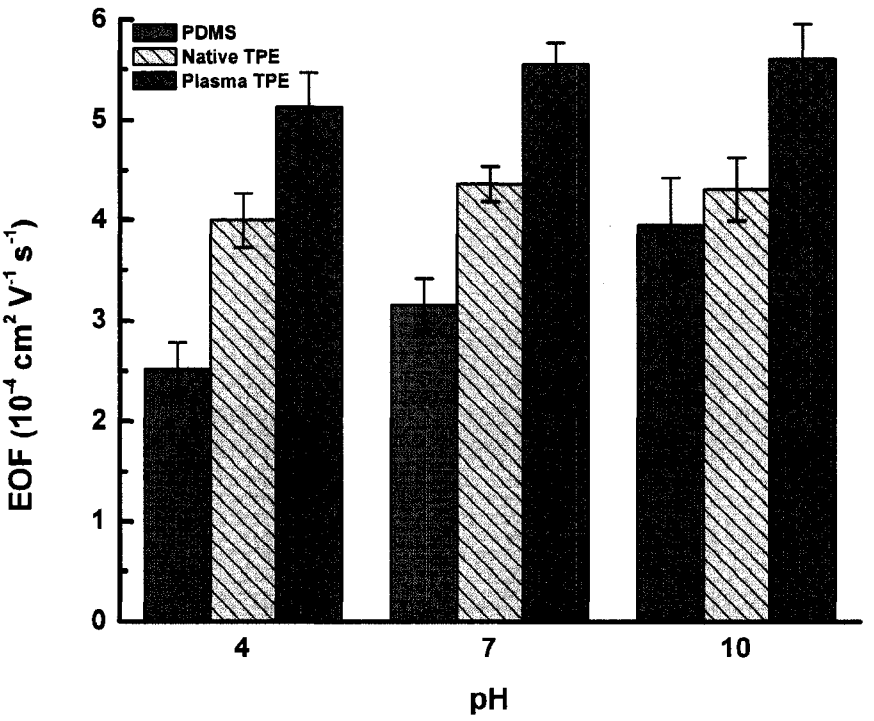

Figure 4.3: EOF measured for five microchips made at different times from different batches of TPE. Each chip was run multiple times are varying pHs (4, 7 and 10) to determine pH effects on reproducibility. Other experimental protocols as in Figure 4.2.

(untreated) TPE, TPE coated with PB, and TPE coated with a bilayer of PB and DS over a pH range of 3 to 10. The EOF for the native TPE microchip stayed consistent across the entire pH range with a value of $4.08 \pm 0.31 \times 10^{-4}$ $cm^2/V \cdot s$ ($n = 10$). Addition of the PB cationic layer to the TPE surface reversed the flow, as expected, but also significantly reduced the magnitude of the EOF. Values for the EOF of the PB treated TPE ranged from -2.69 to -1.51×10^{-4} $cm^2/V \cdot s$ ($n = 3$) in phosphate buffer over the same pH range. Addition of an anionic layer of DS to the PB coated surface, gave EOF magnitudes similar to the native TPE. EOFs between 2.58 ± 0.43 and 4.34 ± 0.83 $cm^2/V \cdot s \times 10^{-4}$ were seen for the 3 to 10 pH range. Control of surface chemistry through a simple and effective PEM coating will allow TPE microchips to be used in variety of ways. PEM coatings may be used to reverse, reduce, or even eliminate EOF. Reversal of EOF is useful in the separation of anionic species because flow direction parallels anion migration allowing for shorter separation time and larger separation efficiency due to the narrower peaks from reduced diffusion. Another benefit to adsorbed PEM coatings is that no additional PE's need be added to the background electrolyte as with dynamic coatings such as surfactants. Here, as expected the polyelectrolytes are strongly held to the surface through electrostatic interactions.

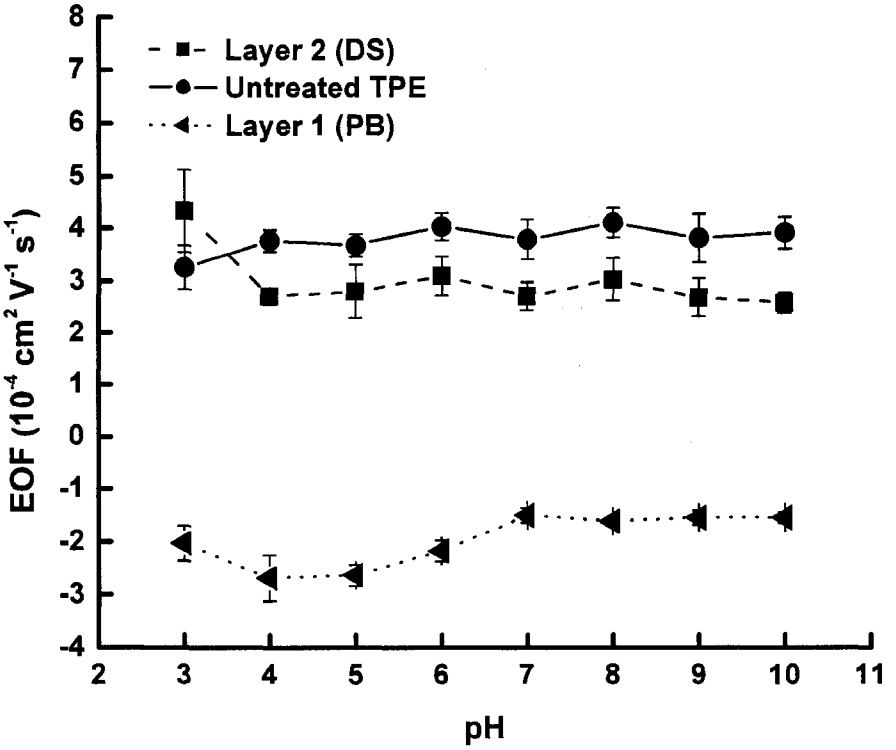

Figure 4.4: EOF values of native TPE (●) modified with a single layer of polybrene (anionic polyelectrolyte) (◀) and a double layer of dextran sulfate (cationic polyelectrolyte) (■) over a pH range from 3 to 10. Other experimental protocols as in Figure 4.2.

4.3.3 Microchip CE-Amperometry. Dopamine, catechol, and ascorbic acid were chosen as model analytes to characterize TPE microfluidic devices and to provide a comparison to PDMS microchips. Figure 4.5 shows representative electropherograms for the separation of 1 μM dopamine, catechol, and ascorbic acid on TPE (top) and PDMS (bottom) microchips. Peak tailing and peak width were dramatically decreased when using TPE over PDMS. Peak skews of 3.2 and 3.8 are observed for dopamine and catechol respectively on the PDMS microchip compared to 1.2 and 1.3 for dopamine and catechol on the TPE devices. The large peak skew values can be attributed to sticking to the hydrophobic surface of PDMS. An 8-fold increase in separation efficiencies when going from PDMS to TPE is shown in Figure 4.6. On TPE separation efficiencies of 49,000 ± 2600, 148,000 ± 4500 and 295,000 ± 12,000 N/m are seen for dopamine, catechol and ascorbic acid respectively as compared to 18,000 ± 1200, 24,000 ± 1400 and 42,000 ± 2100 for PDMS. Higher separation efficiencies seen on the TPE devices can be attributed to the increased hydrophilic nature of the TPE, increased surface charge stability, and lack of hydrophobic recovery over time. The increased separation efficiency allows for a complete baseline resolved separation of all three analytes on TPE in the same time that dopamine is seen

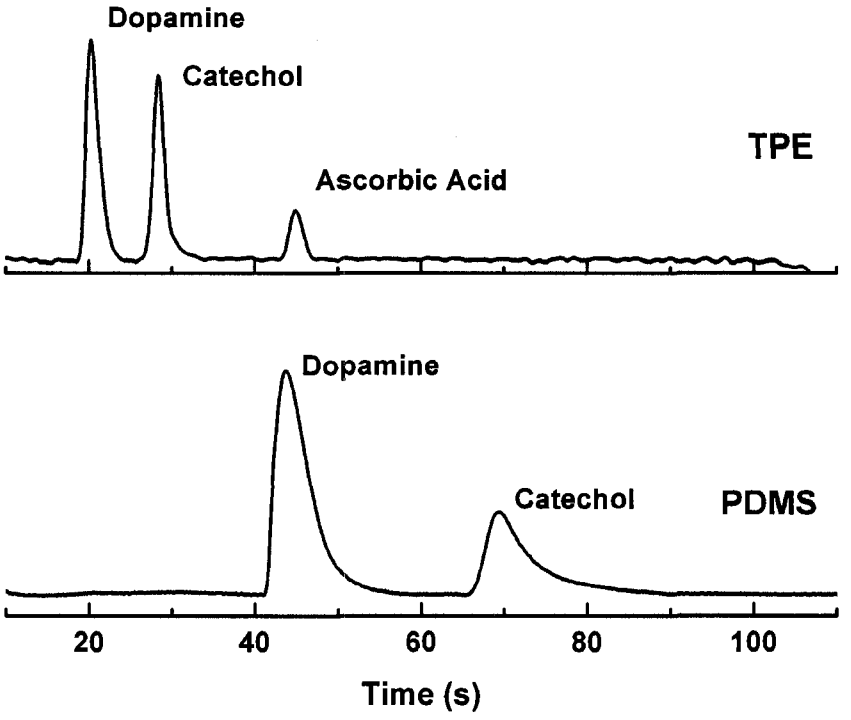

Figure 4.5: Example electropherograms for 1 μM dopamine, catechol and ascorbic acid on a TPE microchip (Top) and PDMS microchip (bottom). Experimental conditions: Field strengths: 300 V/cm and 200 V/cm for TPE and PDMS microchips respectively; pinched injection time: 15 s; Background Electrolyte: 20 mM TES (pH 7.0) Note. Ascorbic acid peak not shown for PDMS.

on a PDMS device. The higher separation efficiencies, better peak skews and faster EOF seen for TPE will allow for a faster and better resolved separation of complex samples.

The effect of field strength on migration time and peak shape were investigated next. Figure 4.7 shows the separation of dopamine, catechol and ascorbic acid on a TPE microchip as a function of separation potential using pH 7.0, 20 mM TES as the run buffer. As expected, as the field strength is increased, the migration times decrease. Migration times were reduced by 31% with microchips at the same field strengths and by 58% with the higher field strength that are possible on TPE microchips compared to PDMS microchips. TPE was able to handle higher field strengths than PDMS in our experiments without the generation of bubbles or destroying the bulk material of the microchip. The exact mechanism that allows higher field strengths to be used is not known, however, improvements of this kind are normally the result of improved heat transfer properties of the substrate material. The optimal separation potential was determined to be 266 V/cm (1600 V) because it offered the fastest separation without sacrificing peak height.

4.3.4 Microchip CE-PAD. As a final test of the compatibility of TPE for MCE-EC, PAD detection of carbohydrates and thiols was performed. 100 μM glucose, cysteine and glutathione were chosen as model analytes. Direct detection has the potential to simplify the quantification of these biologically important compounds. An example electropherogram of the separation of these three analytes is shown in Figure 4.8.

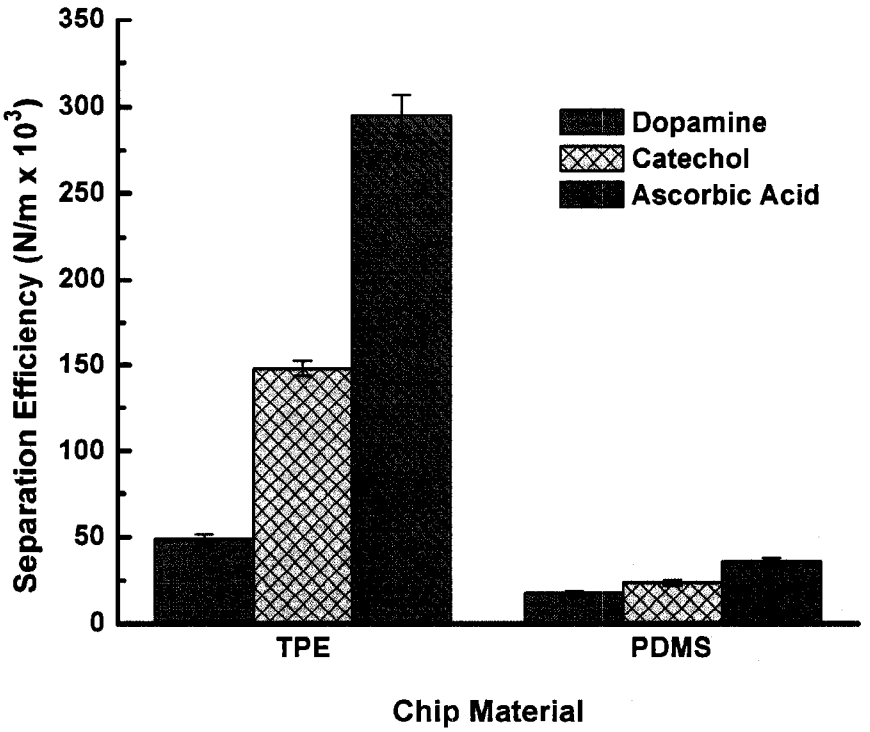

Figure 4.6: Separation efficiencies for 1 μM dopamine, catechol, and ascorbic acid on identical TPE (left) and PDMS (right) microchips.

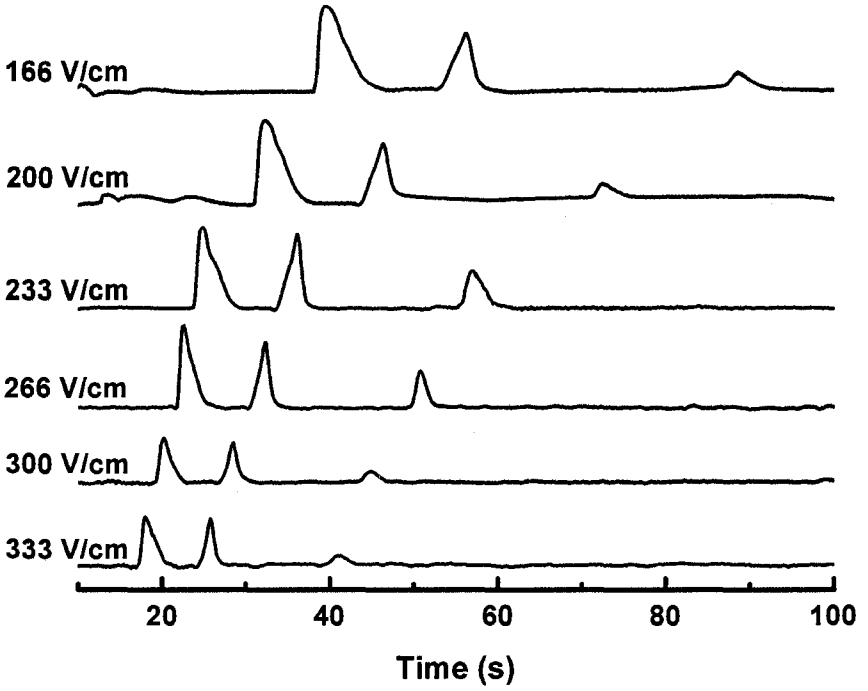

Figure 4.7: Separation of 1 μM dopamine, catechol, and ascorbic acid on a TPE microchip as a function of separation potential. Optimized separation potential is determined to be 266 V/cm (1600V). Experimental conditions as in Figure

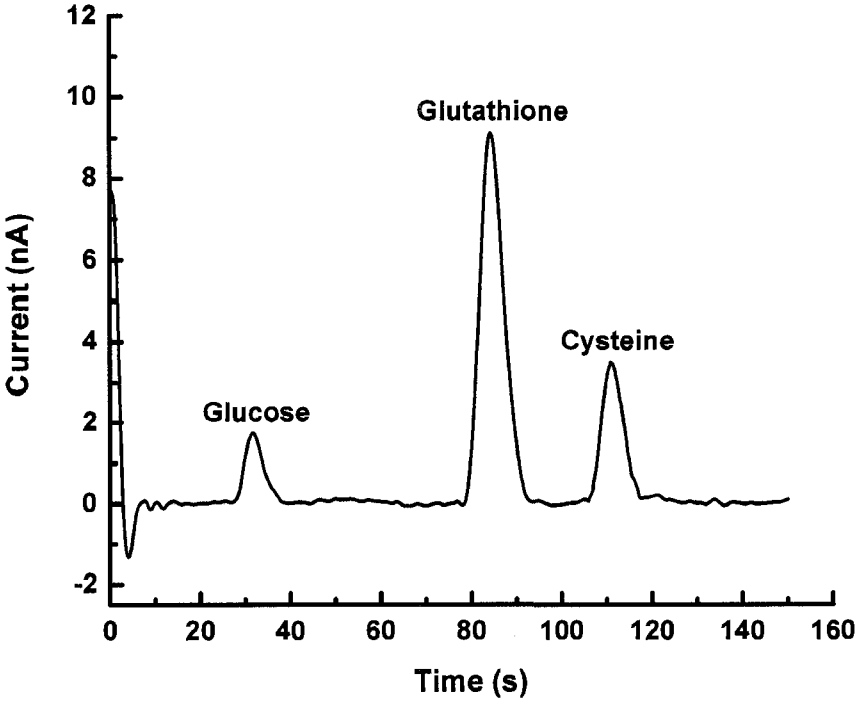

Figure 4.8: Electropherogram for the separation of 100 μM glucose, glutathione, and cysteine on a TPE microchip. Experimental conditions: Field strength: 233 V/cm; Pinched injection time: 15 s; Background electrolyte: 20 mM boric acid (pH 10.0)

The separation was performed using 20 mM boric acid, 0.8 mM SDS (pH 10.0) as the background electrolyte at field strengths of 233 V/cm with a 15 s injection. Baseline resolution of all three analytes is seen. Migration times of 31.7 ± 1.5 s, 84.4 ± 2 s and 110.9 ± 3.2 s (n=4) were seen for glucose, glutathione and cysteine, respectively. The peak broadness can be attributed to the high concentration (100 μM) of the sample used during the separation. This example shows the compatibility of the more general PAD mode with TPE microchips.

4.4 Conclusion

In summary, the ability of TPE, as a material for MCE-EC, to perform the separation of several analytes has been demonstrated. EOF values for TPE microchips have shown to be very stable over a wide pH range and an extended period of time relative to PDMS. Chip-to-chip reproducibility of these devices has also been shown to be very good. The improvement of separation efficiencies on TPE microchips when compared to PDMS chip material gives a good indication of the increased complexity of samples that may be studied with these chips.

4.5 References:

(1) Harrison, D. J.; Manz, A.; Fan, Z. H.; Ludi, H.; Widmer, H. M. *Analytical Chemistry* **1992**, *64*, 1926-1932.

(2) Manz, A.; Harrison, D. J.; Verpoorte, E. M. J.; Fettinger, J. C.; Paulus, A.; Luedi, H.; Widmer, H. M. *J Chromatogr* **1992**, *593*, 253-258.

(3) Liang, Z.; Chiem, N.; Ocvirk, G.; Tang, T.; Fluri, K.; Harrison, D. J. *Anal Chem* **1996**, *68*, 1040-1046.

(4) Salimi-Moosavi, H.; Jiang, Y.; Lester, L.; McKinnon, G.; Harrison, D. J. *Electrophoresis* **2000**, *21*, 1291-1299.

(5) Ramsey, R. S.; McLuckey, S. A. *J Microc Sep* **1997**, *9*, 523-528.

(6) Ramsey, R. S.; Ramsey, J. M. *Analytical Chemistry* **1997**, *69*, 2617.

(7) Jacobson, S. C.; Ramsey, J. M. *Electrophoresis* **1995**, *16*, 481-486.

(8) Jakeway, S. C.; de Mello, A. J.; Russell, E. L. *Fresenius' J Anal Chem* **2000**, *366*, 525-539.

(9) Mayrhofer, K.; Zemann, A. J.; Schnell, E.; Bonn, G. K. *Anal Chem* **1999**, *71*, 3828-3833.

(10) Wang, J.; Polsky, R.; Tian, B.; Chatrathi, M. P. *Anal Chem* **2000**, *72*, 5285-5289.

(11) Ocvirk, G.; Tang, T.; Jed Harrison, D. *Analyst* **1998**, *123*, 1429-1434.

(12) Walker, P. A., 3rd; Morris, M. D.; Burns, M. A.; Johnson, B. N. *Anal Chem* **1998**, *70*, 3766-3769.

(13) Hashimoto, M.; Tsukagoshi, K.; Nakajima, R.; Kondo, K.; Arai, A. *J Chromatogr A* **2000**, *867*, 271-279.

(14) Coltro, W. K.; da Silva, J. A.; da Silva, H. D.; Richter, E. M.; Furlan, R.; Angnes, L.; do Lago, C. L.; Mazo, L. H.; Carrilho, E. *Electrophoresis* **2004**, *25*, 3832-3839.

(15) Kuban, P.; Hauser, P. C. *Electrophoresis* **2005**, *26*, 3169-3178.

(16) Vandaveer, W. R. I. V.; Pasas-Farmer, S. A.; Fischer, D. J.; Frankenfeld, C. N.; Lunte, S. M. *Electrophoresis* **2004**, *25*, 3528-3549.

(17) Wang, J.; Chatrathi, M. P. *Anal Chem* **2003**, *75*, 525-529.

(18) Wang, J. *Talanta* **2002**, *56*, 223-231.

(19) Vandaveer, W. R. I. V.; Pasas, S. A.; Martin, R. S.; Lunte, S. M. *Electrophoresis* **2002**, *23*, 3667-3677.

(20) Backofen, U.; Matysik, F. M.; Lunte, C. E. *Anal Chem* **2002**, *74*, 4054-4059.

(21) Dolnik, V.; Liu, S.; Jovanovich, S. *Electrophoresis* **2000**, *21*, 41-54.

(22) Liu, Y.; Ganser, D.; Schneider, A.; Liu, R.; Grodzinski, P.; Kroutchinina, N. *Anal Chem* **2001**, *73*, 4196-4201.

(23) Reyes, D. R.; Iossifidis, D.; Auroux, P. A.; Manz, A. *Anal Chem* **2002**, *74*, 2623-2636.

(24) McDonald, J. C.; Duffy, D. C.; Anderson, J. R.; Chiu, D. T.; Wu, H.; Schueller, O. J.; Whitesides, G. M. *Electrophoresis* **2000**, *21*, 27-40.

(25) Effenhauser, C. S.; Bruin, G. J. M.; Paulus, A.; Ehrat, M. *Anal Chem* **1997**, *69*, 3451-3457.

(26) Roberts, M. A. *Analytical Chemistry* **1997**, *69*, 2035-2042.

(27) McCormick, R. M. *Analytical Chemistry* **1997**, *69*, 2626-2630.

(28) Martynova, L.; Locascio, L. E.; Gaitan, M.; Kramer, G. W.; Christensen, R. G.; MacCrehan, W. A. *Anal Chem* **1997**, *69*, 4783-4789.
(29) Jikun Liu, T. P., Adam T. Woolley, and Milton L, Lee *Analytical Chemistry* **2004**, *76*, 6948-6955.
(30) Kelly, R. T.; Woolley, A. T. *Anal Chem* **2003**, *75*, 1941-1945.
(31) Roman, G. T.; Culbertson, C. T. *Langmuir* **2006**, *22*, 4445-4451.
(32) Liu, Y.; Fanguy, J. C.; Bledsoe, J. M.; Henry, C. S. *Anal Chem* **2000**, *72*, 5939-5944.
(33) McDonald, J. C.; Whitesides, G. M. *Acc Chem Res* **2002**, *35*, 491-499.
(34) Gonzalez, N.; Elvira, C.; San Roman, J.; Cifuentes, A. *Journal of Chromatography, A* **2003**, *1012*, 95-101.
(35) Garcia Carlos, D. *Electrophoresis* **2005**, *26*, 703-709.
(36) Henry, A. C.; Tutt, T. J.; Galloway, M.; Davidson, Y. Y.; McWhorter, C. S.; Soper, S. A.; McCarley, R. L. *Analytical Chemistry* **2000**, *72*, 5331-5337.
(37) Fiorini, G. S.; Lorenz, R. M.; Kuo, J. S.; Chiu, D. T. *Analytical Chemistry* **2004**, *76*, 4697-4704.
(38) Fiorini, G. S.; Jeffries, G. D. M.; Lim, D. S. W.; Kuyper, C. L.; Chiu, D. T. *Lab Chip* **2003**, *3*, 158-163.
(39) Garcia, C. D.; Henry, C. S. *Anal Chem* **2003**, *75*, 4778-4783.
(40) Vickers, J. A.; Henry, C. S. *Electrophoresis* **2005**, *26*, 4641-4647.
(41) Duffy, D. C.; McDonald, J. C.; Schueller, O. J. A.; Whitesides, G. M. *Anal Chem* **1998**, *70*, 4874-4884.
(42) Huang, X.; Gordon, M. J.; Zare, R. N. *Anal Chem* **1988**, *60*, 1837-1838.
(43) Liu, Y.; Vickers, J. A.; Henry, C. S. *Anal Chem* **2004**, *76*, 1513-1517.
(44) Xu, W.; Uchiyama, K.; Shimosaka, T.; Hobo, T. *Chemistry Letters* **2000**, 762-763.
(45) Kirby, B. J.; Hasselbrink, E. F., Jr. *Electrophoresis* **2004**, *25*, 203-213.
(46) Kim, J.; Chaudhury, M. K.; Owen, M. J. *Journal of Colloid and Interface Science* **2006**, *293*, 364-375.
(47) Kim, J.; Chaudhury, M. K.; Owen, M. J. *J Colloid Interface Sci* **2000**, *226*, 231-236.
(48) Fritz, J. L.; Owen, M. J. *Journal of Adhesion* **1995**, *54*, 33-45.
(49) Barker, S. L. R.; Tarlov, M. J.; Canavan, H.; Hickman, J. J.; Locascio, L. E. *Anal Chem* **2000**, *72*, 4899-4903.

Chapter 5

Influence of Polymer Structure on Electroosmotic Flow and Separation Efficiency in Layer-by-layer Polyelectrolyte Coatings for Microchip Electrophoresis

The effect of Successive Multiple Ionic Layer (SMIL) coatings on the velocity and direction of electroosmotic flow (EOF) and the separation efficiency for poly(dimethylsiloxane) (PDMS) electrophoresis microchips was studied using different polymer structures and deposition conditions. To date, the majority of SMIL studies have used traditional capillary electrophoresis and fused silica capillaries. EOF was measured as a function of polymer structure and number of layers, in one case using the same anionic polymer and varying the cationic polymer and in the second case using the same cationic polymer and varying the anionic polymer. In both situations, the EOF direction reversed with each additional deposited polymer layer. The absolute EOF magnitude, however, did not vary significantly with layer number or polymer structure. Next, different coatings were used to compare separation efficiencies on native and SMIL-coated PDMS microchips.For native PDMS microchips, the average separation efficiency was 4105±1540 theoretical plates. The addition of two layers of polymer increased the separation efficiency anywhere from 2- to 5-fold, depending on the polymer structure. A maximum separation efficiency of 12,880±1050 theoretical plates was achieved for SMIL coatings of polybrene (cationic) and dextran sulfate (anionic) polymers after deposition of six total layers. It was also noted that coating improved run-to-run consistency of the peaks as noted by a reduction of the relative standard deviation of the EOF and separation efficiency. This study shows that the use of polyelectrolyte coatings, irrespective of the polymer structure, generates a consistent EOF in the current experiments and dramatically improves the separation efficiency when compared to unmodified PDMS microchips.

This chapter is a reprint of "Influence of Polymer Structure on Electroosmotic Flow and Separation Efficiency in Layer-by-layer Polyelectrolyte Coatings forMicrochip Electrophoresis" Kanokporn Boonsong, Meghan M. Caulum, Brian M. Dressen, Orawon Chailapakul, Donald M. Cropek, Charles S. Henry, Electrophoresis in press. Written by Kanokporn Boonsong, Meghan M. Caulum, and Brian M. Dressen. Fabrication was performed by all partie. Kanokporn Boonsong and Brian Dressen performed coatings and EOF characterization and Meghan M. Caulum performed separation experiments

5.1 Introduction

Microchip capillary electrophoresis (MCE) has, in recent years, had a major impact on the field of chemical separations. Since the first reports of micro total analysis systems (μTAS)[1], there has been an increase in development of analytical systems in the microchip format because μTAS can be engineered to perform the same analyses as conventional scale systems but with reduced sample and reagent consumption, lower overall cost, and faster analysis times.[2] Early work in MCE used glass substrates for fabrication of capillary channels.[3, 4] Even though glass has several advantages for microchip separations over polymer substrates including chemical stability and high separation efficiency, it also has disadvantages including materials and fabrication cost and time. In light of these problems, many groups have focused efforts on producing microchips from polymer substrates.[2, 5, 6] Polymer microchips have problems of their own, however, including poorly defined and highly variable surface chemistry and the potential for both adsorption and absorption of moderately hydrophobic analytes.[7] As a result, many groups have developed strategies to control the surface chemistry and charge of polymer microfluidic devices.[8-15]

The capillary surface plays an important role in MCE. Control over the surface charge on the capillary wall helps dictate electroosmotic flow (EOF) and therefore the speed of separation.[16, 17] Analyte adsorption and therefore peak tailing is largely

dictated by the polymer surface chemistry with hydrophobic surfaces causing more tailing than hydrophilic surfaces.[18, 19] One polymer in particular, poly(dimethylsiloxane) (PDMS), has gained a great deal of attention due to the ease of fabrication outside a cleanroom, the ease of constructing complex geometries, and the relatively inexpensive per chip cost.[20] Furthermore, pumps and other functional elements can be easily integrated in PDMS devices.[21] Unfortunately, very few methods have been shown to work for controlling the surface chemistry and EOF of PDMS substrates resulting in low separation efficiency for microchips made from this material.[20, 22-26]

Successive Multiple Ionic Layer (SMIL) (also referred to as polyelectrolyte multilayer) coatings have been introduced as semi-permanent coatings for conventional[16, 27-29] and microchip capillary electrophoresis.[25, 30-32] SMIL coatings are formed by the deposition of alternating layers of polyelectrolytes on a surface as first reported by Decher et al.[33, 34] The mechanisms of formation and charge distribution in SMIL coatings have been probed by electrokinetics[16, 33] and radiochemical techniques.[35, 36] In general, the polymers deposit in layers that are intertwined with the last layer determining the net surface charge. Furthermore, alternate adsorption of cationic and anionic polyelectrolytes leads to stable coatings that are simple to deposit, have many potential chemistries, and are robust and reproducible.[36-38]

There have been several reports on the use of polyelectrolytes to stabilize EOF and/or control surface adsorption in CE applications. Maichel et al. and Potocek et al. reported the use of poly(diallyldimethylammonium chloride) (PDADMAC) as a replaceable pseudostationary phase in electrokinetic chromatography.[39, 40] In these reports, PDADMAC served as both a capillary wall coating as well as a stationary

phase for electrochromatography. In a separate report, Wang and Dubin used PDADMAC to minimize protein adsorption.[41] Chiu et al. used polyarginine (PA) as a capillary coating for conventional electrophoretic separations. They showed separation efficiencies of more than 2 million theoretical plates per meter using this coating.[42] Katayama et al. reported the use of polybrene (PB) and dextran sulfate (DS) as SMIL coatings to control EOF as a function of pH.[27] Cordova et al. investigated the properties of four polycationic polymers as noncovalent coatings to address the problem of protein adsorption in conventional CE, showing substantial reduction of adsorption and significant improvement in separation efficiency and peak shape.[43] Graul and Schlenoff characterized formation of adsorbed SMIL coatings composed of PDADMA and poly(styrenesulfonate) (PSS) for capillary zone electrophoresis.[16] All of these reports, however, focused on conventional CE. A smaller number of examples of SMIL coatings have been published for microchip CE devices. Barker et al. used SMIL coatings to alter surfaces in order to control EOF of microchips made from polystyrene (PS) and poly(ethylene terephthalate) glycol (PETG).[23, 24] Our group has previously published on the use of PB and DS for control of EOF as a function of pH in PDMS microchips.[25] In none of the above microchip examples, however, was the impact of SMIL coatings on separation efficiency measured. Furthermore, no systematic studies on the effect of polymer structure on EOF and separation efficiency in microchip devices has been performed.

We report here the characterization of different cationic and anionic multilayer coatings on PDMS microchips for control of EOF and improvement of separation efficiency compared to unmodified PDMS. The goal of this study was to determine what effect, if any, the polyelectrolyte structure and deposition conditions have on separation performance. Three cationic polymers, polybrene (PB),

poly(ethyleneimine) (PEI), and poly(allylamine) hydrochloride (PAH), were used in conjunction with two anionic polymers, dextran sulfate (DS) and poly(acrylic acid) (PAA) to measure the impact of polymer structure. These polymers were chosen for the range of chemical functionalities they possess. It was our initial hypothesis that polymer structure and deposition conditions would have a significant impact on EOF and separation efficiency. Studies showed to the contrary that the EOF magnitude was largely independent of polymer structure or deposition conditions. Finally, separation efficiency was measured for coated microchips and found to be much better (N=12883 ± 1050 plates for PB/DS compared to N=4104.9 ± 1540 plates for native PDMS) on coated microchips as compared to uncoated microchips.

5.2. Materials and Methods

5.2.1 Chemicals. The following chemicals and materials were used as received: SU-8 2035 photoresist (Micro Chem., Newton, MA, USA), propylene glycol methyl ether acetate (Aldrich, St. Louis, MO), 100-mm silicon wafers ((100) Silicon, Boise, ID, USA), poly(dimethylsiloxane) (PDMS) (Dow Corning, San Diego, CA), Sylgard 184 elastomer curing agent (Dow Corning), sodium hydroxide (Fisher, Pittsburgh, PA), *N*-tris[hydroxymethyl]methyl-2-aminoethanesulfonic acid (TES) (Sigma, St. Louis, MO), sodium acetate (Fisher), sodium phosphate (Fisher), boric acid (Fisher), hydrochloric acid (Fisher), phosphoric acid (Mallinckrodt), methanol (Fisher), 2-propanol (Fisher), catechol (Sigma), 3,4-dihydroxyphenethylamine (dopamine) (Sigma), poly(ethyleneimine) (Polysciences, Inc, Warrington, PA), poly(acrylic acid) (Polysciences, Inc), polyallylamine hydrochloride (Polyscience, Inc), hexamethrine bromide (Sigma), dextran sulfate (Polysciences, Inc.), fluorescein isothiocyanate

(FITC) (Invitrogen, Carlsbad, CA), 1,4-diaminobutane (Sigma), and triethylamine (Fisher).

5.2.2 Fabrication of PDMS devices. All experiments were performed using poly(dimethylsiloxane) (PDMS) microchips fabricated using established protocols.[25, 44-46] Briefly, a master mold was fabricated using a SU-8 2035 coated silicon wafer. The wafer was cleaned prior to SU-8 coating using dilute (10%) HF. Once the master was completed, replica molding was used to create channels in PDMS. A degassed mixture of Sylgard 184 elastomer and curing agent (10:1) was poured on the mold master as well as a blank silicon wafer and cured at 65°C for 2 hr. The cured PDMS was removed from the mold and reservoirs punched using a standard 6-mm hole punch.[44] The surfaces of the two pieces of PDMS were cleaned using methanol and placed in an air plasma cleaner (Harrick PDC-45) for 45s at 18 W. Following this, the two pieces of PDMS were immediately brought into conformal contact to form an irreversible seal. The assembled chip was preconditioned by a 30 min rinse with 1M NaOH before use each day.

5.2.3 Layer-by-layer coating procedure. Capillaries were initially coated with either polybrene (PB), poly(ethyleneimine) (PEI), or poly(allylamine) hydrochloride (PAH) followed by an anionic polyelectrolyte (poly(acrylic acid) (PAA) or dextran sulfate (DS)) according to procedures reported by Dai et al.[47] Briefly, the channel was rinsed with 1.0 M NaOH for 30 min followed by a 5 min fill of the positively charged polyelectrolyte solution. After rinsing with water for 1 min, the channel was coated with the negatively charged polymer for 5 min followed by a rinse with water for 1 min. These steps, with the exception of the NaOH rinse were repeated, alternating between anionic and cationic polymers, until the desired layer number was

achieved. All polyelectrolyte concentrations were 3% (w/v) in either 0 or 0.5 M NaCl in deionized water. All rinsing was done by applying a vacuum from a water aspirator or laboratory syringe at the waste outlet of the channels.

5.2.4 Electroosmotic flow measurements. The current monitoring method developed by Huang et al. was used to measure EOF.[48, 49] The polarity of the power supply was chosen so that the EOF was from the electrolyte in one reservoir at (reservoir 1) to the electrolyte reservoir at the other end of the channel (reservoir 2) through a straight channel. The channel and reservoir 2 were filled with 20 mM phosphate buffer while reservoir 1 was filled with 18 mM phosphate buffer. As 18 mM phosphate buffer in reservoir 1 migrates into the channel while the voltage is applied, it displaces an equal volume of 20 mM phosphate buffer. As a consequence, the electrical resistance of the fluid in the channel changes and can be followed by recording the separation current, I_{sep}, during the experiment. A 1.0 kΩ resistor was inserted between the electrode in reservoir 2 and electrical ground. The choice of 1.0 kΩ for this resistor meant that a 1-μA current change produced a 1-mV potential drop across the resistor. A multimeter (Fluke, Model 189) was used to follow the voltage drop across the resistor. The time required for the current to plateau was measured and was indicative of the lower concentration buffer filling the entire separation channel. Sample reservoir 1 was then filled with 20 mM buffer, the potential was reapplied, and the time to reach a current plateau measured. Six to eight consecutive measurements were obtained and averaged for each condition. The time required for the current to reach this plateau was used as the neutral marker, and the EOF determined using Equation 5.1,

$$\mu_{EOF} = L^2/Vt \qquad \text{Equation 5.1}$$

where L is the length of the separation channel (4.4 cm), V is the applied voltage (900 V), and t is the time in s to reach the new current plateau. This is a modification of the traditional mobility equation[25] that takes into account that the total and effective channel lengths are identical.

5.2.5 LIF detection. Fluorescence detection was performed using an epi-fluorescence system with a solid state laser (λ=475nm) for excitation and a photomultiplier tube (PMT) for detection based on similar designs reported by Johnson and Landers.[50] Detection of 1,4-diaminobutane derivatized with FITC (FTPD, 1.5 μM) was performed 2.5 cm down the separation channel using TES (20mM, pH 7.4) as the run buffer. Electropherograms were analyzed using peak fitting algorithms in OriginPro 7.

5.3. Results and Discussion.

Surface modification using SMIL coatings is attractive because of the wide variety of chemistries available for controlling surface properties.[51] In this study, five different polymers that represent primary (PAH), secondary (PEI), tertiary (PEI), and quaternary (PB) amines as well as strong (DS, sulfate) and weak (PAA, carboxylic acid) anions were studied in an effort to understand how differences in polymer chemistry impacted overall separation performance. The structure of each monomer unit is shown in Figure 5.1. It was our hypothesis that polymer structure would have a significant influence on both EOF and separation efficiency. Donath et al.[52] presented the electrophoretic analysis of polyelectrolyte-coated latex particles and

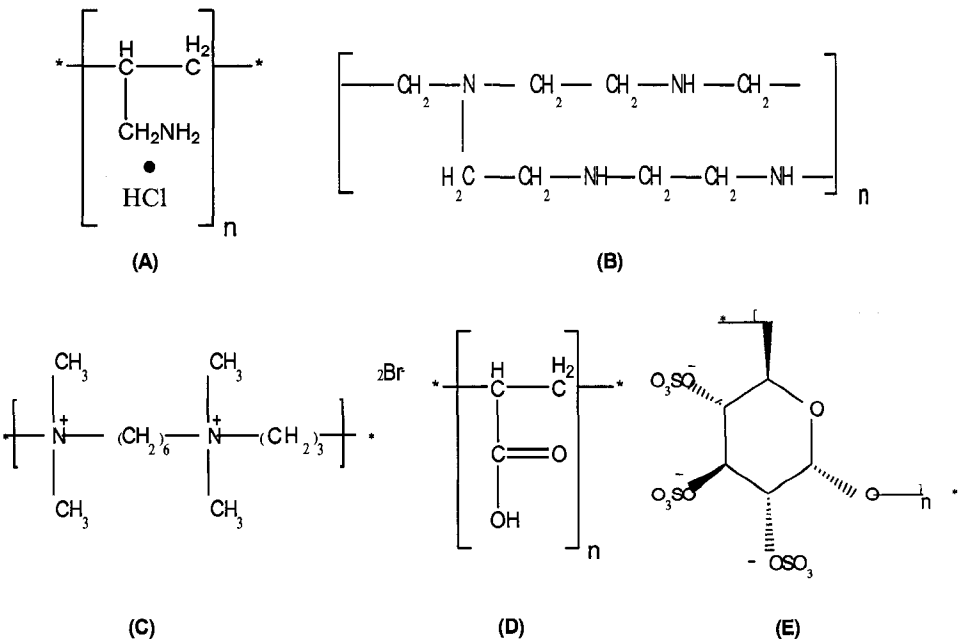

Figure 5.1. Polyelectrolyte structures:
(A) poly(allylamine)hydrochloride, PAH (B) poly(ethyleneimine), PEI
(C) polybrene, PB (D) poly(acrylic acid), PAA (E), dextran sulfate, DS.

found that the surface charge is characterized by an apparent charge density. In the coating process, charges within a thin polymer film were shielded by those at the surface. If thick and highly charged layers are employed, it is necessary to include surface conductivity for the transport of ions on and through the surface layer. If the electrophoretic flow can penetrate the charged polymer layer, the apparent charge density and thus the EOF, are significantly enhanced. In SMIL coatings, the thickness of the film is controlled by the polymer structure and the salt concentration present in the solution during deposition.

The effect of polymer chemistry on surface charge and EOF reproducibility was investigated first. Two experiments were performed; one where the anionic polymer was held constant while the cationic polymer was varied and a second where the cationic polymer was held constant while the anionic polymer was varied. Figure 5.2 shows the EOF with respect to layer number through 10-layers for the cationic polyelectrolytes polybrene (PB), poly(ethyleneimine) (PEI), and poly(allylamine hydrochloride) (PAH) using the anionic polyelectrolyte poly(acrylic acid) (PAA). Likewise, Figure 5.3 shows the comparison EOF for both anionic polyelectrolytes using PEI as the cationic polymer through 10-layers. Odd numbered layers have a cationic outer layer while even numbered layers have an anionic outer layer. Figures 5.2 and 5.3 show the expected EOF reversal when a positively charged polyelectrolyte is adsorbed as the outermost layer and normal EOF when a negatively charged polyelectrolyte is adsorbed as the outermost layer. Of note in both figures is that the magnitude of the EOF values, while varying at low layer numbers, becomes relatively consistent at higher layer numbers. In contrast, the standard deviations improve significantly from low layer numbers to high layer numbers. For example, the standard deviation for layer 1 for all of the data points combined in Figure 5.2 is

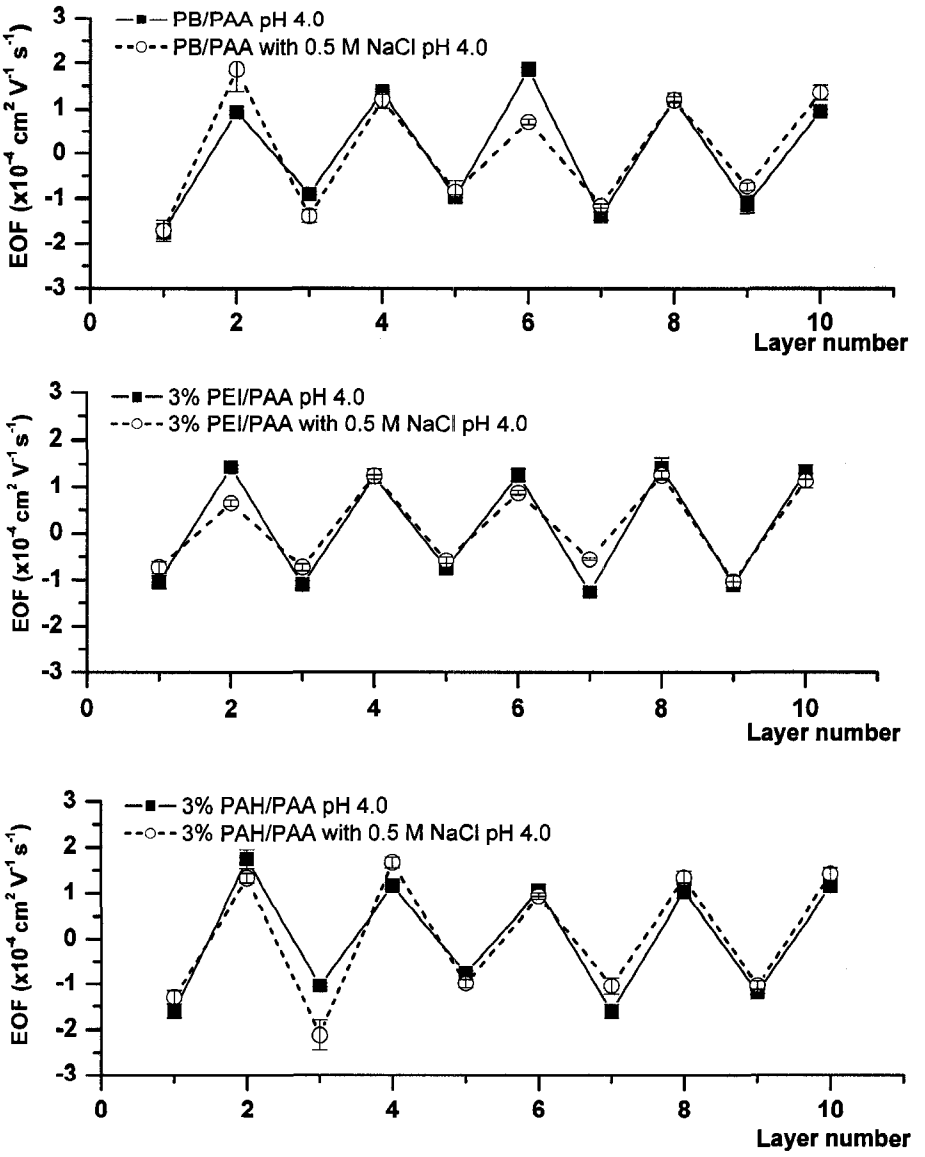

Figure 5.2. Electroosmotic flow as a function of layer number for different polyelectrolyte coating 3% PB/PAA, 3% PB/PAA with 0.5 M NaCl, 3% PEI/PAA, 3% PEI/PAA with 0.5 M NaCl, 3% PAH/PAA, 3% PAH/PAA with 0.5 M NaCl, EOF was measured in 18-20 mM phosphate buffer pH 7.0.

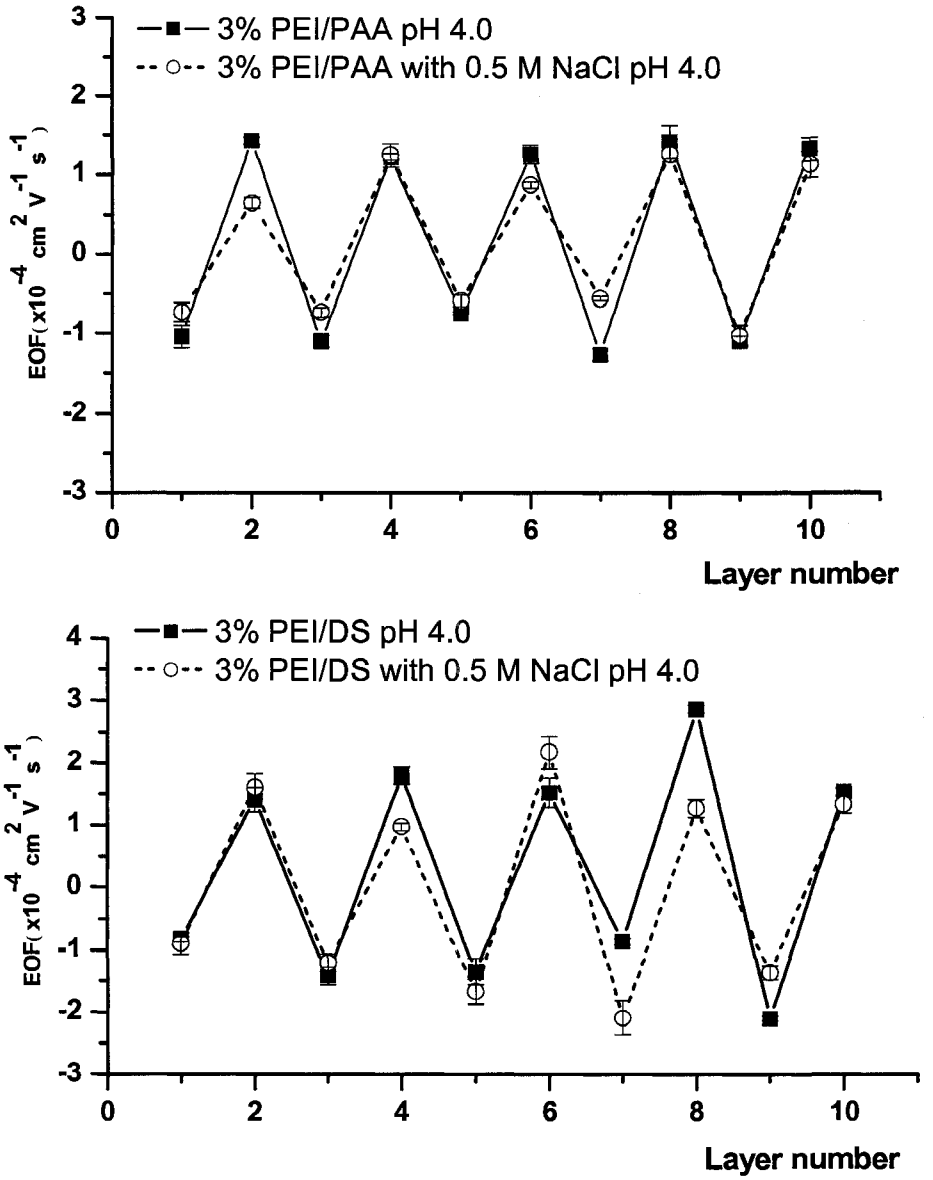

Figure 5.3. Electroosmotic flow as a function of layer number for different polyelectrolyte coating 3% PEI/PAA, 3% PEI/PAA with 0.5 M NaCl, 3% PEI/DS, 3% PEI/DS with 0.5 M NaCl. The EOF was measured in 18-20 mM phosphate buffer pH 7.0.

2.9 x10^{-5} $cm^2V^{-1}s^{-1}$ compared to layer 5 (1.44 x10^{-5} $cm^2V^{-1}s^{-1}$) and layer 10 (1.11 x10^{-5} $cm^2V^{-1}s^{-1}$). This trend is consistent throughout Figures 5.2 and 5.3 for films deposited in the absence and presence of NaCl. Variability in the EOF for films of low layer number most likely comes from variations in the film structure and/or partial surface coverage. As the films become thicker, the overall consistency of the films improves and the surface charge becomes more consistent. This data also suggests that a maximum surface charge exists for these polymers deposited on PDMS. The result is consistent with results seen for similar SMIL films on other surfaces.[23, 53]

The presence of salt during the polyelectrolyte coating step is known to increase the thickness of the resulting films.[16, 51] Results from polyelectrolyte coatings with 0.5 M NaCl versus no NaCl, however, showed no statistical difference in EOF. The adsorption of polyelectrolytes onto an oppositely charged surface is an ion exchange phenomenon where small salt ions are replaced by the polymer ions, negating the surface charge. As previously reported,[54] deposition from low concentration salt solutions makes the polyelectrolytes very efficient at seeking out surface charge. In the current example, the presence of salt in the deposition solution leads to a small reduction in the EOF of $3.40x10^{-5}\pm1.32x10^{-5}$ $cm^2V^{-1}s^{-1}$ when averaged data with salt are compared to averaged data without salt. The slight reduction in EOF is most likely the result of a partial offset of the charged groups of the SMIL layer by the salt.[54] Because the EOF was not significantly impacted by the presence or absence of salt, all additional coating experiments were performed in the absence of NaCl.

In addition to measuring EOF, separation efficiency was measured as a function of film composition and thickness using LIF detection. In all cases, the addition of SMIL coatings resulted in significant improvements in separation efficiency. Figure

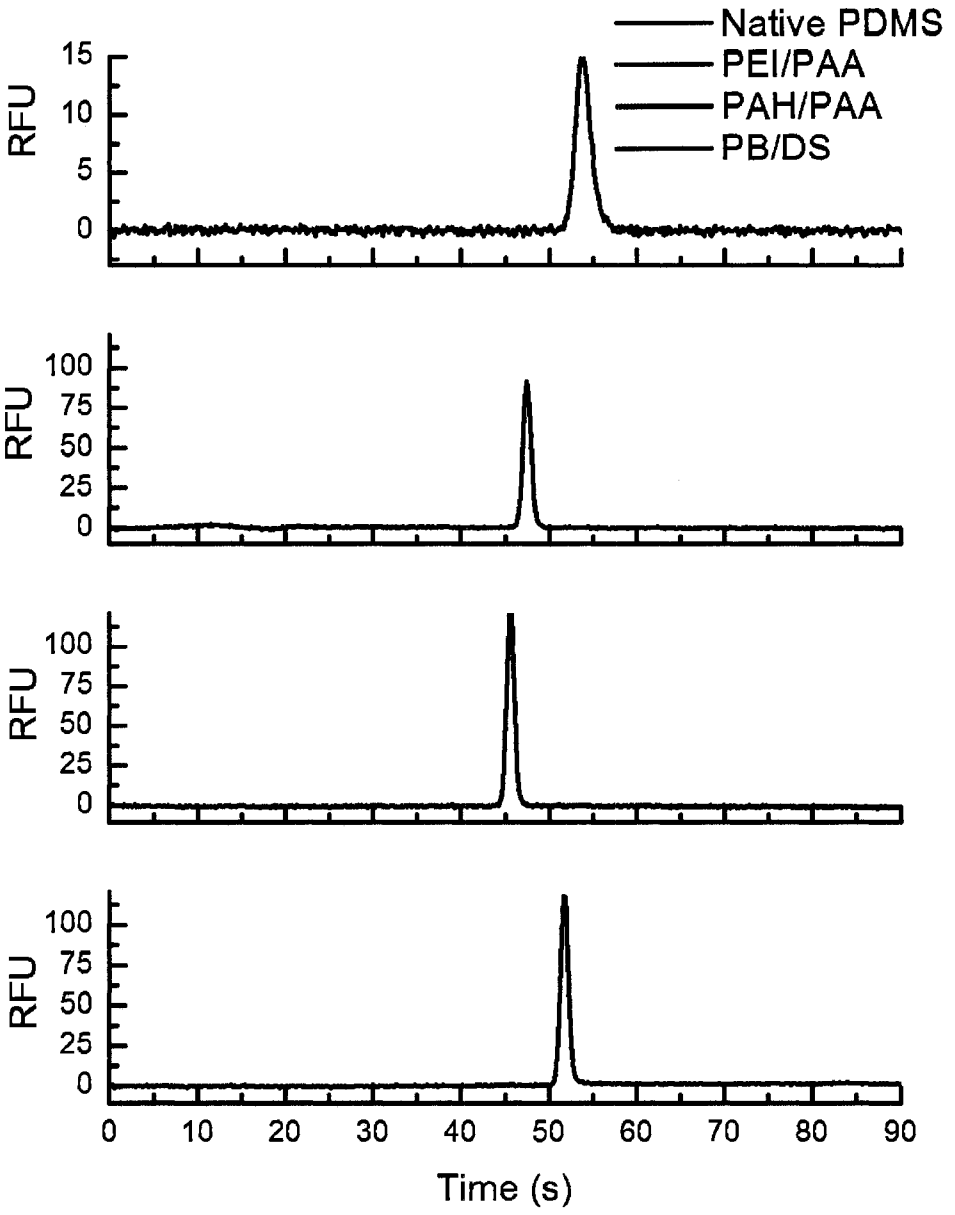

Figure 5.4. Comparison of electropherograms for FTPD using native PDMS and 6-layer coatings of PEI/PAA, PAH/PAA, and PB/DS from top to bottom, respectively.

5.4 shows representative electropherograms for native PDMS and each of the coating types at 6 layers. Separation efficiency for three different coating combinations (PB/DS, PEI/PAA, PAH/PAA) as a function of the layer number for even layer numbers up to 6 is shown in Figure 5.5. In each case there is a layer number where N reaches a maximum: for PB/DS after 6 layers (N=12,883 plates), for PEI/PAA after 6 layers (N=11,402 plates) and for PAH/PAA after 4 layers (N=11,912 plates). These values represent a 2- to 6-fold improvement in separation efficiency at their maximum values for the analyte used in this system as compared to uncoated PDMS. PB/DS generated the highest separation efficiency while PAH/PAA reaches maximum separation efficiency after only four layers. The improvement in separation efficiency is most likely due to an increase in the hydrophilicity of the channel wall.

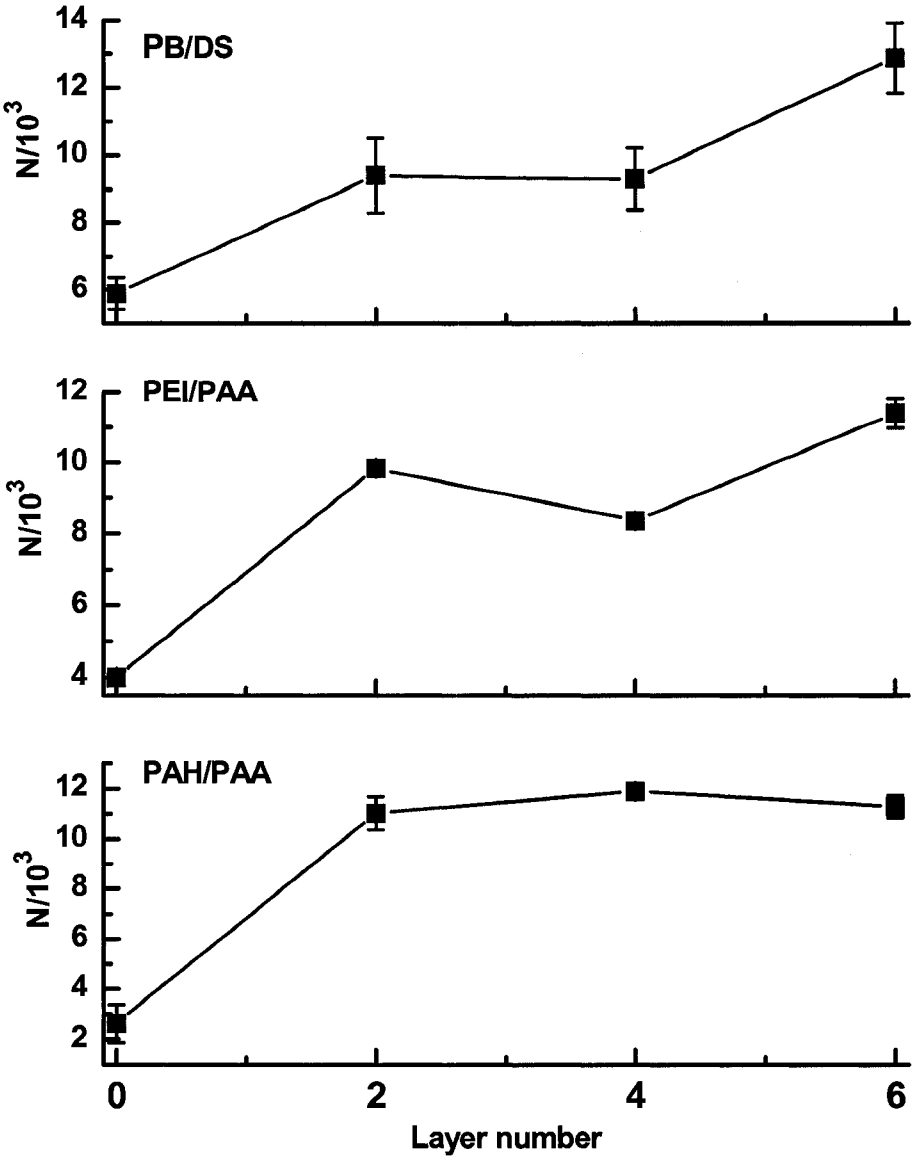

Figure 5.5. Number of theoretical plates (N) as a function of layer number. A) PB/DS alternating layers. B) PEI/PAA alternating layers. C) PAH/PAA alternating layers.

5.4 Conclusion.

In summary, layer-by-layer polyelectrolyte multilayer coatings can stabilize EOF in PDMS microchips while also enhancing separation efficiency. For all systems studied, a consistent EOF of $1.13(\pm 0.45)\times10^{-4}$ $cm^2V^{-1}s^{-1}$ was measured once four or more layers were added, suggesting that it may be possible to vary the coating chemistry to alter the separation without substantially altering the EOF. In addition, the use of SMIL coatings significantly improved separation efficiency for all systems tested. For PAH/PAA, the separation efficiency increased rapidly exhibiting a maximum after only 4 layers. The other two systems tested reached similar separation efficiencies but only after 6 layers of coating. In summary, SMIL coatings provide a simple approach to control EOF and enhance separation efficiency for PDMS microchips.

5.5 Acknowledgements

The authors thank the U.S. Army Corps of Engineers for financial support. KB was supported by a fellowship from the Thailand Research Fund through the Royal Golden Jubilee PhD Program (Grant No. PHD/0063/2547).

5.6 References

(1) Manz, A.; Graber, N.; Widmer, H. M. *Sensors and Actuators, B: Chemical* **1990**, *B1*, 244-248.

(2) Duffy, D. C.; McDonald, J. C.; Schueller, O. J. A.; Whitesides, G. M. *Anal Chem* **1998**, *70*, 4974-4984.

(3) Harrison, D. J.; Fluri, K.; Seiler, K.; Fan, Z.; Effenhauser, C. S.; Manz, A. *Science (Washington, DC, United States)* **1993**, *261*, 895-897.

(4) Harrison, D. J.; Manz, A.; Fan, Z.; Luedi, H.; Widmer, H. M. *Analytical Chemistry* **1992**, *64*, 1926-1932.

(5) Soper, S. A.; Ford, S. M.; Qi, S.; McCarley, R. L.; Kelly, K.; Murphy, M. C. *Anal Chem* **2000**, *72*, 545A.

(6) Fiorini, G. S.; Lorenz, R. M.; Kuo, J. S.; Chiu, D. T. *Analytical Chemistry* **2004**, *76*, 4697-4704.

(7) Toepke, M. W.; Beebe, D. J. *Lab on a Chip* **2006**, *6*, 1484-1486.

(8) Xiao, D.; Le, T. V.; Wirth, M. J. *Anal Chem* **2004**, *76*, 2055-2061.

(9) Garcia, C. D.; Dressen, B. M.; Henderson, A.; Henry, C. S. *Electrophoresis* **2005**, *26*, 703-709.

(10) Cox, M.; Barbier, E. B.; White, P. C.; Newton-Cross, G. A.; Kinsella, L.; Kennedy, H. J. *Prev Vet Med* **1999**, *41*, 257-270.

(11) Makamba, H. *Electrophoresis* **2003**, *24*, 3607-3619.

(12) Wang, W.; Zhao, L.; Zhang, J. R.; Wang, X. M.; Zhu, J. J.; Chen, H. Y. *J Chromatogr A* **2006**, *1136*, 111-117.

(13) Luo, Y. Q.; Huang, B.; Wu, H.; Zare, R. N. *Analytical Chemistry* **2006**, *78*, 4588-4592.

(14) Belder, D.; Ludwig, M. *Electrophoresis* **2003**, *24*, 3595-3606.

(15) Pallandre, A.; de Lambert, B.; Attia, R.; Jonas, A. M.; Viovy, J. L. *Electrophoresis* **2006**, *27*, 584-610.

(16) Graul, T. W.; Schlenoff, J. B. *Anal Chem* **1999**, *71*, 4007-4013.

(17) Jorgenson, J. W.; Lukacs, K. D. *Clin Chem* **1981**, *27*, 1551-1553.

(18) Shariff, K.; Ghosal, S. *Analytica Chimica Acta* **2004**, *507*, 87-93.

(19) Ghosal, S. *Electrophoresis* **2004**, *25*, 214-228.

(20) Hu, S. W.; Ren, X. Q.; Bachman, M.; Sims, C. E.; Li, G. P.; Allbritton, N. *Analytical Chemistry* **2002**, *74*, 4117-4123.

(21) Thorsen, T.; Maerkl, S. J.; Quake, S. R. *Science* **2002**, *298*, 580-584.

(22) Linder, V.; Verpoorte, E.; Thormann, W.; de Rooij, N. F.; Sigrist, H. *Anal Chem* **2001**, *73*, 4181-4189.

(23) Barker, S. L. R.; Ross, D.; Tarlov, M. J.; Gaitan, M.; Locascio, L. E. *Anal Chem* **2000**, *72*, 5925-5929.

(24) Barker, S. L. R.; Tarlov, M. J.; Canavan, H.; Hickman, J. J.; Locascio, L. E. *Anal Chem* **2000**, *72*, 4899-4903.

(25) Liu, Y.; Fanguy, J. C.; Bledsoe, J. M.; Henry, C. S. *Anal Chem* **2000**, *72*, 5939-5944.

(26) Vickers, J. A.; Caulum, M. M.; Henry, C. S. *Anal Chem* **2006**, *78*, 7446-7452.

(27) Katayama, H.; Ishihama, Y.; Asakawa, N. *Anal Chem* **1998**, *70*, 2254-2260.

(28) Katayama, H.; Ishihama, Y.; Asakawa, N. *Anal Chem* **1998**, *70*, 5272-5277.

(29) Kamande, M. W.; Kapnissi, C. P.; Zhu, X.; Akbay, C.; Warner, I. M. *Electrophoresis* **2003**, *24*, 945-951.
(30) Bai, X.; Roussel, C.; Jensen, H.; Girault, H. H. *Electrophoresis* **2004**, *25*, 931-935.
(31) Ro, K. W.; Chang, W. J.; Kim, H.; Koo, Y. M.; Hahn, J. H. *Electrophoresis* **2003**, *24*, 3253-3259.
(32) Xiao, Y.; Wang, K.; Yu, X. D.; Xu, J. J.; Chen, H. Y. *Talanta* **2007**, *72*, 1316-1321.
(33) Decher, G. *Photonic and Optoelectronic Polymers* **1997**, *672*, 445-459.
(34) Decher, G.; Hong, J. D.; Schmitt, J. *Thin Solid Films* **1992**, *210*, 831-835.
(35) Dubas, S. T.; Schlenoff, J. B. *Macromolecules* **2001**, *34*, 3736-3740.
(36) Schlenoff, J. B.; Ly, H.; Li, M. *Journal of the American Chemical Society* **1998**, *120*, 7626-7634.
(37) Gao, H.; Jiang, T.; Heineman, W. R.; Halsall, H. B.; Caruso, J. L. *Fresenius' Journal of Analytical Chemistry* **1999**, *364*, 170-174.
(38) Dubas, S. T.; Farhat, T. R.; Schlenoff, J. B. *Journal of the American Chemical Society* **2001**, *123*, 5368-5369.
(39) Maichel, B.; Gogova, K.; Gas, B.; Kenndler, E. *Journal of Chromatography A* **2000**, *894*, 25-34.
(40) Potocek, B.; Chmela, E.; Maichel, B.; Tesarova, E.; Kenndler, E.; Gas, B. *Analytical Chemistry* **2000**, *72*, 74-80.
(41) Wang, Y.; Dubin, P. L. *Analytical Chemistry* **1999**, *71*, 3463-3468.
(42) Chiu, R. W. *Anal. Chim. Acta* **1995**, 193-201.
(43) Cordova, E.; Gao, J. M.; Whitesides, G. M. *Analytical Chemistry* **1997**, *69*, 1370-1379.
(44) Liu, Y.; Vickers, J. A.; Henry, C. S. *Anal Chem* **2004**, *76*, 1513-1517.
(45) Liu, Y.; Wipf, D. O.; Henry, C. S. *Analyst* **2001**, *126*, 1248-1251.
(46) McDonald, J. C.; Whitesides, G. M. *Acc Chem Res* **2002**, *35*, 491-499.
(47) Wu, D. P.; Zhao, B. X.; Dai, Z. P.; Qin, J. H.; Lin, B. C. *Lab on a Chip* **2006**, *6*, 942-947.
(48) Huang, X.; Gordon, M. J.; Zare, R. N. *Anal Chem* **1988**, *60*, 1837-1838.
(49) Pittman, J. L.; Henry, C. S.; Gilman, S. D. *Anal Chem* **2003**, *75*, 361-370.
(50) Johnson, M. E.; Landers, J. P. *Electrophoresis* **2004**, *25*, 3513-3527.
(51) Schlenoff, J. B.; Ly, H.; Li, M. *J Am Chem Soc* **1998**, *120*, 7626-7634.
(52) Donath, E.; Walther, D.; Shilov, V. N.; Knippel, E.; Budde, A.; Lowack, K.; Helm, C. A.; Mohwald, H. *Langmuir* **1997**, *13*, 5294-5305.
(53) Schlenoff, J. B.; Dubas, S. T. *Macromolecules* **2001**, *34*, 592-598.
(54) Dubas, S. T.; Schlenoff, J. B. *Macromolecules* **1999**, *32*, 8153-8160.

Chapter 6

Monitoring Perchlorate in Water Using

Microchip Capillary Electrophoresis

Perchlorate is a small, persistent, highly water soluble anion arising from both geogenic and anthropogenic sources. Anthropogenic sources include solid rocket fuel, matches, dyes, paints, airbag inflators, pyrotechnics, flares, and fertilizers, with solid rocket fuel being the single largest contributor.[1] Perchlorate is able to travel long distances in groundwater and is therefore a pervasive problem once released into the environment.[2] Widespread ClO_4^- contamination was first discovered in the United States in 1997, when an analytical method with a reporting limit of 4 ppb was developed by Hautman and coworkers.[3] Perchlorate is a significant concern for the water supply because it inhibits the uptake of iodide by the thyroid preventing it from making enough thyroxine for proper endocrine function.[2] Here a new microchip capillary electrophoresis method is reported for determination of perchlorate in surface and drinking water. To achieve the separation, a counter electroosmotic flow separation was developed using the zwitterionic surfactant, N-dodecyl-N, N-dimethyl-3-ammonio-1-propanesulfonate (DDAPS). The method is capable of resolving perchlorate from common interferences in less than four minutes while achieving detection limits of 0.5 (± 0.03) ppb (n = 4). Sample pretreatment is not required as only small, highly mobile anions are injected, while the majority of other interfering compounds and particulate matter contaminants are excluded by the counter flow separation mode. Analysis of waste water, drinking water, explosive residues, and river water samples is presented, illustrating the effectiveness of the overall approach.

This chapter is a modification of a manuscript written by Brian Dressen to be submitted to Analytical Chemistry. All work performed by Brian Dressen.

6.1 Introduction

Human exposure to perchlorate has become an important problem in environmental research.[4] Perchlorate inhibits uptake of iodide into the thyroid gland, leading to irregular production of thyroid hormone and giving rise to developmental problems,[2] neurological disorders,[5] reduced intelligence,[6] and cerebral palsy.[7] Perchlorate is wide spread as a result of both geogenic and anthropogenic[8] sources and has been detected in drinking water,[9] food,[9] and both human and cow milk.[10, 11] The total extent of human exposure to perchlorate is largely unknown at this time because of the limited testing of drinking water and food supplies. Currently, the EPA draft estimate of a regulatory limit for perchlorate in drinking water is 1 ppb, based on toxicity assessment.[12] This would make perchlorate one of the most regulated ions in water with the exception of bromate.[12-16] Sensitive and selective methods for routine, in field monitoring would aid in mitigating exposure as well as tracing remediation efforts.

The most common EPA approved methods for perchlorate detection are ion chromatography (IC) coupled to conductivity detection (CD) and IC coupled to mass spectrometry (MS).[3, 17-19] Ion chromatography coupled to conductivity detection currently dominates environmental perchlorate determination because it has a low limit of detection (0.77 ppb)[13] and the instrumentation is widely available and inexpensive when compared to IC-MS systems. When positive identification of perchlorate is desired, IC coupled to mass spectrometry is used.[20-22] Mass spectrometric detection allows for unequivocal identification of perchlorate and achieves lower limits of detection than CD methods. IC-MS systems are, however,

more expensive to operate and maintain than IC-CD systems and thus few laboratories possess this capability.

While IC methods are capable of isolating and detecting perchlorate, their size, complexity, and cost limit use to established laboratories. Furthermore, these methods non portable, requiring the sample be brought to the instrument. For these reasons, alternative fieldable analytical methods for detecting perchlorate have been explored. Several groups have used capillary electrophoresis (CE) using UV detection for perchlorate analysis.[23-26] Indirect UV detection is required, however, generating detection limits in the μM range. Others have developed infrared (ATR-FTIR)[27, 28] detection systems using affinity chemistry to concentrate the perchlorate within a detection range of 4 ppb. Finally, surface enhanced raman spectroscopy with gold nanoparticles has also been used to achieve detection limits of 500 ppb.[29] These optical methods are simple and robust, but generally lack the limit of detection capabilities needed for trace analysis. In the current report, microchip CE is used to measure ClO_4^-. Previously two examples of portable conventional CE separation of perchlorate have been shown using contactless conductivity detection[30] and indirect photometric detection.[31] These reports show ClO_4^- detection limits of 13 ppb and 900 ppb, respectively, higher than levels targeted by the EPA. All of these methods are less expensive than IC but lack either the LOD or selectivity required for in-field use. Inexpensive, near-real time analyzers are still needed that are capable of field measurements to allow continuous monitoring perchlorate at low ppb levels.

Microchip CE devices enjoy low cost fabrication and instrumentation as well as the potential for portability. In recent years, the microchip field has gained a strong

foothold in emerging laboratory technology.[32-35] Microchip devices promise to be able to perform the same analysis as conventional scale systems with significant reductions in sample and reagent consumption, analysis times, and instrumentation costs.[36] Effective separation of inorganic anions requires an effective detection method. Several research groups have explored electrochemical methods of detection for microchip CE, with amperometry[37, 38] and conductivity[39, 40] being the two most prominent. Amperometry works well for electroactive species but many analytes, such as inorganic ions, cannot be detected with this method. Conductivity detection is universal and does not require sample derivitization. A commercial instrument for contact conductivity for CE detection became available in the 1990s.[41] Microchip conductivity systems have also been developed with either contact or contactless electrode configurations.[30, 42-58]

Micellar electrokinetic chromatography (MEKC), developed by Terabe[59, 60] adds an additional separation regime that relies on the association of analytes with surfactant micelles. In MEKC analytes divide their time between the aqueous phase and the micelle. The surfactant micelles have different migration velocity and/or direction than the analyted[61] and the migration rates of ions will vary with their degree of association. Surfactant micelles act as a chromatographic pseudo-stationary phase enhancing the resolving power through selective interactions. While ionic surfactants such as sodium dodecyl sulfate are the most common stationary phases in MEKC, a number of neutral and zwitterionic surfactants have also been used. Haddad[23] and Lucy[62] described interactions of the zwitterionic surfactant N-dodecyl-N, N-dimethyl-3-ammonio-1-propanesulfonate (DDAPS) with a series of both

polarizable and non-polarizable ions including ClO_4^-. DDAPS was shown to cause significant changes in migration time for ions with increasing polarity when it was added above the critical micelle concentration (CMC).

The mobility of a species is directly related to the ions in the BGE and generally sample stacking will occur when a boundary exists between sample regions and the surrounding BGE.[63] Ions present in low conductivity zones will have higher mobility than in high conductivity zones. The ions in the low conductivity region will migrate rapidly towards the boundary, where they will slow down and "stack" like a traffic jam. This type of sample stacking is known as field amplified sample stacking (FASS).[64] A second method of sample stacking is known as sweeping and occurs when a BGE containing surfactant micelles is used and the sample plug does not contain micelles. The sample ions are slowed down by the micelles as they migrate into the micelle rich region and the sample is concentrated in this boundary zone. Concentration rates exceed 5000 fold.[65] Sweeping is now defined as a situation in which the BGE has a separation vector and the sample plug does not.[66]

In this work I have developed a microchip CE system capable of separating and detecting ClO_4^- in surface and ground water. Separation of ClO_4^- occurs in less than four minutes with no sample pretreatment. The use of the zwitterionic surfactant, N-dodecyl-N, N-dimethyl-3-ammonio-1-propanesulfonate has introduced a chromatographic component to the separation system providing resolution of perchlorate from common high mobility anions such as chloride, nitrate, and sulfate as well as an additional mode of sample stacking, leading to a 0.5 ppb ± 0.03

detection limit. Samples of surface and waste water were analyzed without pretreatment and levels of perchlorate determined.

6.2 Experimental

6.2.1 Materials. The following materials were purchased and used as received: 100 mm silicon wafers ((100) Silicon, Boise, ID, USA), poly(dimethylsiloxane) (PDMS) (Dow Corning, San Diego, CA) as Sylgard 184 elastomer and curing agent (Dow Corning). Biograde morpholinoethanesulfonic acid (MES, Acros Organics), L-histidine, methanol (Fisher Scientific Fair Lawn, NJ), potassium thiocyanate (Sigma-Adrich), Au wire ((99.9% 25 μm diameter) Goodfellow Huntingdon, England), SU-8 2035 photoresist (Micro Chem., Newton, MA, USA), propylene glycol methyl ether acetate (Aldrich, St. Louis, MO) and N-dodecyl-N, N-dimethyl-3-ammonio-1-propanesulfonate (DDAPS) (Sigma-Aldrich).

6.2.2 Fabrication. PDMS microchips were fabricated using existing methodologies.[36, 67] Briefly, SU-8 2035 (Microchem, Newton, MA) was spin-coated onto 100 mm silicon wafers (Silicon Inc, Boise, ID) to a thickness of 50 μm. A high resolution transparency (CSU Printing Services) was used as the mask to define the channel dimensions. After exposure and developing, patterned silicon masters were treated with hexamethyldisilazane (HMDS) (Sigma-Aldrich) to aid the release of PDMS from the mold. Vapor deposition was performed by placing the wafer and a small vial containing 500 μL of HMDS in a crystallization dish, the dish was then covered with foil and placed in a 65° C oven for 4-6 h. PDMS was mixed in a 10:1

with curing agent, degassed and poured over the master. Once cured (at least 2h at 60°C) The PDMS was removed from the mold, trimmed to the desired size, reservoir holes were punched with 5mm biopsy punches (Robbins instruments) and 2 Au electrodes were placed in designated electrode channels located at the end of the separation channel.[68, 69] The final device was assembled and external connections to the microwires made using 18 gauge Cu wire and conductive silver paint. A diagram of the microchip and a photograph of the working electrodes are shown in Figure 6.1.

6.2.3. Electrophoresis. Contact conductivity detection was used for detection in the current application. A Dionex CD20 was modified to work with microchip devices by removing the LC conductivity cell and attaching the leads to the detection electrodes embedded in the microchips. The CD20 range was set to 0-300 μS and output was 0-1 V. Data was collected with a National Instruments USB-6008 DAQ connected to LabView 8.0 software collecting at an effective rate of 16 Hz. A laboratory built high voltage power supply was used for all experiments.[70] Before each use the microchips were rinsed with deionized (18 MΩ, Millipore, Billerica, Massachusetts) water followed by a buffer rinse and equilibration for at least 10 min under an applied potential of either + 400 V or -600 V depending on the application. Solutions were introduced into the reservoirs via volumetric pipette and driven into the capillaries by the application of external pressure applied from a syringe. Each of the reservoirs was loaded with an equal volume of solution to minimize hydrodynamic flow. Injection was performed in gated mode.[71]

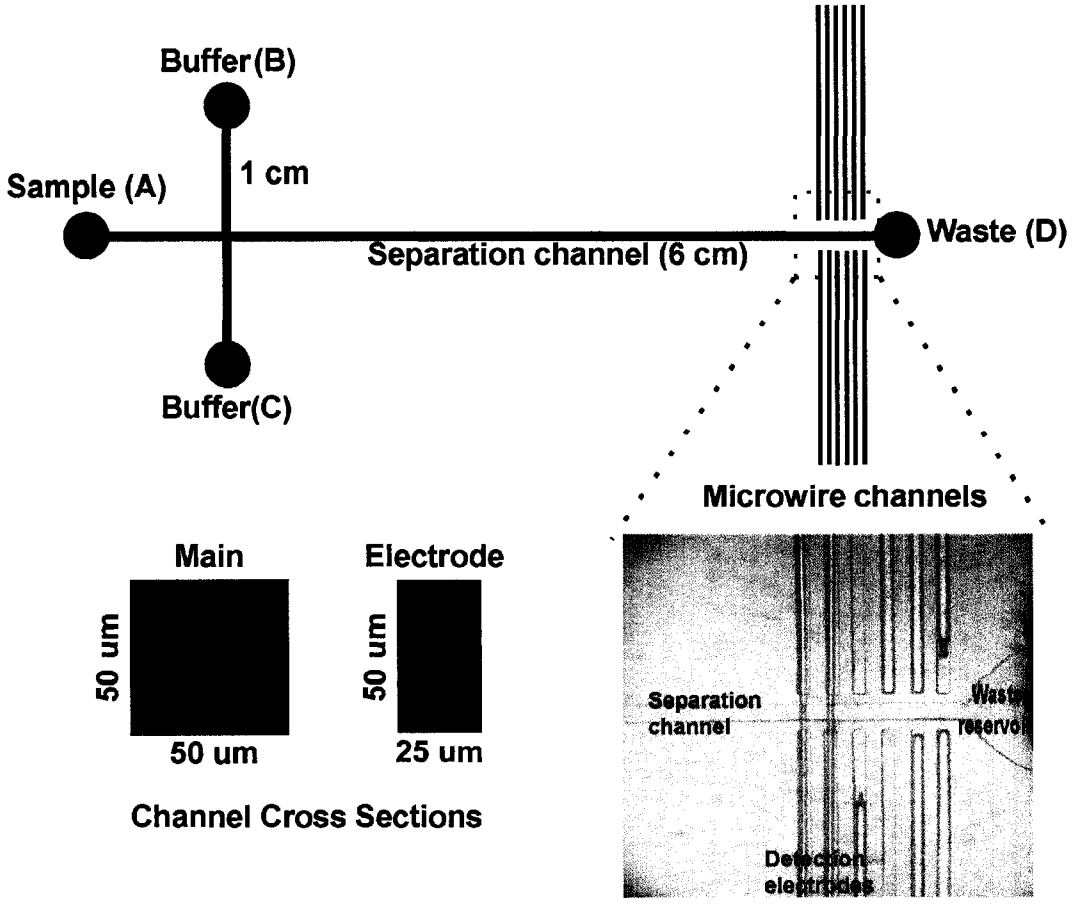

Figure 6.1 Diagram and photograph of microwire electrode area of microchip used for all experiments.

Potassium thiocyanate was added as an internal standard to increase accuracy of migration time and peak height quantification.

6.2.4 Sampling. Sample collection utilized new, DI water rinsed glass vials (3 mL, Fisher, Leicestershire, GB) that were filled and emptied 3 times with the sample water prior to final filling. Nitrile gloves were used to minimize contamination. Each sample location was identified using a handheld GPS (Garmin, Olathe, Ks).

6.3 Results and Discussion

6.3.1 Separation conditions. There are many methods to generate selective separations in CE and the majority of these methods use either low electroosmotic flow (EOF) or co-EOF modes where the velocity of the analyte is in the same direction as the EOF. For high mobility ions, however, this can make separation challenging. In a reverse polarity system perchlorate migration is very similar to likely high abundance ions like nitrate and sulfate, resulting in poor resolution between the peaks. High concentrations of interfering analytes would likely result in a single peak overcoming the perchlorate peak. Moving the separation to the microchip format only compounds this issue because of the short capillary length (4-5 cm) relative to conventional systems (20-50 cm). To overcome this challenge, three general separation approaches were tested in an effort to resolve perchlorate from common interfering anions. Figure 6.2 shows a series of representative electropherograms for different background electrolyte compositions tested in this work, all obtained using 1 mM KCl, KNO_3, K_2SO_4, $KClO_4$, and KI as the standard

mixture. The first system tested consisted of 10 mM MES/His buffer at pH 6 with added TTAB surfactant to reverse the EOF, with positive potential being applied to the sample waste and buffer waste reservoirs. In this scheme the anions are attracted to the positive potential being applied at the sample waste and waste reservoir while the electroosmotic flow (EOF) is moving with the anions. As can be seen in the electropherogram, the electrophoretic velocity of the anions is such that the anions migrate quickly and resolution does not occur. The second approach was to perform a counter EOF separation. If a negative potential is applied, Fig. 2.b results, in which the analytes have an electrophoretic migration towards the ground electrodes, opposing the EOF. Three peaks are observed in this separation, but resolution of perchlorate from possible interferences or high concentrations of other anions is unlikely. In an effort to increase the resolution of perchlorate a third system (Figure 6.2.C) used the surfactant, DDAPS, which has a known strong affinity for perchlorate, to the background electrolyte to further resolve ClO_4^- from other anions.[23] Several reports have shown the migration of anions to be affected by the presence of zwitterionic surfactants, particularly when the surfactants are added above their critical micelle concentration (CMC).[23, 62, 72-76] Micelles interact with analytes in CE separations and because the analyte-micelle complexes have different motilities than the analytes alone, they migrate at a different velocity. This change in migration is due to the creation of a pseudo stationary phase, leading to a chromatography like separation system.[77, 78] In particular, N-dodecyl-N, N-dimethyl-3-ammonio-1-propanesulfonate (DDAPS) (cmc=3 mM)[75] was shown to interact with perchlorate more strongly than either chloride, nitrate, iodide or sulfate.[23]

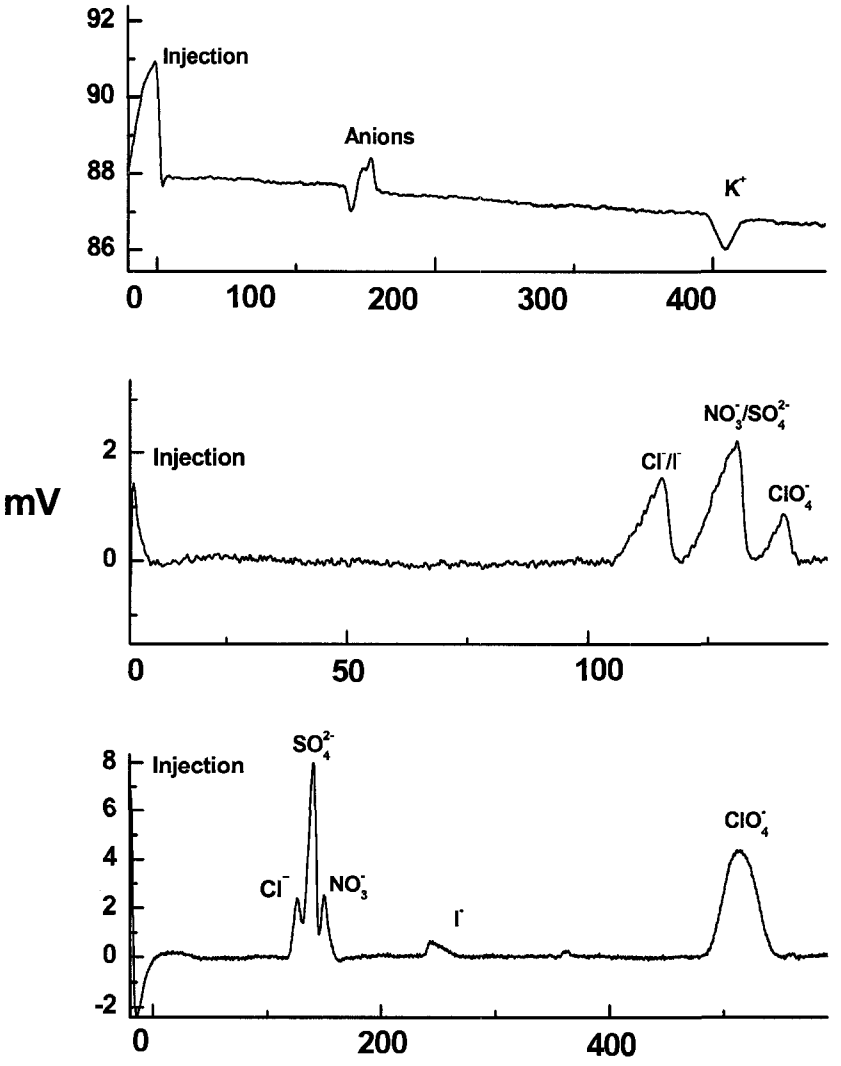

Figure 6.2 Elecropherograms showing progression of separation conditions. A. +400 V potential 1 mM KCl, K_2SO_4, KNO_3, KI, $KClO_4$ 10 mM MES-His TTAB buffer pH 6. B. -600 V potential 10 mM MES-His buffer pH 6. C. -600 V potential 10 mM MES-His buffer pH 6 with 10 mM DDAPS. Injection from water.

This interaction is likely caused by two separate effects.[23, 76] Perchlorate is a polarizable anion, and can interact with the hydrophobic interior of a micelle, increasing the interaction of ClO_4^- with the DDAPS micelle. Perchlorate also interacts with the quaternary amine and sulfate head group found on the surfactant through shifting of the electron cloud on the oxygen atoms to increase its association with the micelle.[79] DDAPS was added at a concentration of 10 mM to the MES-His buffer. Sufficient resolution of perchlorate was achieved from all other analytes.

6.3.2 DDAPS Concentration. In an effort to further optimize the chemistry for perchlorate separation, and to reduce analysis time, a study of varying concentrations of DDAPS was performed (Figure 6.3). As seen previously[75] and supported by Woodland and Lucy,[62] an increase in migration time was observed for those anions most strongly associated with the DDAPS micelle. Perchlorate separation, however, was not shown in the previous reports. Figures 6.3 and 6.4 show a dramatic reduction in migration the time and a decrease in the background noise for reduced surfactant concentration. Resolution of ClO_4^- from other ions was also seen to be dependent on the surfactant concentration as expected, with resolution lost when DDAPS concentrations were below the CMC. Those ions most strongly associated with the DDAPS micelle (ClO_4^-, I^-) show the largest change in migration time. The ions that show little interaction with DDAPS undergo changes in migration time consistent with the EOF changes expected with the addition of the surfactant. While the increasing DDAPS concentration increased the resolution, lower concentrations showed improvement in analysis time, peak shape, and a reduction in background

noise. Resolution of perchlorate from the nitrate/sulfate peak decreased from 13.14 to 4.2 and 0.82 as DDAPS concentration was reduced from 10 to 6.6 to 3.3 mM respectively. The migration and total analysis time was reduced from 446 s to 180 s when the optimized 5 mM DDAPS concentration was used instead of 10 mM. The detection limit was found to be 600 ± 23 ppb (n=3) for a 3 s injection. In an effort to increase the resolution of perchlorate a third system (Figure 6.2.C) added a surfactant, DDAPS, with known strong affinity for perchlorate to the background electrolyte.[23] Several reports have shown the migration of anions to be affected by the presence of zwitterionic surfactants, particularly when the surfactants are added above their critical micelle concentration (CMC).[23, 62, 72-76] Micelles interact with analytes in CE separations and because the analyte-micelle complexes have different motilities than the analytes alone, they migrate at a different velocity. This change in migration is due to the creation of a pseudo stationary phase, leading to a chromatography like separation system.[77, 78] In particular, N-dodecyl-N, N-dimethyl-3-ammonio-1-propanesulfonate (DDAPS) (cmc=3 mM)[75] was shown to interact with perchlorate more strongly than either chloride, nitrate, iodide or sulfate.[23]

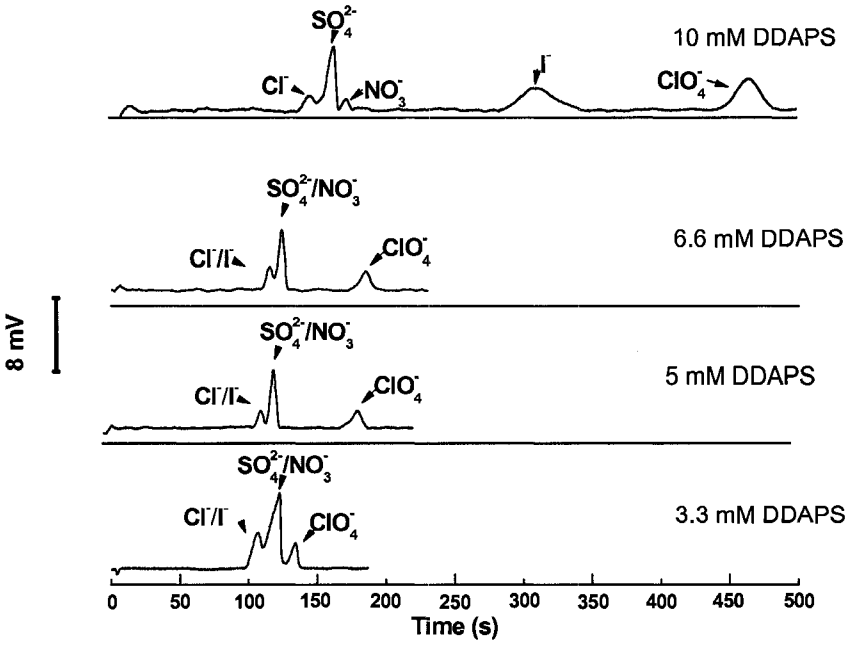

Figure 6.3 Effect of DDAPS concentration on resolution and baseline noise. 100 μM analyte concentration. Other conditions as in Figure 6.2.C

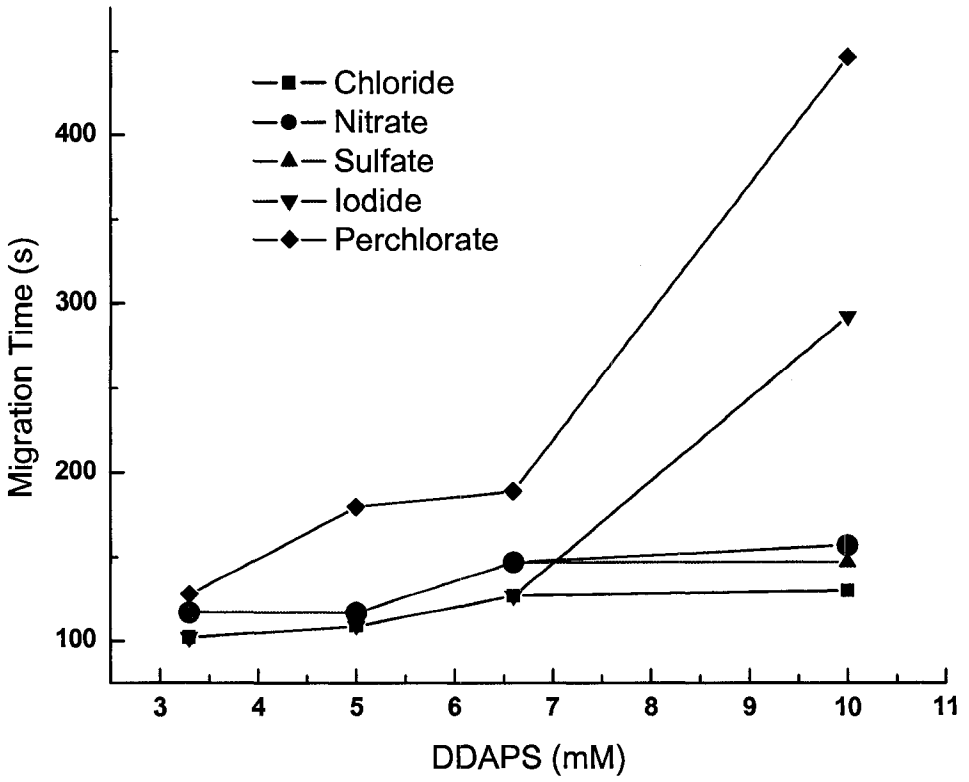

Figure 6.4 Migration time of each analyte at various DDAPS concentration

6.3.3 Improvement of LOD: Stacking. Limits of detection for MCE with conductivity detection has largely been limited to the ppm range for most inorganic species.[58] To be effective for environmental perchlorate, however, detection limits must be pushed to 1 ppb. To achieve this, a combination of stacking techniques was used. First, all samples were injected from water. The injection time of 20 s led to peaks that had a baseline width of 9 ±2.1 s (n=9), indicating significant stacking of the analyte band. The electric field is higher in the water based sample due to its higher resistance than in the relatively high concentration background electrolyte[80] causing field amplified sample stacking (FASS).[81] The difference in field results in the mobility of sample ions being greater in sample solution than the background electrolyte, as a result, the ions are accelerated towards the boundary where they slow down and stack. An additional form of stacking known as sweeping occurs if surfactant above the CMC is present in the BGE and the surfactant has lower or opposite mobility when compared to the analytes.[66] The analytes slow down at the interface of the sample matrix and surfactant-containing BGE. The surfactant micelles interact with the anions as they enter the BGE causing narrowing of the sample band even further and increasing the concentration of anions in the sample plug. By increasing the injection time and using the stacking phenomenon, improvements in the limit of detection were 1100-fold, as the limit of detection for 20 second stacking injections was found to be 0.5 ± 0.03 ppb (n=3). Perchlorate analysis as a function of concentration with the optimized system is shown in Figure 6.5.

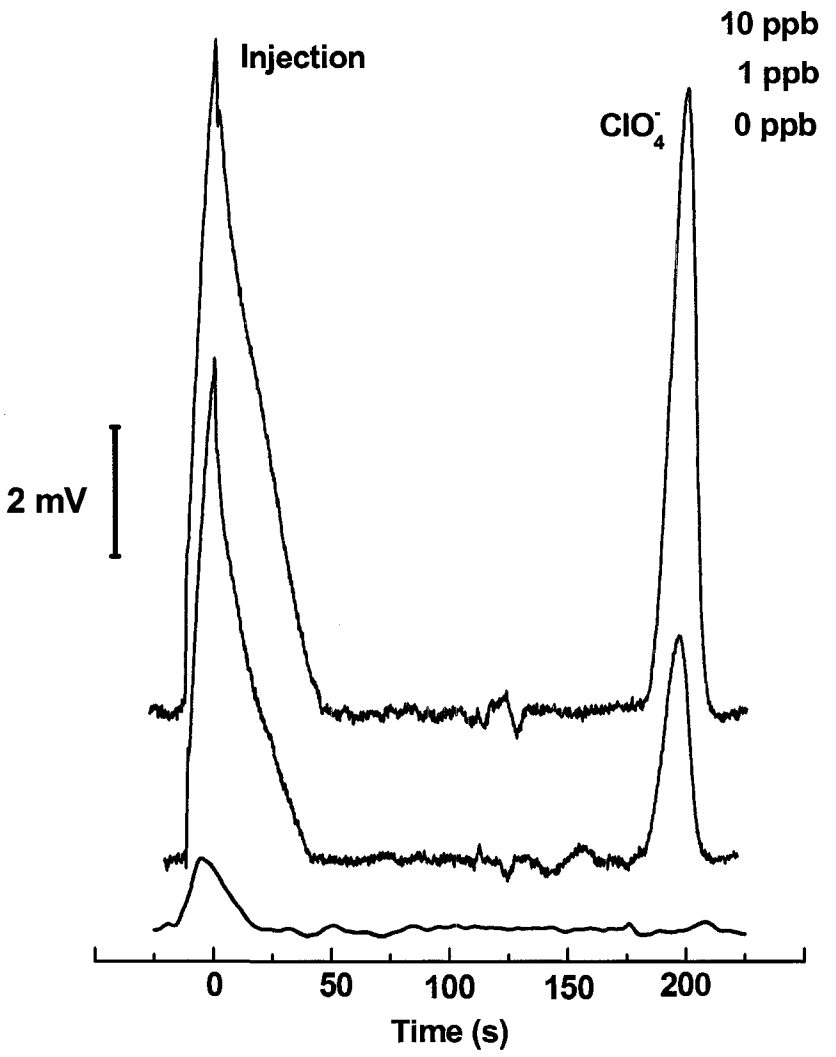

Figure 6.5 Successive injections of 0, 10, and 100 ppb perchlorate on optimized microchip system. 10 mM MES-His pH 6 with 5 mM DDAPS -600 V potential 20 s injection.

6.3.4 Reproducibility. Reproducibility studies were run using optimized separation conditions to elucidate figures of merit. Chip-to-chip quantization variability has shown to be 15% (n = 9) while run-to-run variability is 3.9% (n = 3). While the chip-to-chip variability is larger than we desired, it is within acceptable error for other capillary electrophoresis methods. However, this method in its current sate will not meet EPA requirements for reproducibility. Studies are currently underway to improve repeatability. Three separate chips were used for this study and were fabricated by two different workers, illustrating reproducibility for multiple users. Percent recovery within the linear range was found to be 91-108% across 3 chips. All calculations performed with raw data, while data for figures has been baseline adjusted and smoothed by boxcar averaging.

6.3.5 Analysis of Surface Water. To demonstrate the ability to detect perchlorate in surface and drinking water, samples were taken from a Lake Agnes where human impact should be minimal. Subsequent samples were collected approximately every 10 miles down river for a total of 9 samples. Figure 6.6 shows elecropherograms of the pristine lake sample as well as one sample collected at a popular spot along the river where human activity is more significant. Also shown is the same sample spiked with 0.5 ppb ClO_4^-. Thiocyanate (SCN^-) was added as an internal standard to correct for any changes in peak area caused by the sample matrix as well as variations in migration time. The pristine lake sample contained no detectable perchlorate, nor did all the downstream samples except the final 2 where more human activity was observed. The samples collected at these locations show low levels of perchlorate 0.5

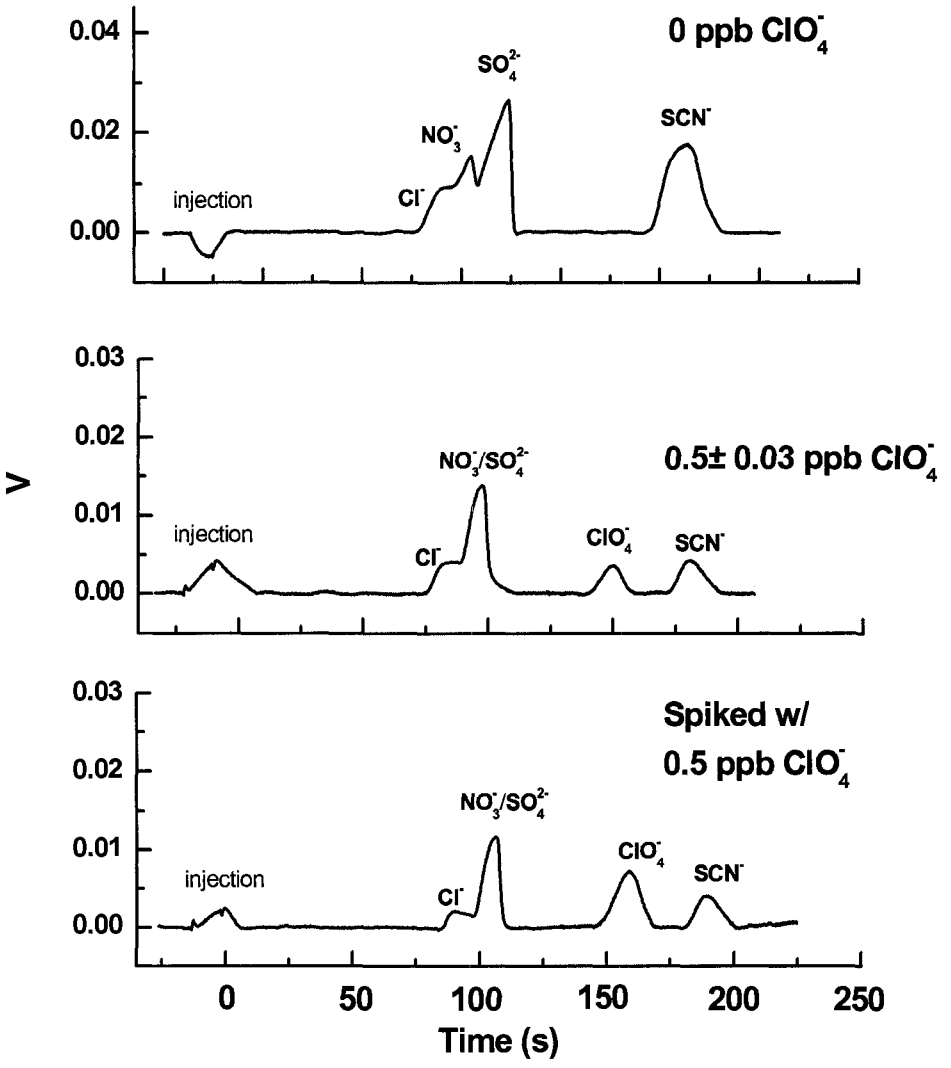

Figure 6.6 Analysis of Lake Agnes, downstream Poudre River sample, and downstream spiked sample Conditions as in figure 6.5.

± 0.03 ppb (n=3) and 0.7 ± 0.03 ppb (n=3). It should be noted that these values are below EPA action limits and not likely to be reported even if testing occurred in this watershed. To the best of our knowledge, perchlorate levels have not been measured at these locations. These data demonstrate the ability of the method for determination of perchlorate in surface water. It should also be noted that very small volumes of sample are required to perform these analysis. 1 mL was sufficient for many replicate analyses, making this method extremely amenable to analysis of remote areas where bringing back large volumes of sample is impractical. The other significant item of merit is that all cations, neutrals, organics, and other interfering analytes are selected out before separation begins due to the counter EOF separation, giving elecropherograms that are simple and free from extraneous peaks. The presented method requires only simple filtration of very turbid waters for analysis.

6.3.6 Wastewater from Explosives Packing Facility. A sample from a military explosives packing plant was obtained and perchlorate levels determined (Figure 6.7). This sample contained known high levels of perchlorate reported by EPA method 314 to be 247.8 ±12.39 ppb. Our analysis showed 270 ± 13 ppb, 109% of the known. EPA method 314 specifies 10% allowable error. The agreement between the two methods illustrates the viability of the microchip CE device for trace analysis of perchlorate in water samples. The sample tested here contained high levels of dissolved solids, which were not injected with the sample anions into the separation channel, eliminating the need for pretreatment of samples. High background levels of ions leads to an increase in the LOD for this method

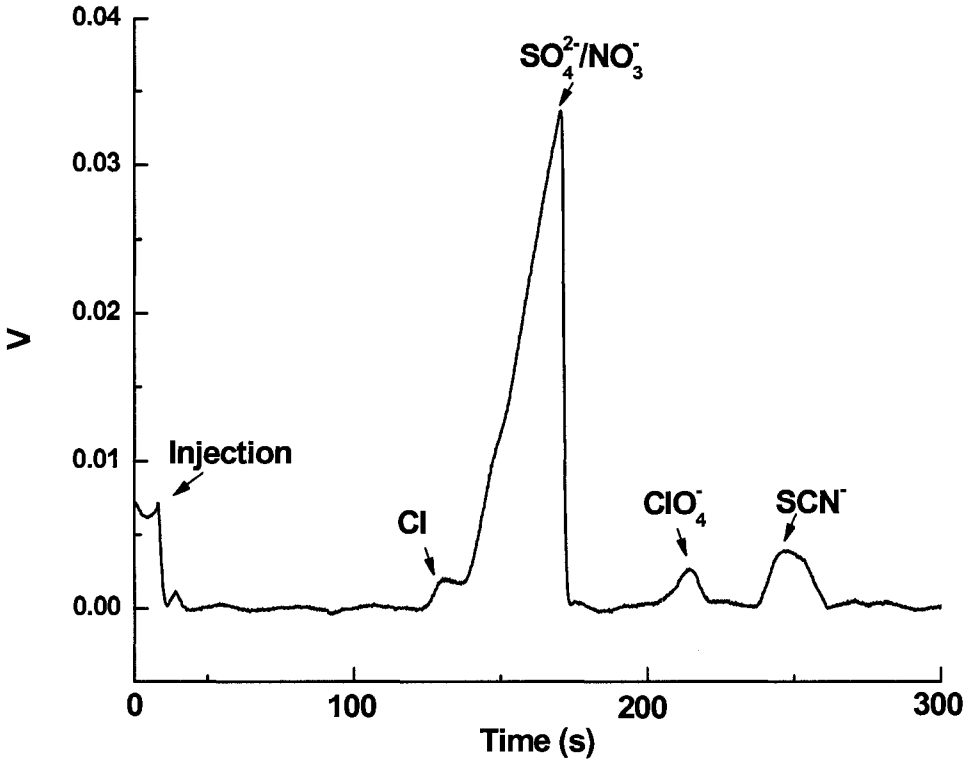

Figure 6.7 Analysis of waste water sample from explosives packing facility. Conditions as in figure 6.5.

arising from loss of FASS as the ionic strength of the sample approaches or even exceeds that of the background electrolyte. Methods of overcoming this limitation are under investigation currently.

6.3.7 Analysis of Fort Collins Drinking Water. Samples of Fort Collins, Colorado drinking water supply were collected before and after a tap mounted home filtration system (PUR, Windsor, CA) and analyzed (Figure 6.8). The ClO_4^- levels are low 3.1 ± 0.03 ppb (n=3) and below EPA reporting limits. A reduction in Cl^- and ClO_4^- of approximately one-half is seen after the carbon filtration. ($ClO_4^- = 1.4 \pm 0.03$ ppb (n=3))

6.3.8 Analysis of Explosives Residues. To further illustrate the effectiveness of the method for complex samples, explosives residue from rifle casings were analyzed (Figure 6.9). Five freshly discharged shell casings were collected and agitated for 10 min in 10 mL DI water. The solution was then analyzed without any pretreatment and perchlorate levels were determined to be 0.8 ±0.03 ppb (n=3). This sample contains large amounts of debris and was a yellow color (Figure 6.9 inset). The MCE system was able to reject these interferences and analyze for perchlorate.

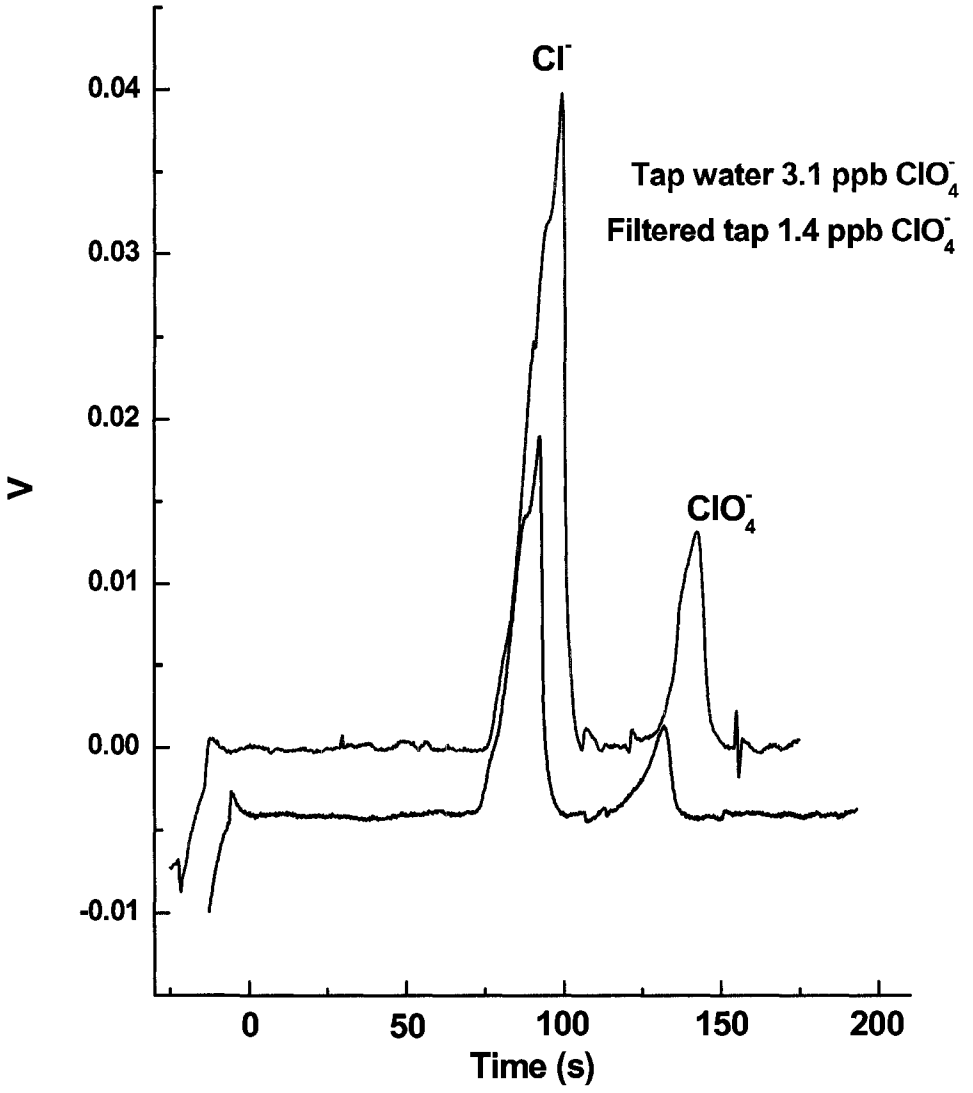

Figure 6.8 Analysis of Fort Collins, CO drinking water before and after a home filtration unit. Conditions as in Figure 6.4

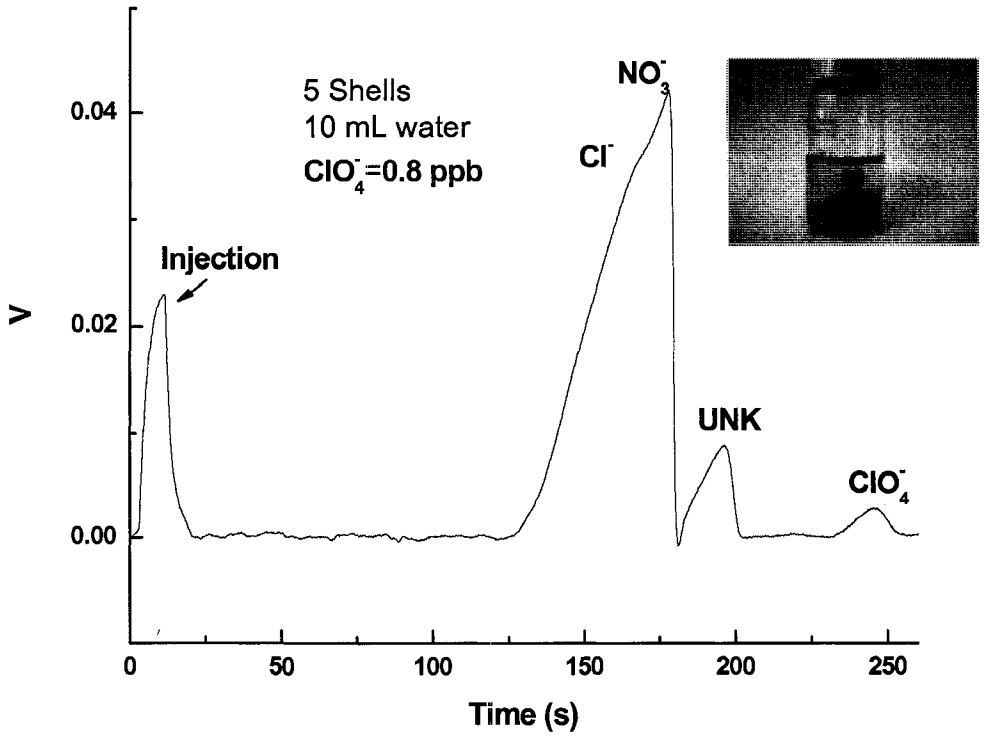

Figure 6.9 Analysis of explosives residues from rifle shell casings. 5 22LR Cal rifle shells in 10 mL DI water. Conditions as in Figure 6.4

6.4 Conclusion. I have developed a microchip capillary electrophoresis device capable of perchlorate analysis in surface and ground water samples in under 4 minutes. No pretreatment of samples is required because of an opposed flow system that rejects all but highly mobile anions such as perchlorate. Detection limits have shown to be comparable to IC-MS method described in EPA method 330. These results bode well for the development of a rapid on-site monitoring system for ClO_4^-.

6.5 References

(1) Environmental Protection Agency, C., OH, 1999; EPA, Ed.; EPA, 2004.
(2) Kirk, A. B. *Analytica Chimica Acta* **2006**, *567*, 4-12.
(3) D.P. Hautman, D. J. M., A.D. Eaton, A.W. Haghani; Environmental Protection Agency, C., OH, 1999, Ed.; Environmental Protection Agency, 1999.
(4) Dasgupta, P. K. *Analytica Chimica Acta* **2006**, *567*, 1-3.
(5) Herschkowitz, N.; Kagan, J.; Zilles, K. *Neuropediatrics* **1997**, *28*, 296-306.
(6) Dussault, J. H.; Ruel, J. *ANNU. REV. PHYSIOL.* **1987**, *Vol. 49*, 321-334.
(7) Jacobsson, B.; Hagberg, G. *Best Practice & Research Clinical Obstetrics & Gynaecology* **2004**, *18*, 425-436.
(8) US Govt. Acountability Office, May 2005; Vol. GAO-05-462.
(9) FDA www.cfsan.fda.gov/dms/clo4data.html, 2003.
(10) Kirk, A. B.; Smith, E. E.; Tian, K.; Anderson, T. A.; Dasgupta, P. K. *Environmental Science and Technology* **2003**, *37*, 4979-4981.
(11) Kirk, A. B.; Martinelango, P. K.; Tian, K.; Dutta, A.; Smith, E. E.; Dasgupta, P. K. *Environmental Science and Technology* **2005**, *39*, 2011-2017.
(12) EPA/815/F-98/002, U. S. E. P. A. D. n.; Fed. Regist., 1998, pp 10273.
(13) Tian, K.; Dasgupta, P. K.; Anderson, T. A. *Analytical Chemistry* **2003**, *75*, 701-706.
(14) http://www.epa.gov/ogwdw000/ccl/perchlor/perchloro.html.
(15) http://www.epa.gov/ncea/perh.htm.
(16) EPA *http://frwebgate.access.gpo.gov/cgi-bin/multidb.cgi?WAIStemplate=multidb_results.html&WAISqueryRule=%24WAISqueryString&WAISdbName=1998_register+Federal+Register%2C+Volume+63+%281998%29&WAISqueryString=drinking+water+contaminant+list&WAISmaxHits=50&WrapperTemplate=fr_wrapper.html.*
(17) Wagner, H. P.; Pepich, B. V.; Hautman, D. P.; Munch, D. J. *Journal of Chromatography A* **2002**, *956*, 93-101.
(18) Wagner, H. P.; Pepich, B. V.; Hautman, D. P.; Munch, D. J. *Journal of Chromatography A* **2000**, *882*, 309-319.
(19) Wagner, H. P.; Suarez, F. X.; Pepich, B. V.; Hautman, D. P.; Munch, D. J. *Journal of Chromatography A* **2004**, *1039*, 97-104.
(20) Buchberger, W.; Haider, K. *Journal of Chromatography A* **1997**, *770*, 59-68.
(21) Roehl, R.; Slingsby, R.; Avdalovic, N.; Jackson, P. E. *Journal of Chromatography A* **2002**, *956*, 245-254.
(22) El Aribi, H.; Le Blanc, Y. J. C.; Antonsen, S.; Sakuma, T. *Analytica Chimica Acta* **2006**, *567*, 39-47.
(23) Yokoyama, T.; Macka, M.; Haddad, P. R. *Analytica Chimica Acta* **2001**, *442*, 221-230.
(24) Pirogov, A. V.; Yur'ev, A. V.; Shpigun, O. A. *Journal of Analytical Chemistry* **2003**, *58*, 781-784.
(25) Giblin, T.; Frankenberger, W. T. *Chromatographia* **2000**, *52*, 505-508.

(26) Park, S. W.; Jin, K. H.; You, J. H.; Kim, T. J.; Paeng, K. J.; Kong, K. H. *Analytical Sciences* **1997**, *13*, 243-246.
(27) Hebert, G. N.; Odom, M. A.; Bowman, S. C.; Strauss, S. H. *Analytical Chemistry* **2004**, *76*, 781-787.
(28) Strauss, S. H.; Odom, M. A.; Hebert, G. N.; Clapsaddle, B. J. *Journal American Water Works Association* **2002**, *94*, 109-115.
(29) Ruan, C. M.; Wang, W.; Gu, A. H. *Analytica Chimica Acta* **2006**, *567*, 114-120.
(30) Wang, J.; Chen, G.; Muck, A., Jr.; Collins, G. E. *Electrophoresis* **2003**, *24*, 3728-3734.
(31) Hutchinson, J. P.; Evenhuis, C. J.; Johns, C.; Kazarian, A. A.; Breadmore, M. C.; Macka, M.; Hilder, E. F.; Guijt, R. M.; Dicinoski, G. W.; Haddad, P. R. *Analytical Chemistry* **2007**, *79*, 7005-7013.
(32) Wang, H.; Zhang, Y.; Yan, B.; Liu, L.; Wang, S. P.; Shen, G. L.; Yu, R. Q. *Clinical Chemistry* **2006**, *52*, 2065-2071.
(33) Ressine, A.; Ekstrom, S.; Marko-Varga, G.; Laurell, T. *Analytical Chemistry* **2003**, *75*, 6968-6974.
(34) Garcia, C. D.; Engling, G.; Herckes, P.; Collett, J. L., Jr.; Henry, C. S. *Environ Sci Technol* **2005**, *39*, 618-623.
(35) Sano, M.; Nishino, I.; Ueno, K.; Kamimori, H. *Journal of Chromatography B-Analytical Technologies in the Biomedical and Life Sciences* **2004**, *809*, 251-256.
(36) Duffy, D. C.; McDonald, J. C.; Schueller, O. J. A.; Whitesides, G. M. *Analytical Chemistry* **1998**, *70*, 4974-4984.
(37) Wang, J. *Electroanalysis* **2005**, *17*, 1133-1140.
(38) Vandaveer, W. R.; Pasas-Farmer, S. A.; Fischer, D. J.; Frankenfeld, C. N.; Lunte, S. M. *Electrophoresis* **2004**, *25*, 3528-3549.
(39) Pumera, M. *Talanta* **2007**, *74*, 358-364.
(40) Guijt, R. M.; Evenhuis, C. J.; Macka, M.; Haddad, P. R. *Electrophoresis* **2004**, *25*, 4032-4057.
(41) Haber, C.; Jones, W. R.; Soglia, J.; Surve, M. A.; McGlynn, M.; Caplan, A.; Reineck, J. R.; Krstanovic, C. *Journal of Capillary Electrophoresis* **1996**, *3*, 1-11.
(42) Galloway, M.; Stryjewski, W.; Henry, A.; Ford, S. M.; Llopis, S.; McCarley, R. L.; Soper, S. A. *Anal Chem* **2002**, *74*, 2407-2415.
(43) Shadpour, H.; Hupert, M. L.; Patterson, D.; Liu, C. G.; Galloway, M.; Stryjewski, W.; Goettert, J.; Soper, S. A. *Analytical Chemistry* **2007**, *79*, 870-878.
(44) Vrouwe, E. X.; Luttge, R.; Vermes, I.; van den Berg, A. *Clinical Chemistry* **2007**, *53*, 117-123.
(45) Wang, J.; Pumera, M.; Collins, G.; Opekar, F.; Jelinek, I. *Analyst* **2002**, *127*, 719-723.
(46) Pumera, M.; Wang, J.; Opekar, F.; Jelinek, I.; Feldman, J.; Lowe, H.; Hardt, S. *Anal Chem* **2002**, *74*, 1968-1971.
(47) Baltussen, E.; Guijt, R. M.; van der Steen, G.; Laugere, F.; Baltussen, S.; van Dedem, G. W. *Electrophoresis* **2002**, *23*, 2888-2893.

(48) Berthold, A.; Laugere, F.; Schellevis, H.; de Boer, C. R.; Laros, M.; Guijt, R. M.; Sarro, P. M.; Vellekoop, M. J. *Electrophoresis* **2002**, *23*, 3511-3519.
(49) Laugere, F.; Guijt, R. M.; Bastemeijer, J.; van der Steen, G.; Berthold, A.; Baltussen, E.; Sarro, P.; van Dedem, G. W.; Vellekoop, M.; Bosschet, A. *Anal Chem* **2003**, *75*, 306-312.
(50) Macka, M.; Hutchinson, J.; Zemann, A.; Zhang, S.; Haddad, P. R. *Electrophoresis* **2003**, *24*, 2144-2149.
(51) Zemann, A. J. *Electrophoresis* **2003**, *24*, 2125-2137.
(52) Zemann, A. *GIT Labor-Fachzeitschrift* **2003**, *47*, 22-24.
(53) Unterholzner, V.; Macka, M.; Haddad, P. R.; Zemann, A. *Analyst (Cambridge, United Kingdom)* **2002**, *127*, 715-718.
(54) Zemann, A. J. *TrAC, Trends in Analytical Chemistry* **2001**, *20*, 346-354.
(55) Mayrhofer, K.; Zemann, A. J.; Schnell, E.; Bonn, G. K. *Anal Chem* **1999**, *71*, 3828-3833.
(56) Zemann, A. J.; Mayrhofer, K.; Schnell, E.; Bonn, G. K. *Book of Abstracts, 216th ACS National Meeting, Boston, August 23-27* **1998**, ANYL-075.
(57) da Silva, J. A. F.; Guzman, N.; do Lago, C. L. *Journal of Chromatography A* **2002**, *942*, 249-258.
(58) Guijt, R. M.; Evenhuis, C. J.; Macka, M.; Haddad, P. R. *Electrophoresis* **2004**, *25*, 4032-4057.
(59) Terabe, S.; Otsuka, K.; Ichikawa, K.; Tsuchiya, A.; Ando, T. *Analytical Chemistry* **1984**, *56*, 111-113.
(60) Terabe, S.; Otsuka, K.; Ando, T. *Analytical Chemistry* **1985**, *57*, 834-841.
(61) Landers, J. P. *Handbook of Capillary Electrophoresis*; CRC Press: Boston, 1997.
(62) Woodland, M. A.; Lucy, C. A. *Analyst* **2001**, *126*, 28-32.
(63) Landers, J. P. *Handbook of of capillary and microhip electrophoresis and associated microtechniques* 3rd ed.; CRC Press: Boca Raton, 2008.
(64) Landers, J. P. *Handbook of Capillary Electrophoresis*, 1 ed., 1993.
(65) Quirino, J. P.; Terabe, S. *Science* **1998**, *282*, 465-468.
(66) Sera, Y.; Matsubara, N.; Otsuka, K.; Terabe, S. *Electrophoresis* **2001**, *22*, 3509-3513.
(67) Duffy, D. C.; McDonald, J. C.; Schueller, O. J. A.; Whitesides, G. M. *Anal Chem* **1998**, *70*, 4874-4884.
(68) Garcia, C. D.; Henry, C. S. *Anal Chem* **2003**, *75*, 4778-4783.
(69) Vickers, J. A.; Henry, C. S. *Electrophoresis* **2005**, *26*, 4641-4647.
(70) Garcia, C. D.; Liu, Y.; Anderson, P.; Henry, C. S. *Lab Chip* **2004**, *3*, 324-328.
(71) Jacobson, S. C.; Hergenroder, R.; Moore, A. W., Jr.; Ramsey, J. M. *Anal Chem* **1994**, *66*, 4127-4132.
(72) Zhou, J.; Lunte, S. M. *Electrophoresis* **1995**, *16*, 498-503.
(73) Liu, Y.; Foote, R. S.; Culbertson, C. T.; Jacobson, S. C.; Ramsey, R. S.; Ramsey, J. M. *Journal of Microcolumn Separations* **2000**, *12*, 407-411.
(74) Yan, Z.; Yanyan, L.; Fritz, J. S.; Haddad, P. R. *J Chromatogr A* **2003**, *1020*, 259-264.

(75) Zajac, J.; Chorro, C.; Lindheimer, M.; Partyka, S. *Langmuir* **1997**, *13*, 1486-1495.
(76) Cook, H. A.; Dicinoski, G. W.; Haddad, P. R. *Journal of Chromatography A* **2003**, *997*, 13-20.
(77) Wallenborg, S. R.; Bailey, C. G. *Anal Chem* **2000**, *72*, 1872-1878.
(78) Rodriguez, I.; Jin, L. J.; Li, S. F. *Electrophoresis* **2000**, *21*, 211-219.
(79) Cook, H. A.; Hu, W. Z.; Fritz, J. S.; Haddad, P. R. *Analytical Chemistry* **2001**, *73*, 3022-3027.
(80) Breadmore, M. C. *Electrophoresis* **2007**, *28*, 254-281.
(81) Chien, R. L. *Electrophoresis* **2003**, *24*, 486-497.

Chapter 7

Conclusions and Future Directions

7.1 Conclusion

The work presented in this doctoral dissertation focused on improvements in the microchip CE field. Improvements in separation efficiency, surface chemistry, and EOF control within the microchip devices using: surfactants, PEMs, PECVD, and bulk material selection were made. These experiments resulted in published journal articles for each method. Surfactant addition proved to be the most useful and simplest modification method which resulted in increased EOF velocity, stability, and separation efficiency. PEMs showed improved EOF stability, good flow direction control and an increase in the number of theoretical plates. PECVD coatings were tested for EOF control as well as analyte absorption properties into the bulk PDMS. Decreases in analyte absorption resulted when argon plasma pretreatment was performed. Control of EOF magnitude was also demonstrated with increases or decreases in the measured EOF values depending on the desired effect and the modification method used. The PEM and PECVD coatings however, coated microwires rendering them useless and limiting detection to optical methods. Two alternate polymer materials were demonstrated for use in microchip CE-ECD increases in EOF and separation efficiencies were observed as well as increased stability and reproducibility. Only slight variations in fabrication were needed and the overall cost was reduced relative to PDMS devices for TPE microfluidic devices. For perchlorate separations, the surfactant used to achieve resolution dominated the separation in such a way that no change in migration order was seen. Small changes in the overall separation time were noticed due to the differences in electroosmotic

flow of the PMMA device in its native state. Peak shape remained essentially unchanged.

The last goal of my doctoral dissertation research was the development of fast, sensitive microchip CE separation devices and the associated separation and surface chemistry needed to resolve analytes of environmental importance and prevent absorption into the bulk material. After studying the separation chemistry, surface chemistry, and characterization, I moved on to the development of a small, inexpensive, fast, and sensitive detector for perchlorate. Perchlorate is of concern because it inhibits uptake of iodide into the thyroid impairing its function as the master gland in the endocrine system and causing a wide range of health effects. Perchlorate also migrates with the groundwater due to its low absorption to organic matter and soils and high solubility. Monitoring perchlorate release and remediation as well as tracking the extent of contamination has become a major concern for water quality. I have developed the needed separation chemistry and an analytical device capable of determining levels of perchlorate in surface and groundwater in less than three minutes with no sample pretreatment. Limits of detection have shown to be 0.5 ppb, which is on par with much more expensive methods of analysis (IC-MS). Separation conditions were optimized to achieve perchlorate resolution from interfering analytes. I have made use of sample stacking to preconcentrate sample prior to injection to allow for sub ppb detection limits. Effectiveness of the method was demonstrated on both surface (Poudre River) and wastewater (Explosives packing facility) samples. Validation was performed by comparison to EPA established methods for the analysis of the wastewater sample. I also made a

significant step towards a field portable system in the creation of a computer controlled, battery operated, power supply.

7.2 Future Directions

The next step in the perchlorate project is to develop a portable detector for in field monitoring. A portable detector would consist of similar electronics to the Dionex CD-20 currently used to achieve the required sensitivity; however the electronics must be powered by battery. Of major importance in a portable system is form factor, encompassing size and weight as well as robustness. I envision an auto-sampler like microchip consisting of several sample reservoirs that are connected to the injection cross with individually addressable leads from the power supply. This would allow for field testing of multiple samples without changing BGE or excessive sample introduction. The computer controlled power supply already built can be programmed to control flow within the microchip allowing for semi-autonomous use, furthermore, a bank of relays would allow for multiplication of the number of sample reservoirs that could be incorporated. I also foresee the application of this analysis device to other analytes of interest such as active pharmaceutical agents, pesticides, and heavy metals, by varying separation conditions, and microchip configurations. The basic configuration of the microchip can be modified to meet many specialized needs from on-line monitoring by using a flow through injection system, to incorporation of on-chip filtration and sample handling. The broad applicability of conductivity detection lends itself well to analysis of many biological analytes as well as other classes.

Further exploration into the modification of polymeric microfluidic devices is needed to resolve issues stemming from surface chemistry and irregularities in polymer surface morphology. The application of various plasma systems to modify polymers used in microchip CE is virtually untapped. This dissertation covers just two examples of the nearly endless possibilities of PECVD modification. Further exploration into creating stable, uniform surface coatings is needed. Coatings providing an increase in hydrophilicity would increase the separation efficiency of polymer microchips, while selective chemistries could be applied for complex analysis.

Appendix 1: Research Proposal
Micro-Total Analysis Device for Detection of Prostate Specific Antigen for Early Diagnosis of Prostate Cancer

Brian M. Dressen, Department of Chemistry, Colorado State University
Original Research Proposal

A. Summary and Specific Aims

Prostate cancer is currently the second leading cause of cancer related death in American males,[2] second only to lung cancer. An estimated 218,890 new cases, and 41,800 deaths are reported each year.[2, 3] Prostate cancer develops in the prostate,[3] a gland in the male reproductive system when cells of the prostate mutate and multiply out of control. These cancerous cells often metastasize to other parts of the body with the lymph nodes and bones being the most likely targets. As with all cancers, early diagnosis is key to treatment and most importantly, survivability. Currently two tests exist for routine screening for prostate cancer, the digital rectal exam (DRE) and prostate specific antigen (PSA) screening. DRE is the most common screening method for prostate cancer but lacks the ability to detect reliably and early enough to be effective at improving prognosis. PSA is a single-chain glycoprotein commonly used as a prostate cancer biomarker. Data suggests that PSA testing will detect only progressed prostate cancer cases, which are usually too late for effective treatment[4] and reports suggest that PSA screening only reflects prostate size. New, more effective tests are needed in order to reduce the unnecessary suffering and treatment costs associated with prostate cancer. Few other biomarkers exist; therefore researchers are searching for new biomarkers of prostate cancer.[5, 6] Recently variants of PSA have been identified that can provide additional specificity for prostate cancer prognosis.[7] PSA electrophoretic subforms F_2 and F_3 behave inversely, as patients with prostate cancer show decreased F_2 levels and increased F_3 levels.[7] Free electrophoretic subforms of PSA can be analyzed from serum or semen samples by 2D electrophoresis with identification through western blotting techniques.[7] Comparison of the ratio of F_2 and F_3 provides for more positive diagnosis of prostate cancer.[8] Here we propose to develop a novel micro-total analysis system (μTAS) for the detection and quantification of free electrophoretic subforms of PSA, F_2 and F_3, for early diagnosis of prostate cancer. The μTAS system will provide reduced sample consumption, decreased analysis time, lower cost, and size. The specific aims of this proposal are:

1. Develop a microfluidic system for isolation of PSA from serum using micro-fluidic bead chemistry methods.
2. Optimize the separation of free PSA isoforms by microchip capillary electrophoresis separation to allow for rapid analysis of isoforms.
3. Develop a robust microchip interface to ESI-MS system for quantification of F_2 and F_3.
4. Integrate isolation, purification, separation, and detection system, using microfluidics to create a μTAS chip for the early diagnosis of prostate cancer.

The final PSA-μTAS device will provide a rapid, sensitive method to quantify PSA levels in serum samples and monitor prostate cancer prognosis by comparing ratios of F_2 to F_3 PSA subforms. Early diagnosis of prostate cancer will become more selective, producing more accurate testing, improved patient survivability, and a higher quality of life.

B. Background

Prostate cancer is the most common form of cancer in American males and is responsible for 41,800 deaths each year. Common symptoms and effects of prostate cancer include genital pain, difficulty urinating, and erectile dysfunction. Prostate cancer occurs most frequently in men over fifty and like all cancers, early detection is key in treating the disease. Therefore there is a need to improve existing diagnostic methods as well as develop new tools that will allow prostate cancer to be detected 5-10 years before a patient would present with clinically diagnosable prostate cancer. Current diagnostic methods are invasive as the most common method is digital palpation through the rectal wall (DRE). Figure 1 shows the location of the prostate as well as surrounding organs.[9] The DRE method can only yield a useful diagnosis if the physician conducting the exam has prior knowledge and experience of the patient's prostate size through previous DRE tests. Furthermore, diagnosis using DRE is often realized too late, when effective treatments are no longer an option.

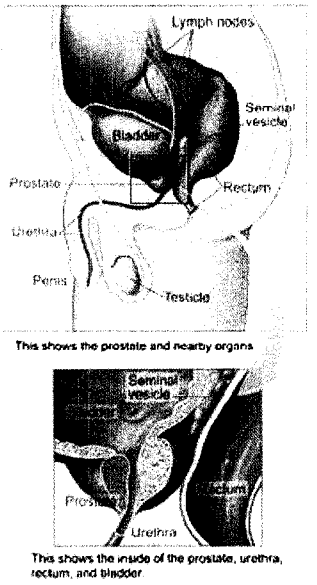

Figure 1

Total PSA (tPSA) testing has long been used in an effort to diagnose prostate cancer. tPSA is commonly measured using enzyme linked immunosorbent assay (ELISA) chemistry.[10] Alternatively PSA testing can be done using direct immunoadsorption methods, separation using 2-D gel electrophoresis (2DE), followed by antibody based identification or mass spectrometry analysis.[11] Men showing levels above 10 μg/L are at high risk of prostate cancer while the risk is low below 4 μg/L. PSA concentrations detected in the 4-10 μg/L range are more ambiguous but accurate diagnosis in this range is critical to effective treatment. Men with PSA levels in the 4-10 μg/L range may harbor an early stage malignancy which is curable with surgery if detected early enough. Unfortunately, the measurement of tPSA in this range using conventional methods lacks the specificity and sensitivity required for diagnosis. At the present time, electrophoretic subforms F_2 and F_3 offer the most promising route of biomarker detection for prostate cancer diagnosis.[7, 8] The following sections detail the steps currently used to determine tPSA levels and some electrophoretic subforms.

B.1. Direct Immunoadsorption. Proteins that are not in sufficient abundance in serum must be isolated and collected in sufficient yield and purity prior to analysis. If

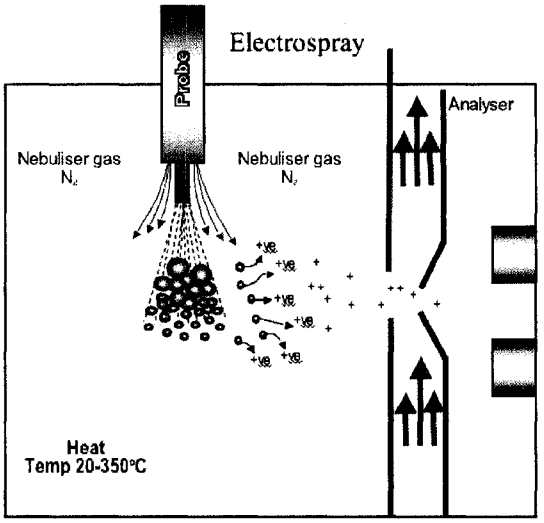

Figure 2 Schematic of ESI-MS[1]

antibodies are available, immunopurification is the method of choice. PSA is present in serum at concentrations10^5-10^8 times lower than other proteins, such as albumin.[11] PSA is then bound to a streptavidin-coated surface by monoclonal antibody complexes of anti-DIG-IgG bound to the surface. Washing steps remove impurities and detergents leaving behind bound PSA. A competing binding agent such as digoxigenin-lysine at neutral pH is used to elute off the bound PSA. Neutral pH is used to minimize the amount of bound impurities come off with the PSA. After lyophilization, the PSA enriched sample can be analyzed immediately or frozen for future use.

B.2. 2-D Gel Electrophoresis. 2-D gel electrophoresis 2DGE is a powerful method for the analysis of protein mixtures.[12] Two forms of electrophoresis are used together to produce the two-dimensional separation. The first is isoelectric focusing in which proteins are separated according to their isolelectric point. The second dimension uses sodium dodecyl sulfate (SDS) and polyacrylamide gel to denature proteins and separate them according to their molecular weights. 2-D gel electrophoresis is time consuming (hours) and requires several mL of sample. Staining, excising, preparation and analysis add hours to processing time.

B.3. Antibody Identification. Following 2DGE, samples are stained with common staining reagents to visualize their location on a gel and excise them if needed. Often rabbit polyclonal anti-PSA is combined with chemiluminescence reactions to provide identification via fluorescent imaging of spots of interest.[13] Ratios of free PSA forms are ultimately determined with densitometric intensities.

B.4. Electrophoresis. Protein analysis using capillary electrophoresis (CE) is useful as a second dimension separation step in liquid chromatography–CE systems or as a single dimension separation scheme for the analysis of PSA.[14] 2D separations can also be realized by coupling two CE systems in CE-CE methods. Single dimension CE separations of PSA have been performed through the modification of electroosmotic flow to enhance resolution.[15] CE is typically not capable of separating large numbers of proteins

B.5. Mass Spectrometry. Electrospray ionization mass spectrometry (ESI-MS) is a mass analysis method that can be used for positive identification of proteins. ESI forces liquid sample through a charged capillary. The liquid forms charged droplets that increase in charge density as the solvent evaporates. Once past a critical charge density, the droplets explode into ions that are accelerated towards the mass analyzer by the potential between the capillary tip and the entrance to the mass analyzer. (Figure 2) Low flow preparative systems such as CE. MS is used for proteomics research for positive

identification of proteins as well as quantification can be directly fed into an ESI-MS system, easing the coupling of CE to MS.

C. Methods/Experimental Design

The creation of a micrototal analysis system for isolation, separation, and detection of free electrophoretic subforms of PSA from human serum will take place in 4 steps.

1. Develop a microfluidic system for isolation of PSA from serum using micro-fluidic bead chemistry methods.
2. Optimize the separation of free PSA isoforms by microchip capillary electrophoresis separation for rapid analysis of the isoforms, F_2 and F_3.
3. Develop a robust microchip interface to ESI-MS system for quantification of F_2 and F_3.
4. Integrate isolation, purification, separation, and detection systems to create a μTAS chip for the early diagnosis of prostate cancer.

C.1. Purification/isolation of PSA. The purification of PSA will occur through indirect immunoadsorption of PSA on streptavidin coated latex beads modified with anti-DIG-IgG and digoxigenylated anti-PSA/PSA. Elution with digoxigenin-lysine conjugate will result in highly purified fPSA. Microbeads will be packed into microchip LC channels and exposed to reagents to chemically modify the bead surface with streptavidin and anti-DIG-IgG. Sample solutions containing PSA will be pumped into the affinity purification column and allowed to incubate with the bead material to form antibody complexes on the surface. After incubation, fPSA will be eluted off and analyzed via SDS-PAGE to assess purity. The beads will be carried into the microchip column under pressure and blocked from exiting the channel by a narrow passageway that will serve as a frit from the purification column to the CE system. Three inlet ports; sample, binding buffer, and elution buffer will be used to control flow within the column. (Figure 3) Initially the devices would be used for only one patient, given that the immunoadsorption chemistry is not reusable. Multiplexing the system to include additional purification columns could allow for higher throughput and extended usage of the uTAS system the use of magnetic beads that could be trapped for use and then released, could allow for multi use chips.

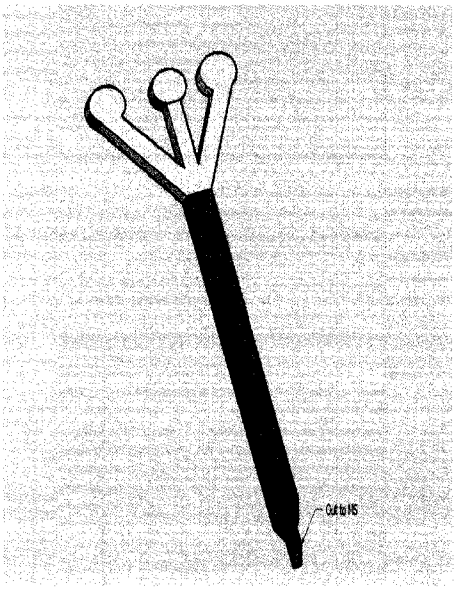

Figure 3 Micro LC channel design

C.2. CE separation of PSA. The second step will be to determine the separation conditions needed to resolve F_2, F_3 and other isoforms of PSA. Separation conditions will be first determined on conventional CE instrumentation using fused silica capillaries. CE separation relies on differences in the charge to hydrodynamic radius ratio to resolve analyte components. Given that this ratio does not vary much for each protein isoform, enhancing selectivity and control of flow within the device will be paramount. Separation of PSA isoforms has been demonstrated with conventional CE using borate buffer and the amine additive 1,3-diaminopropane.[15] The electrophoretic subforms of PSA, F_2, and F_3 have masses in the 33 kDa range as opposed to 237 kDa for tPSA; the pI for each form ranges from 6.6 to 6.8. The first method of CE separation will be to vary the buffer pH in the pI range, resulting in differing charges for F_2 and F_3 PSA subforms. The hydrodynamic radius is essentially identical for these biomarkers, and this varying of the charge will provide the most promising method of separation while minimizing buffer complexity. If resolution of F_2 and F_3 is not possible with pH modification, buffer additives will be used to control flow and selectivity. Numerous groups have used surfactants and other additives to control electroosmotic flow within the capillary[14, 16] and in the case of surfactants, when used above the critical micelle concentration, micellar electrokinetic chromatography (MEKC) results in an additional mode of separation. MEKC relies on micelles acting as a psudostationary phase in which the proteins will interact with the micelles and the degree of interaction affects the migration time of the proteins. Additives such as morpholine, 1,3-diaminopropane, 1,5-diaminopentane, and 1,7-diaminoheptane enhance the selectivity of CE to glycoproteins and allow high resolution separation.[15] Additives will be used to optimize the separation performance if needed to achieve the desired resolution of the free forms of PSA. During the development stage, UV detection of analytes at 214 nm wavelength will be used to monitor the successful separation of PSA subforms F_2 and F_3.[15] ESI-MS is sensitive to salt and surfactant concentration, therefore separation conditions will be carefully chosen to minimize buffer effects on MS analysis. TRIS or HEPS buffers are tolerated if they are in low enough concentration.[17] If adequate separation conditions cannot be found, a sheath flow ESI emitter will be used.[18]

C.3.1. Microchip CE. Figure 4 shows a schematic of the CE microchip. Purified PSA from the micro LC purification section will be introduced in to the sample reservoir. An electric potential applied between the sample and sample waste reservoirs will generate electroosmotic flow (EOF), causing flow of sample across the separation channel. Identical EOF will be generated between the buffer and waste reservoirs to cause migration of sample towards the detector. Injection will be performed by momentarily switching the buffer reservoir to a lower potential. Proteins will be separated while migrating at different electrophoretic velocities within the separation channel. During the microchip development stage, F_2 and F_3 will be detected using UV detection monitored at 254 nm.

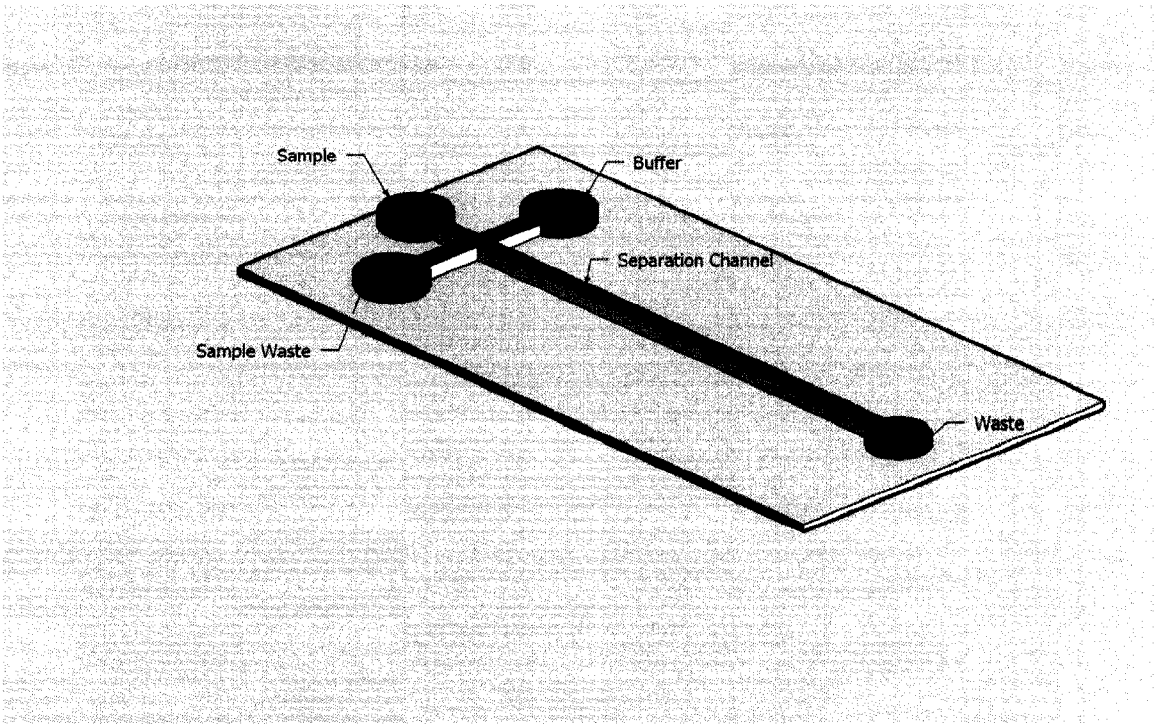

Figure 4: Schematic of CE microchip

C.3.2. Coupling Microchip to Mass Spectrometry. Following optimization of F_2 and F_3 separation on the microchip CE device, the separation system will be coupled to mass spectrometry for detection of individual cancer biomarkers. Mass spectrometry provides for positive identification of proteins and their fragments. When dealing with cancer diagnosis, false positives and negatives must be avoided. CE separation and UV detection alone are not usually sufficient to unequivocally guarantee identification of analytes. Low flow systems such as capillary electrophoresis, lend themselves well to ESI-MS.[17] The proposed microchip design will have an integrated ESI connector in lieu of the waste reservoir. F_2 and F_3 will be spatially separated in the separation portion of the device, pass into the ESI tip where ionization will occur. Identification will be made using the known molecular masses of F_2 and F_3 and comparing the ratio of the ion currents. Sheathed and sheathless emitters for microchip devices have been created and allow for facile coupling of microchip CE devices to ESI-MS systems.[19, 20] Sheathed emitters allow for addition of BGE modifiers to allow MS to be used with buffer systems that may otherwise interfere.

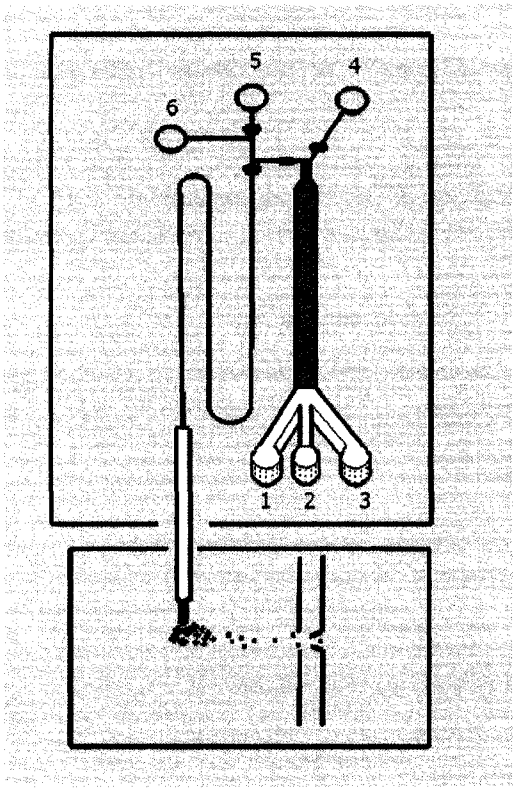

Figure 5: Schematic of μ-TAS Device

C.4. Integration of Systems into μ-TAS. The final steps toward device completion will be joining the previous systems into one integrated micro analysis device. A set of valves[21] will be used to control pressure driven flow within the capillaries. The device will consist of 3 main parts; immunoadsorption/ isolation, CE separation of F_2 and F_3 and analysis by ESI-TOF. A total of 6 reservoirs will be employed to add sample and buffers as well as serving as ports for pumping systems. Two high voltage systems will be used, one to control the CE separation and one for the ESI system. Valves[21] will allow fluid manipulation from the Micro LC column to the injection zone of the microchip or to waste during loading and washing steps. Voltage will be applied between reservoir 5 and the ESI tip during the separation step. The whole blood samples will be added to reservoir 1 and flowed onto the micro affinity column under pressure from a syringe pump. PSA will be retained and all other interfering proteins will be washed with rinse buffer from reservoir 2. Following PSA capture and washing, the purified PSA will be eluted from the column and injected onto the CE separation channel where the various forms of PSA will be resolved from one another and enter the ESI tip to be ionized and detected in the mass spectrometry portion of the device.

D. Summary and Broader Impacts.

The goal of this project is to develop an analysis system capable of analyzing prostate cancer biomarker PSA subforms F_2 and F_3 in serum or semen samples, providing a quick and reliable method of screening for prostate cancer. Prostate cancer is the number two cancer killer of American men. Current diagnostic methods do not provide early detection, and there is a need for sensitive and selective instrumentation that can reliably diagnose clinically significant prostate cancer cases with enough advance notice to allow for best possible survival. Total analysis of free PSA can provide a more definitive early diagnosis of prostate cancer. Simple blood or semen samples can be taken and analyzed in a fraction of the time, with fewer steps using the proposed μ-TAS system than with currently available methods. As future biomarkers for prostate cancer are identified, the proposed system can be adapted to perform total analysis of these biomarkers, thereby increasing the accuracy of diagnosis even farther by analyzing for a larger set of biomarkers simultaneously.

The proposed μ-TAS system has application in a much broader field of diagnostics by changing the specificity of the system through immunoadsorption column selection as well as separation conditions within the CE portion of the device. Mass spectrometric detection will provide for unequivocal identification of proteins, reducing the occurrence of false positives. Cost can be reduced by using other detection modes such as UV or electrochemical methods common to CE if absolute identification is not needed.

(1) Institute, C. H.; UCL Institute of Child Health, 2008.
(2) Physicians, A. A. o. F. *Diagnosisi and Treatment of Prostate Cancer* http://www.aafp.org/afp/980401ap/naitoh.html, 1998.
(3) *National Cancer Institute: US National Institutes of Health 2007,* http://www.cancer.gov.
(4) Humphrey PA, K. D., Smith DS, Shepherd D, Catalona WJ. *Journal of Urology* **1996**, 816-820.
(5) Stamey, T. A.; Caldwell, M.; McNeal, J. E.; Nolley, R.; Hemenez, M.; Downs, J. *Journal of Urology* **2005**, *174*, 1155-1156.
(6) van Gils, M.; Stenman, U. H.; Schalken, J. A.; Schroder, F. H.; Luider, T. M.; Lilja, H.; Bjartell, A.; Hamdy, F. C.; Pettersson, K. S. I.; Bischoff, R.; Takalo, H.; Nilsson, O.; Mulders, R.; Bangma, C. H. *European Urology* **2005**, *48*, 1031-1041.
(7) Jung, K.; Hoesel, W.; Reiche, J.; Deger, S.; Kramer, J.; Loening, S. A.; Lein, M.; Stephan, C. *Urology* **2007**, *69*, 320-325.
(8) Jung, K.; Reiche, J.; Boehme, A.; Stephan, C.; Loening, S. A.; Schnorr, D.; Hoesel, W.; Sinha, P. *Clinical Chemistry* **2004**, *50*, 2292-2301.
(9) Wikipedia http://en.wikipedia.org/wiki/Image:Prostatelead.jpg.
(10) Wiese, R.; Belosludtsev, Y.; Powdrill, T.; Thompson, P.; Hogan, M. *Clin Chem* **2001**, *47*, 1451-1457.
(11) Peter, J.; Unverzagt, C.; Lenz, H.; Hoesel, W. *Analytical Biochemistry* **1999**, *273*, 98-104.
(12) Carrascal, M.; Caruio, S.; Bachs, O.; Abian, J. *Proteomics* **2002**, *2*, 455-468.
(13) Tabares, G.; Jung, K.; Reiche, J.; Stephan, C.; Lein, M.; Peracaula, R.; de Llorens, R.; Hoesel, W. *Clinical Biochemistry* **2007**, *40*, 343-350.
(14) Badal, M. Y.; Wong, M.; Chiem, N.; Salimi-Moosavi, H.; Harrison, D. J. *J Chromatogr A* **2002**, *947*, 277-286.
(15) Donohue, M. J.; Satterfield, M. B.; Dalluge, J. J.; Welch, M. J.; Girard, J. E.; Bunk, D. M. *Analytical Biochemistry* **2005**, *339*, 318-327.
(16) Garcia, C. D.; Dressen, B. M.; Henderson, A.; Henry, C. S. *Electrophoresis* **2005**, *26*, 703-709.
(17) He, T.; Quinn, D.; Fu, E.; Wang, Y. K. *Journal of Chromatography, B: Biomedical Sciences and Applications* **1999**, *727*, 43-52.
(18) Li, J.; Thibault, P.; Bings, N. H.; Skinner, C. D.; Wang, C.; Colyer, C.; Harrison, J. *Anal. Chem.* **1999**, *71*, 3036-3045.
(19) Li, F. A.; Wang, C. H.; Her, G. R. *Electrophoresis* **2007**, *28*, 1265-1273.
(20) Mao, X. L.; Chu, I. K.; Lin, B. C. *Electrophoresis* **2006**, *27*, 5059-5067.
(21) Grover, W. H.; Skelley, A. M.; Liu, C. N.; Lagally, E. T.; Mathies, R. A. *Sens. Act. B* **2003**, *89*, 315-323.